Targeting of nanoparticles to cell adhesion molecules for potential immune therapy

By

Chuda Chittasupho

Submitted to the graduate degree program in Pharmaceutical Chemistry and the Graduate Faculty of the University of Kansas in partial fulfillment of the requirements for the degree of Doctor of Philosophy.

_____

Cory J. Berkland, Committee Chairperson

_____

Teruna J.Siahaan

_____

Laird Forrest

_____

Susan M. Lunte

_____

Prajna Dhar

Date Defended: December 10th

The Dissertation Committee for Chuda Chittasupho

certifies that this is the approved version of the following dissertation:

Targeting of nanoparticles to cell adhesion molecules for potential immune therapy

_____

Cory J. Berkland, Chairperson

Date approved:

Abstract

Cell adhesion molecules including leukocyte function associated antigen-1 (LFA-1) and intercellular adhesion molecule-1 (ICAM-1) play an important role in regulating inflammatory responses. For circulating leukocytes to enter inflamed tissue or peripheral lymphoid organs, the cells must adhere to and transmigrate between endothelial cells lining blood vessel wall by binding of LFA-1 on leukocytes to ICAM-1 on endothelial cells. In addition, interaction of LFA-1 expressed on T cells and ICAM-1 expressed on antigen presenting cells (APCs) is crucial for immunological synapse formation and hence T cell activation. Clustering of LFA-1 and ICAM-1 by multivalent ligands increases binding avidity of these cell adhesion molecules. In this thesis, multivalent ICAM-1 or LFA-1 ligands were conjugated to the surface of polymeric nanoparticles (NPs) to target the clustering of these receptors and increase the avidity of binding to ICAM-1 or LFA-1. Polymeric nanoparticles possess some advantages over other multivalent ligands since drugs can be protected and released. This delivery system permits modification of the nanoparticle surface without compromising the activity of the drug carried.

In chapter 2 of this thesis, a peptide ligand targeting ICAM-1 (cLABL) was conjugated to poly (DL-lactic-co-glycolic acid) (PLGA) nanoparticles. The cellular uptake of cLABL conjugated NPs (cLABL-NPs) by lung carcinoma epithelial cells upregulating ICAM-1 was significantly more rapid than control NPs. The specificity of ICAM-1 mediated internalization was confirmed by blocking the uptake of cLABL-NPs to ICAM-1 using free cLABL peptide. Cell studies suggested that cLABL-NPs targeted encapsulated doxorubicin to ICAM-1 expressing cells and

provided sustained release of doxorubicin. In chapter 3, a peptide ligand targeting LFA-1 (cIBR) was conjugated to PLGA NPs to specifically target T cells expressing LFA-1. The specificity of NPs targeting LFA-1 was demonstrated by competitive inhibition using free cIBR peptide or by using the I domain of LFA-1 to inhibit the binding of cIBR-NPs. In addition, T-cell adhesion to epithelial cells was inhibited by cIBR-NPs. In chapter 4, nanoparticles capable of blocking LFA-1/ICAM-1 interaction were then studied as inhibitors of T cell conjugation to DCs. LABL-NPs and cIBR-NPs rapidly bound to DCs and inhibited T cell conjugation to DCs to a greater extent than the free peptides, unconjugated NPs, anti-ICAM-1 antibodies and anti-LFA-1 antibodies. In addition, DCs treated with NPs or with cIBR-NPs stimulated the proliferation of T cells, but DCs treated with LABL-NPs did not stimulate T cell proliferation. LABL-NPs and cIBR-NPs also altered cytokine production compared to free ligands suggesting these NPs may offer a unique tool for shaping T cell response. In chapter 5, multivalent ligands having both ovalbumin (OVA) antigen and LABL peptide grafted to hyaluronic acid (HA) were found to bind professional APCs and may offer an alternative targeting approach for inducing immune tolerance. Collectively, results verified that cyclic and linear LABL and cIBR peptides can target NPs to ICAM-1 and LFA-1, respectively, to deliver encapsulated agent or to provide function as potent immune modulators.

Acknowledgements

I would like to gratefully and sincerely thank my advisor, Cory Berkland, for his support, guidance, understanding, and most importantly, his friendship during my graduate studies at KU. I have been amazingly fortunate to have an advisor who gave me a great opportunity to develop my own individuality by being allowed to work with such independence and at the same time his guidance. His mentorship was paramount in providing a well-rounded experience consistent my long-term career goals. He encouraged me to not only grow as a researcher but as an instructor and an independent thinker. For everything you have done for me, Professor Berkland, I greatly appreciate. I hope that one day I would become as good an advisor to my students as you have been to me.

My research for this dissertation was made more efficient and also much more extensive through the guidance and assistance of my collaborative professors. Thus I gladly express my gratitude to Dr. Teruna J. Siahaan, Dr. Charlotte M. Vines, Dr. Jeffrey Krise and Dr. Laird Forrest. I appreciate their insightful comments and constructive criticisms at different stages of my research. I am grateful to them for holding me to a high research standard and enforcing strict validations for each research result.

Additionally, I am very grateful for help, support and the friendship of all of my friends and colleagues: Na Zhang, Sheng-Xue Xie, Prakash Manikwar, Rosemary Ndolo, Laurie Shannon, all previous and present Berkland lab members, and friends in the department.

I would like to thank the members of my oral prelims and dissertation committee: Dr. Cory Berkland, Dr. Teruna J. Siahaan, Dr. Laird Forrest, Dr. Susan M. Lunte, Dr. Prjana Dhar, Dr. Elizabeth M. Topp and Dr. Steven Gehrke for their input, valuable discussions and accessibility. I would like to acknowledge all faculty members in the department of Pharmaceutical chemistry for numerous discussions and lectures that helped me improve my knowledge in the area.

The years spent in Lawrence would not have been as wonderful without my Thai roommates, Supang Khondee and Wanrangkana Pornputtapitak. I greatly value their friendship and I deeply appreciate their belief in me. I am also indebted to the Prestons for allowing me to stay in such a great place and their warm friendship.

Most importantly, none of this would have been possible without the love and patience of my family. My special thanks to the persons whom I owe everything I am today, my parents Chucheep and Patcharee Chittasupho, for their constant love, concern, support and strength all these years. Their faith and confidence in my abilities and in me is what has shaped me to be the person I am today.

Finally, I am also grateful to Royal Thai Government scholarship for the financial support to live, learn and experience beyond education here in such a great country, the United States.

ChudaChittasupho

November 2010

Table of Contents

Chapter 1

Targeting T cell costimulation in autoimmune disease

1.1 Autoimmune disease

Autoimmunity results from the breakdown of mechanisms controlling immune tolerance and the failure of the host immune system to distinguish self from non-self-antigens. Autoimmunity produces an attack on self-cells and organs by autoantibodies and auto-reactive T cells. Central tolerance in primary lymphoid organs (thymus and bone marrow) provides the mechanism by which T cells and B cells are removed if they carry receptors that recognize self-antigens. For self-reactive T cells or B cells that escape from the thymus or bone marrow, there is a backup mechanism of 'peripheral tolerance' that renders these cells inactive or anergic by several processes such as apoptosis or by the function of regulatory T cells.[1, 2] Despite tight regulation, inappropriate humoral and cellular-mediated immune responses against self-antigens occasionally occur. Autoimmune reactions propagate a number of autoimmune diseases such as rheumatoid arthritis, multiple sclerosis, Graves' disease, Crohn's disease, lupus erythematosus and insulin-dependent diabetes mellitus. Autoimmune diseases are chronic inflammatory diseases assumed to arise from a combination of genetic traits, environmental factors and the breakdown of regulatory mechanisms.[1-5]Both humoral (autoantibodies) and cellular (autoreactive lymphocytes) responses mediate autoimmune diseases. Some autoimmune diseases are mediated by cellular damage. Autoimmune diseases that are mediated by cellular damage occur when lymphocytes or antibodies bind to cell membrane antigens and stimulate cellular lysis and inflammatory response. Insulin-dependent diabetes mellitus is caused by the attack of auto-reactive T cells against insulin-producing cells (beta cells) in the pancreas. In multiple sclerosis, patients produce autoreactive T

cells that infiltrate brain tissue and cause inflammatory lesions along the myelin sheath of nerve fibers.[2] Some autoimmune diseases are mediated by stimulating or blocking autoantibodies. In Graves' disease, autoantibodies are produced and bind to thyroid stimulating hormone (TSH) receptor without regulation, hence overstimulating the production of thyroid hormone. Myasthenia gravis is an autoimmune disease mediated by autoantibodies that block acetylcholine receptors on the motor end plate of muscles and inhibit the binding of acetylcholine to this receptor, hence weakening skeletal muscle.

Current therapies for autoimmune diseases only reduce symptoms to provide an acceptable quality of life; for example, by general suppression of the immune system. The problem of using non-selective immunosuppressants, cytotoxic drugs or corticosteroids that threaten the overall immune response is that patients are then susceptible to opportunistic infections and other side effects.[6]

Chronic inflammation is one target for autoimmune disease intervention.[5] The inflammatory pathway involves several steps including leukocyte transmigration and cytokine production. Advances in discoveries of pathogenetic mechanisms of autoimmune diseases have contributed to the introduction of biologics as new therapies for autoimmune diseases. TNF-α inhibitors (infliximab, etanercept, and adalimumab) have been used for treatment of rheumatoid arthritis, psoriasis and Crohn's disease. There are several other cytokines that modulate inflammatory responses such as IL-1, IL-6, IL-17 and IL-23. The rationale behind attempts to block the biological effects of cytokines is that an imbalance of proinflammatory cytokines

and anti-inflammatory cytokines may be responsible for the induction of autoimmunity.[5]

Besides inhibition of cytokine production or signaling, blockade of cell trafficking, B cell depletion and blocking of T cell activation are used as therapeutic intervention strategies. Tysabri® (natalizumab), an $\alpha_4\beta_1$ integrin blocker, acts as an inhibitor of leukocyte extravasation and was approved for the treatment of multiple sclerosis. The drug was withdrawn later due to cases of opportunistic infections in the brain, but was later reintroduced to treat relapsing forms of multiple sclerosis. Rituximab, a monoclonal antibody against CD20 antigen presented on the surface of B cells, kills B cells via complement-mediated cytotoxicity, antibody-dependent cytotoxicity and apoptosis.[5] In the United States, it has been approved for use in combination with methotrexate (MTX) for reducing symptoms in patients with rheumatoid arthritis who have had an inadequate response to one or more anti-TNF-alpha therapies.

1.2 T cell activation and costimulatory molecules

In autoimmune diseases, T cell activation is initiated by presentation of self-antigen to T cells. Antigen presenting cells (APCs) capture self antigen and load it onto major histocompatibilty complex (MHC) class II. The antigen-primed APC then presents the self antigen to T cells which express T cell receptors that recognize self antigen.T cell activation requires two signals, the interaction of TCR on T cells and antigenic peptide-MHC complex on APCs (Signal 1) and a costimulatory signal (Signal 2), to promote T cell proliferation, cytokine secretion, and effector function. [7, 8] Signal 1, which imparts specificity to the immune response, must occur through the antigen

specific receptor of T cells. Signal 2, the costimulatory signal, is composed of several receptor/ligand interactions including the binding of CD28 on T cells and B7 on professional APC, and the binding of leukocyte function associated antigen-1 (LFA-1) primarily on T cells and intercellular cell-adhesion molecule 1 (ICAM-1) primarily on APC.[9-11] Activated T cells then either transmigrate to the tissue where antigen is located (beta cells in type I diabetes or CNS in multiple sclerosis) or T cells proceed to activate B cells to secrete antibodies (myasthenia gravis or systemic lupus erythematosis). The activation of T cells in the absence of the costimulatory signal can lead to T cell anergy and interrupt the immune response. Abatacept, a CTLA4-Ig fusion protein, blocks T cell costimulation and has been approved to treat rheumatoid arthritis and is now in clinical trials for other autoimmune diseases.[12]

The costimulaltory signal is important in determining T cell activation since the TCR has low affinity for the antigen-peptide complex, has a small size hindering engagement, and is only present in small quantities.[6] In the absence of the costimulatory signal, antigen-specific T cells fail to respond effectively and become anergic or die.Several costimulatory molecules have been identified and classified in families. Among these molecules, there are both stimulatory and inhibitory signals. T cell costimulation plays an important role in the development of effective immune response including T cell proliferation, differentiation and survival (Table 1).

Table 1 Summary of costimulatory molecules

Molecule	Expression	Ligands	Expression	Ligation to its receptor	Drugs/mAb
CD28	T cells[6,8]	CD80 (B7-1) CD86 (B7-2)	Constitutively expressed on DCs and inducible on activated B cells and macrophages.[6] Constitutively expressed on monocytes, DCs and B cells and inducibly upregulated on both T cells and APCs.[6]	- Enhance T cell proliferation and cytokine production through induction of IL-2 production.[6] - Promote T cell differentiation into IL-4 producing T helper 2 cells.[6, 13] -Stimulate B cells for antibody production.[8] - Augment the kinetics and level of expression of OX40, 4-1BB and CD30.[6, 13, 14] -Inhibition of CD28/B7 reduces specific Ab production, prolongs the survival of organ transplants and inhibits autoimmune diabetes and lupus.	-Abatacept (CTLA-4-Ig) targeting CD80/86 has been approved by FDA to use in RA. It is also in Phase I clinical trials in psoriasis.[15, 16] -Belatacept (CTLA-4-Ig) has a clinical indication in renal transplantation.[17, 18] -Galiximab is a chimeric antibody targeting CD80/86. It has clinical indications in Non-Hodgkin's B cell lymphoma (NHL)[9], and psoriasis.[16] It is now in Phase III clinical trials.
PD-1	Activated T, B cells, monocytes and macrophages[20]	PD-L1 (B7-H1) PD-L2 (B7-DC)	-APC and nonhematopoietic cells[20] -Inducibly expressed on dendritic cells and macrophages[20]	-Transmit signals that inhibit T cell and B cell activation.[20]	-PD-L1 Ig fusion protein reduced clinical score in CIA mice model and prolonged graft survival in mice[20, 21] -Anti PD-1 antibody antagonists (MDX 1106, CT-011) are currently in Phase I/II clinical trials in melanoma.[22, 23]
CTLA-4 (CD152)	Activated T cells[13]	B7-1 (CD80) and B7-2 (CD86)	T, B cells, macrophages, DCs, endothelial cells, epithelial cells and fibroblasts[13]	-Transmits an inhibitory signal to T cells and inhibit T cell activation.[13] -Deplete the expression of IL-2 and IL-2R.[8] -CTLA-4 binds B7 with a much higher affinity than CD28.	-Anti CTLA-4 mAb (Ipilimumab and tremelimumab) have clinical indications in melanoma and other tumors. They have been studied in Phase II/III clinical trials.[24-27]
ICOS	Activated T cells[28]	ICOSL (B7RP-1)	Constitutively expressed as a monomer on B cell, dendritic cells, monocytes, endothelial cells, fibroblasts, epithelial cells[27]	-Enhance T cell differentiation, cytokine production and survival.[28]	Anti-ICOSL mAb antagonist has shown to reduce the severity of G6PI-induced arthritis[29], reduce lethality and symptoms in GVHD.[30] -Anti ICOS mAbprolongs cardiac and bone marrow graft survival in mice.[31, 32]
BTLA (CD272)	B cells and inducible during activation of T cells.[33, 34]	HVEM	Naïve or resting T cells, NK cells, B cells and DCs, myeloid cells.[31,32]	-Deliver the inhibitory signal of T cell activation.[32] -Decrease IL-2 production[32]	Anti-BTLA in a combination with CTLA-4-Ig has shown efficacy in allograft rejection.[35, 36]
CD40	B cells, monocytes, macrophages, DCs, platelets and inducibly expressed on non-hematopoietic cells such as epithelial cells and fibroblasts.[37]	CD40L (CD154)	Activated T cells, activated B cells and platelets.[37]	-Promote B cell activation and DC maturation.[8] - Induce memory B cells maturation.[37, 38] CD40 ligation leads to the upregulation of B7-1 and B7-2 on APCs and enhances the ability of APCs to activate naïve T cells.[37, 38]	-Dacetuzumab (anti-CD40 mAb) has clinical indications in multiple myeloma, Non-Hodgkin's lymphoma (Phase I)[39, 40], diffuse large B-cell lymphoma (Phase II)[41] and CLL (Phase I).[42] - Anti-CD40L MAb has clinical indications in allograft rejection (Phase I/II).[43, 44]

OX40 (CD134)	Activated T cells.[14]	OX40L (CD252)	Professional APCs and can be induced on activated B cells, mature DCs and macrophages.[14]	-Promote T cell proliferation, differentiation, survival, differentiation, cytokine production and effector cell function of T cells.[14] -OX40-OX40L interactions additionally modulate the differentiation and activity of regulatory T cells (both suppress and promote proliferation of these cells).[14]	-Anti OX40 and OX40L mAb agonists have shown benefits in cancer.[45-47] -Neutralizing anti OX40L ameliorated the severity of disease in EAE[48], colitis[49], arthritis[50], asthma[51], and diabetes [52] *in vivo*.
GITR	Naïve T cells and Treg. It is upregulated on effector T cell upon activation.[53]	GITRL	B cells, macrophages, DCs, endothelial cells and activated T cells.[53]	-Suppress function of Treg.[54] -Activation of effector T cells and NK cells.[54] -Induce inflammatory activation of macrophage.[53]	-Anti GITR mAb agonist induced potent antitumor immunity.[55, 56] -GITR fusion protein binding to GITRL prolonged allograft survival and showed potential anti-inflammatory properties in animal studies.[57, 58] -Neutralizing anti GITRL MAb protected the progression of diabetes.[59]
CD27	Naïve T cells, B cells, NK cells, memory and antigen-exposed T cells.[60, 61]	CD70	Activated T cells and activated APCs.[60, 61]	- Stimulate T cell activation and survival.[62] -Promote B cell activation and production of antibodies.[60]	-Anti CD70 exhibited antitumor immunity in *in vivo* studies.[63, 64] -Improved disease severity in inflammatory and autoimmune disease.[65, 66]
LIGHT (TNFSF14)	Activated T cells and immature DCs.[61, 67]	HVEM	T cells, B cells and NK cells.[61, 67]	-Promote T cell proliferation, cytokine production, and activation of NF-κB[8]	-LTβR–Ig fusion protein improved ACR scores in RA patients[68, 69] and prolonged survival of GVHD mice [70] -anti–HVEM mAb profoundly ameliorated GVHD in mice[71] -HVEM Ig fusion protein plus cyclosporine A prolonged allograft survival in mice.[72]
4-1BB (CD137)	Activated T cells and activated NK cells.[73-75]	4-1BBL	Activated DCs, B cells and macrophages.[73-75]	-Provide costimulation of T cell activation and promote T cell survival.[73-75]	-Anti 4-1BB MAb has clinical indication in cancers. It is now being studied in Phase II clinical trials.[76] -Anti 4-1BBL attenuated acute rejection in rat liver transplantation.[77]
VLA-4	T cells, B cells, monocytes, NK cells, eosinophils, neutrophils and hematopoietic cells.[75]	VCAM-1 (CD106) and fibronectin	Endothelial cells[75]	-Regulate adult hematopoiesis.[75] -Promote the adhesion of lymphocytes, monocytes, eosinophils, and basophils.[8]	-Natalizumab (anti VLA-4 antagonist) was approved by FDA for the treatment of relapsing forms of multiple sclerosis (MS)[78]
LFA-1	Leukocytes.[79]	ICAM-1 (CD54) and ICAM-2 (CD102)	Vascular endothelium, macrophages and lymphocytes.[8]	-Mediate adhesive interaction between T cell and APC in the immunological synapse and mediate leukocyte trafficking during inflammation.[79]	-Efalizumab (anti LFA-1 mAb) was approved to use in psoriasis but withdrawn due to an increased risk of progressive multifocal leukoencephalopathy (PML).[80] -Anti ICAM-1 mAb were studied in clinical trials for Crohn's disease (Alicaforsen)[81] and Ischemic stroke's disease (Enlimomab).[82] None of them were continued in post marketing phase.
Mac-1	Leukocytes [79]	ICAM1 (CD54)	Vascular endothelium, macrophages, and lymphocytes.[8]	-Mediate leukocyte trafficking during inflammation and contributes to leukocyte activation in immune responses.[79]	-Anti-Mac-1 showed no effect in graft survival.[83]

1.2.1 Costimulatory molecules of the immunoglobulin superfamily

CD28-B7 costimulatory pathway

The interaction of CD28 on T cells and B7 family on APC provides a crucial positive costimulatory signal for T cell activation. CD28 is a disulfide linked homodimeric transmembrane member of Immunoglobulin superfamily constitutively expressed on CD4+ T cells and CD8+ T cells. The ligands for CD28 are B7-1 (CD80) and B7-2 (CD86). They are constitutively expressed on DCs and induced on activated macrophages and activated B cells. Binding of CD28 and their ligands promotes proliferation of activated T cells and differentiation of T cells into T helper cells and enhances the production of antibodies by B cells.[8, 84]

CTLA-4-B7 costimulatory pathway

CTLA-4 (CD152) is structurally homologous to CD28. CTLA-4 is expressed on T cell membrane and binds to the same two ligands as CD28 (B7-1 and B7-2) with higher affinity. CTLA-4 is upregulated and activated after binding of CD28 and B7 ligands and T cell activation and undetectable on resting T cells, whereas CD28 is expressed on both resting and activated cells.[2, 17]CTLA-4 has similar structure as CD28, but their functions are different. CD28-B7 interaction delivers a positive costimulatory signal to T cells, whereas CTLA-4-B7 interaction delivers an inhibitory signal to T cells resulting in the attenuation of T cell activation and proliferation. Due to the higher binding affinity to B7, the upregulated CTLA-4 competes for the B7-1 or B7-2 ligands to turn off T cell activation and hence regulating the lymphocyte homeostasis.[84]

Therapeutics targeting CD28-mediated costimulation

Abatacept (CTLA-4-Ig) is a fusion protein composed of the extracellular binding domain of CTLA-4 fused to an Fc domain of human IgG. It was developed to block the binding of CD28 to B7.[84] Abatacept was approved for the treatment of moderate to severe rheumatoid arthritis (RA) in the case of inadequate response to anti-TNFα therapy.[84, 85] A recent report, however, has shown that RA patients respond poorly to abatacept.[86] Furthermore, abatacept was shown to lack efficacy in organ transplantation in non-human primates, which was suggested to be due to the lower avidity of abatacept to CD86 compared to CD80.[8] For this reason, belatacept was developed. Belatacept is a second-generation CTLA-4-Ig, differing from abatacept only by 2 amino acids leading to a superior binding to CD80 (2 fold) and CD86 (4 fold) compared to abatacept.[87] Belatacept provided more potent immunosuppressive properties required for transplantation.[17] Belatacept is intended to provide extended graft survival and is under currently continuing through clinical trials.

PD-1-PD-L Costimulatory pathway

Programmed death-1 (PD-1 or CD279) is an inhibitory costimulatory molecule.[88] It is a member of the immunoglobulin superfamily expressed on activated T cells, B cells, monocytes, and macrophages.[89] PD-1 binds PD-L1 (B7-H1) and PD-L2 (B7-DC). PD-L1 is expressed on B cells, DCs, and T cells including Treg. PD-L2 expression is limited to DCs and macrophages. Ligation of PD-1 on lymphocytes delivers a negative costimulatory signal to T cells and plays a critical role in the regulation of peripheral tolerance.[90-93] Engagement of PD-1 by its ligands PDL-1 or PDL-2 blocks TCR signaling and transduces a signal that inhibits T and B cell proliferation, cytokine production and cytotoxicity of CD8+ T cells.[89, 93]

Therapeutic targeting of PD-1-PDL interactions

An *in vitro* study has shown that PD-L1 Ig stimulated PD-1, thus inhibiting CD4+ and CD8+ T cell proliferation.[8] PD-L1 Ig has been shown to ameliorate collagen-induced arthritis (CIA) in the CIA mouse model as evaluated by clinical score and histology and reduce the production of inflammatory cytokines. These results suggested a beneficial effect of PD L1 Ig in this arthritis model via anti-inflammatory actions and inhibition of cell proliferation.[20] PD-L1 Ig prolonged corneal allograft survival in mice by augmented ligation of the PD-1 negative costimulatory molecule.[21]

ICOS-ICOSL costimulatory pathway

Inducible costimulator (ICOS) is also a member of the immunoglobulin superfamily of costimulatory molecules. ICOS is induced after TCR engagement upon T cell activation. ICOSL (B7H) is constitutively expressed on DCs, monocytes, macrophages, B cells, endothelial cells, fibroblasts, and renal epithelial cells.[28] ICOS has similar sequence with CD28 and CTLA-4. Unlike other costimulatory molecules such as CTLA-4, ICOS can be upregulated in the absence of CD28-B7 interaction.[6] ICOS promotes T cell differentiation and cytokine production.[8, 94] ICOS can stimulate both Th1 and Th2 effector cytokine production, especially IL-4 and IL-10.[8, 94] Since ICOS signaling does not sustain IL-2 production, it does not stimulate T cell clonal expansion.[95, 96]

Therapeutic targeting of ICOS-ICOSL interactions

The ICOS-ICOSL costimulatory pathway is crucial for T cell activation, differentiation and effector function. Anti-ICOS mAb treatment resulted in significant

inhibition of graft versus host disease (GVHD) and reduced the number of Ag-specific T cells that reject the bone marrow graft.[32] The blockade of ICOS-ICOSL was effective in prolonging cardiac and liver allograft survival.[8] ICOS blockade also prevented development of spontaneous disease in pre-diabetic NOD mice.[97] Transient blockade of ICOS/ICOSL interactions profoundly reduced the severity of glucose-6 phosphate isomerase (G6PI) induced arthritis.[29] These observations suggested that ICOS costimulation may be a beneficial therapeutic target for allograft transplantation and autoimmune diseases.[94]

BTLA-HVEM costimulatory pathway

B and T lymphocyte attenuator (BTLA or CD272) is an immunoglobulin-like molecule belonging to the immunoglobulin superfamily. BTLA is not expressed by naive T cells, but it is induced during activation and remains expressed on T_H1 but not on T_H2 cells.[34] It is also constitutively and highly expressed on B cells. BTLA was identified as an inhibitory receptor with structural and functional similarities to CTLA-4 and PD-1.[98] The engagement of BTLA and herpes virus entry mediator (HVEM), which is a member of the TNF receptor (TNFR) superfamily delivers an inhibitory signal. BTLA interaction with HVEM impairs T cell activation resulting in decreased T cell proliferation and cytokine production.

Therapeutic targeting of BTLA-HVEM interactions

Blockade of BTLA-HVEM costimulation has been suggested that anti-BTLA mAb in a combination with CTLA-4-Ig can prolong cardiac allograft survival.[35] In a different study, combination therapy between anti-BTLA mAb and CTLA-4-Ig induced donor-specific tolerance in murine islet allograft.[36]

1.2.2 Costimulatory molecules of the TNF-TNFR family

CD40-CD40L costimulatory pathway

CD40 is constitutively expressed on B cells, dendritic cells, monocytes, platelets, and macrophages, and can be inducibly expressed on non-hematopoietic cells such as endothelial cells and fibroblasts in the presence of inflammation.[37] Ligation of CD40 and its subsequent signaling leads to activation of B cells, as well as activation and maturation of dendritic cells, priming of helper and cytotoxic T cells, and propagation of a variety of inflammatory reactions.[38] The ligand for CD40 (CD40L or CD154), a member of the TNF family, is expressed on activated T cells, after stimulation by TCR-antigenic peptide/MHC complex engagement and signaling from CD28-B7 interaction.[8] Blockade of the CD40-CD40L pathway alone or together with the CD28-B7 pathway can lead to long-term allograft survival in animal transplantation models and can inhibit development of autoimmune diseases.[38]

Therapeutic targeting of CD40-CD40L interactions

Blocking the CD40-CD40L costimulatory pathway was examined by using anti-CD40L mAb, which has shown promise in both rodent and non-human primate models.[99] Anti-CD40L mAb can prevent acute allograft rejection and promote allograft and xeno-graft survivals in rodents and non-human primates.[8] Although treatment with anti-CD40L mAb promoted long term allograft survival in experimental transplantation, clinical trials in autoimmune diseases and transplantation were halted due to unanticipated thromboembolic complications. This complication may be explained by the high expression of CD40L on platelets; however, observed stabilization of arterial thrombi were thought not to involve CD40

molecules.[99] An anti-CD40 mAb has also been developed and was shown to block binding of CD154 and to inhibit CD154-induced B cell proliferation *in vitro*. Anti-CD40 mAbs promoted moderate prolongation of graft survival when used alone. When combined with belatacept, anti-CD40 mAbs synergized the effect in prolonging graft survival in non human primate models of renal and islet transplantation.[99]

OX40-OX40L costimulatory pathway

OX40 (CD134) is predominantly expressed on activated T cells, but not naïve CD4+, CD8+ T cells, and memory T cells.[14] Following activation, OX40L is induced on activated B cells and mature dendritic cells, endothelial cells and T cells. It is not expressed on resting APC. Expression of OX40 is delayed and decreased in the absence of CD28. OX40-positive T cells are found at the site of inflammation in experimental allergic encephalomyelitis (EAE), graft-vs-host disease (GVHD) and rheumatoid arthritis (RA).[100] Targeting the OX40-OX40L interaction with anti-OX40L mAb can delay disease progression in EAE, colitis, arthritis, asthma and diabetes.[48-52]

GITR-GITRL costimulatory pathway

Glucocorticoid-induced TNFR-related gene (GITR or TNFRSF18) is a transmembrane protein of the TNFR superfamily. GITR is preferentially expressed by Treg and is also upregulated in conventional effector T cells upon activation.[57] GITR ligand (GITRL) is mainly expressed on B cells, macrophages, dendritic cells, endothelial cells, and activated T cells but not on resting T cells.[53, 57] Binding of GITRL to its receptor is involved in the development of autoimmune or inflammatory

responses due to costimulation of effector T cells, inhibition of Treg cells, and activation of macrophages.[54]GITR fusion protein binding to GITRL prolonged allograft survival and showed potential anti-inflammatory properties in animal studies.[57, 58] Neutralizing anti GITRL MAb protected the progression of diabetes.[59]

1.2.3 Costimulatory molecules of the integrin family

Leukocyte function associated antigen-1 (LFA-1) and Intercellular adhesion molecule-1 (ICAM-1) belong to the integrin family and immonuglobulin superfamily, respectively. They are critical costimulatory molecules since they mediate strong interaction and enhance T cell activation signaling.[101] Binding of LFA-1 and ICAM-1 stabilizes the interaction of TCR and MHC-peptide complex in immunological synapse.

Therapeutic targeting for ICAM-1/LFA-1 mediated signaling

The effect of anti-ICAM-1 mAb on preventing rejection was reported in a rat transplantation model.[102] Intravenous administration of anti ICAM-1mAb alone could not prevent acute lung allograft rejection; however, combination with cyclosporine significantly reduced infiltration of leukocytes into the allograft.[102] Anti ICAM-1 mAb were studied in clinical trials for Crohn's disease (Alicaforsen) and Ischemic stroke's disease (Enlimomab). [81, 82] None of them were continued in post marketing phase.

Anti-LFA-1 mAb (efalizumab) has been shown to be effective in reducing the severity of chronic psoriasis without lymphocyte depletion and prevented rejection in kidney transplantation. Recently, efalizumab was withdrawn from clinical use due to

concerns about the development of progressive multifocal myeloencephalopathy (PML) in several patients receiving the drug as treatment for psoriasis.[103] In other studies, Posselt et al. described a novel immunosuppressive regimen using efalizumab which permitted long-term islet allograft survival while reducing the need for corticosteroids and calcineurin inhibitors (CNI).[104]

1.3 Immunological synapse (IS)

Immunological synapse is a specialized junction between cells, within which a variety of receptors and adhesion molecules engage their ligands on the apposed cell surface.[105] One such junction occurs between T cells and APCs and includes the specific binding of antigenic peptide-MHC class II and TCR recognizing this particular antigen surrounded by a ring of LFA-1 and ICAM-1, among other receptor/ligand pairs.[105] T cell activation requires sustained conjugate formation between T cells and APCs because the number of peptide-MHC complexes can be very low, in the range of 10 to 100 per APC, and because the interaction between the TCR and its ligand has low affinity.[106-108] In the immunological synapse, the ligands and their receptors are arranged in an orderly manner to enhance binding specificity and to prolong the duration of signaling.[109] Reports suggest that, T cell activation requires more than 1 hr which is mediated by the longevity of stabilized IS.[109] The activation signals are sustained by localization of TCR and MHC complexes to the center of the IS.[107, 109] Pairs of costimulatory receptors and their ligands also accumulate at the center of the IS while clusters of LFA-1 and ICAM-1 among others are localized to the peripheral ring of the IS.[110]

The surface proteins located within the immunological synapse on T cells include T cell receptors, costimulatory molecules CD2, CD28, CD40L, LFA-1, VLA-4, ICAM-1, ICAM-3, and various cytokine and chemokine receptors.[111] The immunological synapse on APCs contains surface proteins including CD80, CD86, CD40, ICAM-1, ICAM-3 and other surface and cytoplasmic proteins.[112] The structure of the mature IS was described as a 'bull's eye' arrangement with three distinct regions.[110] The central region of the IS, called the central supramolecular activation cluster (cSMAC), contains TCR complexes interacting with peptide-MHC complexes as well as interactions of costimulatory molecules such as CD4, CD2, CD28 and CD40.[109-111, 113] The intermediate ring of the bull's eye, called the peripheral supramolecular activation cluster (pSMAC), contains complexes of integrin LFA-1 binding to ICAM-1 and the cytoskeletal protein talin, among others.[113] The outermost region is the distal supramolecular activation cluster (dSMAC), containing CD45 and CD43.[110]

After T cell and APC contact, the binding of TCR to peptide-MHC complexes leads to the formation of small TCR microclusters containing about 100 TCR/ MHC each, distributed in the periphery of the T cell-APC interface (dSMAC).[114, 115] The increased density of TCR and MHC by forming microclusters facilitates the engagement of this low affinity pair. The segregated microclusters of LFA are also formed in d-SMAC.[116] TCR and LFA-1 microclusters then translocate to pSMAC. After T cells begin to contract, TCR microclusters migrate towards the center region of the contact area (cSMAC), while integrin microclusters accumulate in a surrounding area (pSMAC).[106, 116-118] At the center, TCR microclusters assemble to

form larger clusters and a stable cSMAC to sustain the activation signal.[119] Similarly, MHC and ICAM-1 microclusters are also formed at the contact interface on the APC. cSMAC is surrounded by peripheral SMAC (pSMAC) containing adhesion molecules such as LFA-1 and ICAM-1. ICAM-1 on APCs forms oligomers that bind to LFA-1 clusters on T cells.[111, 120] The interactions of integrins and their ligands enable the formation of tight and prolonged contacts between T cells and APCs. The stable IS cannot be formed in the absence of integrins.[111]

In addition to the formation of TCR clusters, clustering of costimulatory molecules and their ligands is also required for T cell activation to occur. The costimulatory molecules CD28 and CTLA-4 have been reported to accumulate in the cSMAC.[107] The accumulation of CD28-B7 enhanced T cell response by modifying T cell signaling and stabilize the arrangement of immunological synapse.[110] Other costimulatory receptor-ligand pairs, including PD-1-PD-L1/PD-L2, ICOS-ICOSL and CD40-CD40L were reported to localize and function in the cSMAC.[110] CD28 and CTLA-4 are expressed as homodimers on the T cell surface with monovalent and bivalent binding capacities, respectively. B7-1 is also present on the surface as a homodimer, while B7-2 is monomeric.[114] A homodimeric CTLA-4 molecule can bind two B7-1 molecules at low concentration of CTLA-4. At high concentration, CTLA-4 can form an linear array of B7-1-CTLA-4 multimers containing 7-18 receptor-ligand pairs.[121] At low concentration, one CD28 molecule can bind two molecules of B7-1. At high concentration, two molecules of CD28 can bind a dimer of B7-1 without forming a multimeric array.[121] As a result of multimerization, CTLA-4 has 10-100 fold higher binding avidity for B7 ligands than CD28.[114]

1.4 The importance of mutivalency of LFA-1 and ICAM-1

LFA-1 mediates multiple events in the immune system, such as leukocyte trafficking, transmigration, and formation of the IS. Binding of LFA-1 to ICAM-1 is needed for the initiation and stabilization of T cell-APC conjugation. Avidity is the overall strength of cellular adhesive interactions resulting from the combination of both the affinity of individual receptor-ligand bonds and the total number of bonds formed (i.e., the valency of the interaction).[122] The affinity of integrin is regulated by the alteration of integrin conformation, whereas valency regulation is mediated by changes in cell surface receptor diffusivity or density that alter the number of adhesive bonds that can form.[123] The ligands of LFA-1 are members of the immunoglobulin superfamily known as intercellular adhesion molecules (ICAMs) expressed on APCs, endothelial cells and epithelial cells, and are inducible by inflammatory cytokines.

LFA-1 on resting leukocytes circulating in the blood is normally inactive (i.e. a non-ligand-binding conformation). The conformational change of LFA-1 from low to high affinity state can be activated by several factors including the binding of other receptors on leukocytes, such as chemokine receptors, antigen-specific TCRs or B-cell receptors (BCRs).[124] The high affinity state of LFA-1 induces its ability to bind ICAMs. There are three different LFA-1 conformations that occur at different stages of activation.[124] The low affinity conformation of LFA-1 is a bent form where the LFA-1 I domain is bent and close to cell membrane, whereas the extended form with a closed binding domain has an intermediate affinity, and the extended form in which the ligand-binding I-domain of is opened to bind domain 1 of ICAM-1 with the

highest affinity.[79, 125] Microclusters of LFA-1 on T cells are formed after initial multivalent binding of LFA-1 to ICAM-1.[67] The interaction of intermediate affinity LFA-1 with ICAM-1 induces the high affinity conformation that stabilizes adhesion. Change in affinity is not the only means to regulate the binding of LFA-1. The dynamic adhesion of LFA-1 is also controlled by its avidity resulting from clustering, which is driven by outside-in signals from activated LFA-1 itself.[124]

ICAM-1 is the primary ligand of LFA-1, expressed on both T cells and APCs. ICAM-1 on APC may act as a costimulatory receptor and receives signal that facilitates immune response .[120] ICAM-1 is composed of five immunoglobulin-like domains. Oligomerization and clustering of ICAM-1 increase its ligand binding avidity by allowing the rebinding of receptors and ligands after dissociation, since monomeric adhesion molecules tend to have fast dissociation rates.[120] The crystal structure analysis of ICAM-1 reveals that this molecule organizes into non-covalently linked homodimer via D4-D4 interaction on the cell surface, and two homodimers bind each other by using D1, resulting in W shaped tetramers.[120] These tetramers can form linear arrays zigzagging between the T cell and APC.[120] This linear structure can bend and close to form a peripheral ring in IS facilitating the adhesion between APC and T cells.[120] The adhesion ring can be composed of thousands of circular LFA-1/ICAM-1 pairs and has a diameter of several microns.[120]

1.5 Strategies and rational design of multivalent, targeted drug delivery system

Targeted drug delivery is a strategy to preferentially increase the concentration of drug in the diseased cells relative to normal cells.[126] This strategy results in an increased therapeutic efficacy and reduced side effects and toxicity of the targeted

drug.[126] Targeted drug delivery often uses specific types of membrane-bound protein including surface antigens or cell surface receptors as a target. Tools for targeting specific cellular populations have been widely explored by using various targeting ligands including antibodies, aptamers, peptides, and small molecules.[127-130]

High affinity binding and selectivity are important properties of targeted drug delivery systems.[100, 131, 132] The ideal targeted delivery system should have a low affinity for its targeted receptor expressed in normal cells but high affinity to receptors on diseased or activated cells.[100] However, high affinity delivery systems can have low specificity if the target receptors are expressed in both diseased and healthy cells.[100] One active targeting method for cancer treatment focuses on transferrin and folate receptors that are upregulated in cancer cells. Ligands targeting transferrin receptor increased uptake of targeted nanoparticles by cancer cells; however, since these receptors are expressed to some degree on many types of normal cells, side effects may occur. An example of a more selective targeting strategy is the use of antibodies to target prostate-specific membrane antigen (PSMA) exclusively expressed on prostate cancer cells. Anti-PSMA conjugated dendrimers were found to bind preferentially to prostate adenocarcinoma, whereas the untargeted dendrimer did not. Furthermore, the targeted dendrimer did not bind to cells which do not express PSMA.[126]

The specificity of targeting can also be improved if there are more ligands bound to target cells than to untargeted cells. The low affinity of ligand reduces specific binding in monovalent form but binding of ligand can be increased through multivalent presentation (higher avidity). Multivalent ligands consist of multiple

monomeric ligands attached to a single backbone carrier such as quantum dots, polymers, microparticles or nanoparticles, creating an array that can bind to multiple receptors simultaneously. Due to the multiple, simultaneous binding events, multimeric ligands often exhibit stronger binding compared to their corresponding monomers.[133] Several investigators have designed delivery systems with multiple ligands to achieve more effective targeting through multivalent interaction.[133] Studies have shown the enhanced binding avidities of biological multivalent inhibitors on the order of 1 to 9 orders of magnitude.[131] However, the specificity of targeting can be achieved when ligands have low binding affinity For some ligands such as antibodies having high binding affinities, using multivalent interaction of multiple antibodies to increase binding specificity would be possible at much lower concentrations.[134]

Many proteins that participate in multivalent interactions (e.g. cell adhesion) are oligomeric. One of the most studied members of this type of surface proteins is LFA-1 and ICAM-1. LFA-1 and ICAM-1 possess characteristics which can serve as a target for multivalent targeted drug delivery systems. First, LFA-1 and ICAM-1 on resting leukocytes, APC, endothelial and epithelial cells are normally inactive (i.e. a non-ligand binding conformation).Once triggered (e.g. by binding of TCR to MHC class II complex), molecules like LFA-1 change conformation to enhance binding to ICAM-1.[120] Second, LFA-1 and ICAM-1 are upregulated on activated T cells and on endothelial cells in inflammatory diseases or autoimmune diseases. Third, both LFA-1 and ICAM-1 ligand bindings are controlled by their avidities resulting from clustering.[120, 124]Cell adhesion mediated by ICAM-1 and LFA-1 involves multivalent interaction between these two molecules on opposing cells (APC and T cell).

In order to design a system that could specifically target the multivalent state of LFA-1 and ICAM-1 on activated T cells and APC populations, multiple copies of their ligands were conjugated to NPs to facilitate receptor binding through multivalent presentation. LFA-1 and ICAM-1 exhibit clustering during activation, which should promote the proper geometry for multivalent interaction of receptors with their ligands presented on NPs. Thus, this targeting strategy should yield a benefit when targeting receptor clusters.

Besides increasing therapeutic efficacy and reducing side effects, internalization of targeted drug delivery system can also be critical. LFA-1 and ICAM-1 targeting offers the possibility of improved inhibition since receptor internalization is triggered by the multivalent engagement of ligands.[135] The conjugation of LFA-1 and ICAM-1 ligands on NPs is, therefore, hypothesized to preferentially target specific immune cell populations, increase the binding avidity of these ligands to receptors, inhibit receptor signaling by blocking binding and reduce the number of surface receptors by facilitating the internalization of these receptors via endocytosis.

The use of targeted nanoparticles (NPs) in drug delivery is expected to increase specificity of the encapsulated drugs and thus reduce side effects and decrease the dose of administration. In addition, encapsulation of drugs in NPs may increase the bioavailability of drug, offer sustained release, andprotect against degradation. Encapsulation of drug into NPs can also alter pharmacokinetics of the drug, while maintaining its pharmacological action.

In this thesis work, PLGA NPs targeting ICAM-1 (cLABL-NPs) were loaded with the anticancer drug, doxorubicin. Binding specificity to lung carcinoma epithelial cells was confirmed. Drug release and microscopy studies indicated that the cLABL-NPs sustained drug release and confirmed the localization of drug to the target site (chapter 2). In chapter 3, an LFA-1 targeting peptide was conjugated to PLGA NPs to target T cells (cIBR-NPs). The results revealed that the binding of cIBR-NPs was specific to LFA-1 compared to untargeted NPs and binding was dependent on the surface ligand concentration. The internalization of cIBR-NPs was suggested by the reduced uptake of NPs at low temperature. In addition, cIBR-NPs were able to block the binding of T cells to lung epithelial cells. In chapter 4, cIBR-NPs and LABL-NPs were found to shift immune cell responses when compared to monomeric ligands (free cIBR and LABL peptides). Finally, in chapter 5, the performance of hyaluronic acid as a multivalent nanomaterial for targeting DC and inhibiting T cell proliferation and proinflammatory cytokine expression (TNF-α and IL-17) were reported.

References

1. Wraith DC (2009) *Therapeutic peptide vaccines for treatment of autoimmune diseases* , 134-136.
2. Kindt TJ, Goldsby RA, Osborne BA, & Kuby J (2007) *Kuby immunology* (W.H. Freeman, New York) 6th Ed pp 402.
3. Wraith DC, Goldman M, & Lambert PH (2003) Vaccination and autoimmune disease: what is the evidence? *Lancet* 362, 1659-1666.
4. Larche M & Wraith DC (2005) Peptide-based therapeutic vaccines for allergic and autoimmune diseases. *Nat Med* 11, S69-76.
5. Balague C, Kunkel SL, & Godessart N (2009) Understanding autoimmune disease: new targets for drug discovery. *Drug Discov Today* 14, 926-934.
6. Stuart RW & Racke MK (2002) Targeting T cell costimulation in autoimmune disease. *Expert Opin Ther Targets* 6, 275-289.
7. Bucks CM & Katsikis PD (2009) New insights into classical costimulation of CD8+ T cell responses. *Adv Exp Med Biol* 633, 91-111.
8. Ma A, Zhang L, Wang X, & Chen H (2009) New look at therapeutic strategies for blocking costimulatory signal in experimental and pre-clinical transplantation. *Curr Drug Saf* 4, 155-166.
9. Jois SD & Teruna TJ (2003) A peptide derived from LFA-1 protein that modulates T-cell adhesion binds to soluble ICAM-1 protein. *J Biomol Struct Dyn* 20, 635-644.

10. Anderson ME & Siahaan TJ (2003) Targeting ICAM-1/LFA-1 interaction for controlling autoimmune diseases: designing peptide and small molecule inhibitors. *Peptides* 24, 487-501.

11. Murray JS, Fois SD, Schountz T, Ford SR, Tawde MD, Brown JC & Siahaan TJ (2002) Modeling alternative binding registers of a minimal immunogenic peptide on two class II major histocompatibility complex (MHC II) molecules predicts polarized T-cell receptor (TCR) contact positions. *J Pept Res* 59, 115-122.

12. Perry JJ, Fleming RA, Rocco MV, Petros WP, Bleyer AJ, Radford JE Jr, Powell BL & Hurd DD (1999) Administration and pharmacokinetics of high-dose cyclophosphamide with hemodialysis support for allogeneic bone marrow transplantation in acute leukemia and end-stage renal disease. *Bone Marrow Transplant* 23, 839-842.

13. Alegre ML, Frauwirth KA, & Thompson CB (2001) T-cell regulation by CD28 and CTLA-4. *Nat Rev Immunol* 1, 220-228.

14. Croft M (2010) Control of immunity by the TNFR-related molecule OX40 (CD134). *Annu Rev Immunol* 28, 57-78.

15. Gottlieb AB, Kang S, Linden KG, Lebwohl M, Menter A, Abdulghani AA, Goldfarb M, Chieffo N & Totoritis MC (2004) Evaluation of safety and clinical activity of multiple doses of the anti-CD80 monoclonal antibody, galiximab, in patients with moderate to severe plaque psoriasis. *Clin Immunol* 111, 28-37.

16. Gottlieb AB, Lebwohl M, Totoritis MC, Abdulghani AA, Shuey SR, Romano P, Chaudhari U, Allen RS & Lizambri RG (2002) Clinical and histologic response to single-dose treatment of moderate to severe psoriasis with an anti-CD80 monoclonal antibody. *J Am Acad Dermatol* 47, 692-700.

17. Rangel EB (2010) Belatacept in clinical and experimental transplantation - progress and promise. *Drugs Today (Barc)* 46, 235-242.

18. Rostaing L, Massari P, Garcia VD, Mancilla-Urrea E, Nainan G, Rial MD, Steinberg S, Vincenti F, Shi R, Di Russo G, Thomas D & Grinyó J. (2010) Switching from Calcineurin Inhibitor-based Regimens to a Belatacept-based Regimen in Renal Transplant Recipients: A Randomized Phase II Study. *Clin J Am Soc Nephrol*. (e-published)

19. Leonard JP, Friedberg JW, Younes A, Fisher D, Gordon LI, Moore J, Czuczman M, Miller T, Stiff P, Cheson BD, Forero-Torres A, Chieffo N, McKinney B, Finucane D & Molina A (2007) A phase I/II study of galiximab (an anti-CD80 monoclonal antibody) in combination with rituximab for relapsed or refractory, follicular lymphoma. *Ann Oncol* 18, 1216-1223.

20. Wang G, Hu P, Yang J, Shen G, & Wu X (2009) The effects of PDL-Ig on collagen-induced arthritis. *Rheumatol Int*. (e-published)

21. Watson MP, George AJ, & Larkin DF (2006) Differential effects of costimulatory pathway modulation on corneal allograft survival. *Invest Ophthalmol Vis Sci* 47, 3417-3422.

22. Brahmer JR, Drake CG, Wollner I, Powderly JD, Picus J, Sharfman WH, Stankevich E, Pons A, Salay TM, McMiller TL, Gilson MM, Wang C, Selby M, Taube JM, Anders R, Chen L, Korman AJ,Pardoll DM, Lowy I & Topalian SL (2010) Phase I study of single-agent anti-programmed death-1 (MDX-1106) in refractory solid tumors: safety, clinical activity, pharmacodynamics, and immunologic correlates. *J Clin Oncol* 28, 3167-3175.

23. Benson DM Jr, Bakan CE, Mishra A, Hofmeister CC, Efebera Y, Becknell B, Baiocchi RA, Zhang J, Yu J, Smith MK, Greenfield CN, Porcu P, Devine SM, Rotem-Yehudar R, Lozanski G, Byrd JC & Caligiuri MA (2010) The PD-1/PD-L1 axis modulates the natural killer cell versus multiple myeloma effect: a therapeutic target for CT-011, a novel monoclonal anti-PD-1 antibody. *Blood* 116, 2286-2294.

24. Kaehler KC, Piel S, Livingstone E, Schilling B, Hauschild A & Schadendorf D (2010) Update on Immunologic Therapy With Anti-CTLA-4 Antibodies in Melanoma: Identification of Clinical and Biological Response Patterns, Immune-Related Adverse Events, and Their Management. *Semin Oncol* 37, 485-498.

25. O'Day SJ, Maio M, Chiarion-Sileni V, Gajewski TF, Pehamberger H, Bondarenko IN, Queirolo P, Lundgren L, Mikhailov S, Roman L, Verschraegen C, Humphrey R, Ibrahim R, de Pril V, Hoos A & Wolchok JD. (2010) Efficacy and safety of ipilimumab monotherapy in patients with pretreated advanced melanoma: a multicenter single-arm phase II study. *Ann Oncol* 21, 1712-1717.

26. Wolchok JD, Neyns B, Linette G, Negrier S, Lutzky J, Thomas L, Waterfield W, Schadendorf D, Smylie M, Guthrie T Jr, Grob JJ, Chesney J, Chin K, Chen K, Hoos A, O'Day SJ & Lebbé C. (2010) Ipilimumab monotherapy in patients with pretreated advanced melanoma: a randomised, double-blind, multicentre, phase 2, dose-ranging study. *Lancet Oncol* 11, 155-164.

27. Kirkwood JM, Lorigan P, Hersey P, Hauschild A, Robert C, McDermott D, Marshall MA, Gomez-Navarro J, Liang JQ & Bulanhagui CA. (2010) Phase II trial of tremelimumab (CP-675,206) in patients with advanced refractory or relapsed melanoma. *Clin Cancer Res* 16, 1042-1048.

28. Yong PF, Salzer U, & Grimbacher B (2009) The role of costimulation in antibody deficiencies: ICOS and common variable immunodeficiency. *Immunol Rev* 229, 101-113.

29. Frey O, Meisel J, Hutloff A, Bonhagen K, Bruns L, Kroczek RA, Morawietz L & Kamradt T (2010) Inducible costimulator (ICOS) blockade inhibits accumulation of polyfunctional T helper 1/T helper 17 cells and mitigates autoimmune arthritis. *Ann Rheum Dis* 69, 1495-1501.

30. Fujimura J, Takeda K, Kaduka Y, Saito M, Akiba H, Yagita H, Yamashiro Y, Shimizu T & Okumura K. (2010) Contribution of B7RP-1/ICOS co-stimulation to lethal acute GVHD. *Pediatr Transplant* 14, 540-548.

31. Zhang QW, Rabant M, Schenk A, & Valujskikh A (2008) ICOS-Dependent and -independent functions of memory CD4 T cells in allograft rejection. *Am J Transplant* 8, 497-506.

32. Taylor PA, Panoskaltsis-Mortari A, Freeman GJ, Sharpe AH, Noelle RJ, Rudensky AY, Mak TW, Serody JS & Blazar BR. (2005) Targeting of inducible costimulator (ICOS) expressed on alloreactive T cells down-regulates graft-versus-host disease (GVHD) and facilitates engraftment of allogeneic bone marrow (BM). *Blood* 105, 3372-3380.

33. Murphy KM, Nelson CA, & Sedy JR (2006) Balancing co-stimulation and inhibition with BTLA and HVEM. *Nat Rev Immunol* 6, 671-681.

34. Watanabe N, Gavrieli M, Sedy JR, Yang J, Fallarino F, Loftin SK, Hurchla MA, Zimmerman N, Sim J, Zang X, Murphy TL, Russell JH & Allison JP, Murphy KM. (2003) BTLA is a lymphocyte inhibitory receptor with similarities to CTLA-4 and PD-1. *Nat Immunol* 4, 670-679.

35. Truong W, Plester JC, Hancock WW, Kaye J, Merani S, Murphy KM, Murphy TL, Anderson CC & Shapiro AM (2007) Negative and positive co-signaling with anti-BTLA (PJ196) and CTLA4Ig prolongs islet allograft survival. *Transplantation* 84, 1368-1372.

36. Truong W, Plester JC, Hancock WW, Merani S, Murphy TL, Murphy KM, Kaye J, Anderson CC & Shapiro AM (2007) Combined coinhibitory and costimulatory modulation with anti-BTLA and CTLA4Ig facilitates tolerance in murine islet allografts. *Am J Transplant* 7, 2663-2674.

37. Elgueta R, Benson MJ, de Vries VC, Wasiuk A, Guo Y & Noelle RJ (2009) Molecular mechanism and function of CD40/CD40L engagement in the immune system. *Immunol Rev* 229, 152-172.

38. Law CL & Grewal IS (2009) Therapeutic interventions targeting CD40L (CD154) and CD40: the opportunities and challenges. *Adv Exp Med Biol* 647, 8-36.

39. Hussein M, Berenson JR, Niesvizky R, Munshi N, Matous J, Sobecks R, Harrop K, Drachman JG & Whiting N (2010) A phase I multidose study of dacetuzumab (SGN-40; humanized anti-CD40 monoclonal antibody) in patients with multiple myeloma. *Haematologica* 95, 845-848.

40. Advani R, Forero-Torres A, Furman RR, Rosenblatt JD, Younes A, Ren H, Harrop K, Whiting N & Drachman JG (2009) Phase I study of the humanized anti-CD40 monoclonal antibody dacetuzumab in refractory or recurrent non-Hodgkin's lymphoma. *J Clin Oncol* 27, 4371-4377.

41. Khubchandani S, Czuczman MS, & Hernandez-Ilizaliturri FJ (2009) Dacetuzumab, a humanized mAb against CD40 for the treatment of hematological malignancies. *Curr Opin Investig Drugs* 10, 579-587.

42. Furman RR, Forero-Torres A, Shustov A, & Drachman JG (2010) A phase I study of dacetuzumab (SGN-40, a humanized anti-CD40 monoclonal antibody) in patients with chronic lymphocytic leukemia. *Leuk Lymphoma* 5, 228-235.

43. Jiang XF, Zhu L, Cui ZM, Guo DW, Sun WY, Lin L, Tang YF, Wang XF & Liang J (2010) Transplant long-surviving induced by CD40-CD40 ligand costimulation blockade is dependent on IFN-gamma through its effect on CD4(+)CD25(+) regulatory T cells. *Transpl Immunol*. (e-published)

44. Aoyagi T, Yamashita K, Suzuki T, Uno M, Goto R, Taniguchi M, Shimamura T, Takahashi N, Miura T, Okimura K, Itoh T, Shimizu A, Furukawa H & Todo S (2009) A human anti-CD40 monoclonal antibody, 4D11, for kidney transplantation in cynomolgus monkeys: induction and maintenance therapy. *Am J Transplant* 9, 1732-1741.

45. Redmond WL, Gough MJ, Charbonneau B, Ratliff TL, & Weinberg AD (2007) Defects in the acquisition of CD8 T cell effector function after priming with tumor or soluble antigen can be overcome by the addition of an OX40 agonist. *J Immunol* 179, 7244-7253.

46. Weinberg AD (2010) The role of OX40 (CD134) in T-cell memory generation. *Adv Exp Med Biol* 684, 57-68.

47. Sadun RE, Hsu WE, Zhang N, Nien YC, Bergfeld SA, Sabzevari H, Lutsiak ME, Khawli L, Hu P & Epstein AL (2008) Fc-mOX40L fusion protein produces complete remission and enhanced survival in 2 murine tumor models. *J Immunother* 31, 235-245.

48. Nohara C, Akiba H, Nakajima A, Inoue A, Koh CS, Ohshima H, Yagita H, Mizuno Y & Okumura K (2001) Amelioration of experimental autoimmune encephalomyelitis with anti-OX40 ligand monoclonal antibody: a critical role for OX40 ligand in migration, but not development, of pathogenic T cells. *J Immunol* 166, 2108-2115.

49. Totsuka T, Kanai T, Uraushihara K, Iiyama R, Yamazaki M, Akiba H, Yagita H, Okumura K & Watanabe M (2003) Therapeutic effect of anti-OX40L and

anti-TNF-alpha MAbs in a murine model of chronic colitis. *Am J Physiol Gastrointest Liver Physiol* 284, G595-603.

50. Yoshioka T, Nakajima A, Akiba H, Ishiwata T, Asano G, Yoshino S, Yagita H & Okumura K (2000) Contribution of OX40/OX40 ligand interaction to the pathogenesis of rheumatoid arthritis. *Eur J Immunol* 30, 2815-2823.

51. Huang L, Ji W, Zhou WF, Shi Q, Chen XY & Hu YM (2006) Effects of costimulatory pathway OX40/OX40L on the pathogenesis of allergic asthma in mice. *Zhonghua Er Ke Za Zhi* 44, 455-458.

52. Pakala SV, Bansal-Pakala P, Halteman BS, & Croft M (2004) Prevention of diabetes in NOD mice at a late stage by targeting OX40/OX40 ligand interactions. *Eur J Immunol* 34, 3039-3046.

53. Hwang H, Lee S, Lee WH, Lee HJ, & Suk K (2010) Stimulation of glucocorticoid-induced tumor necrosis factor receptor family-related protein ligand (GITRL) induces inflammatory activation of microglia in culture. *J Neurosci Res* 88, 2188-2196.

54. Nocentini G & Riccardi C (2009) GITR: a modulator of immune response and inflammation. *Adv Exp Med Biol* 647, 156-173.

55. Zhou P, Qiu J, L'Italien L, Gu D, Hodges D, Chao CC & Schebye XM (2010) Mature B cells are critical to T-cell-mediated tumor immunity induced by an agonist anti-GITR monoclonal antibody. *J Immunother* 33, 789-797.

56. Côté AL, Zhang P, O'Sullivan JA, Jacobs VL, Clemis CR, Sakaguchi S, Guevara-Patiño JA & Turk MJ (2010) Stimulation of the Glucocorticoid-Induced TNF Receptor Family-Related Receptor on CD8 T Cells Induces

Protective and High-Avidity T Cell Responses to Tumor-Specific Antigens. *J Immunol*. (e-published)

57. Kim JI, Sonawane SB, Lee MK, Lee SH, Duff PE, Moore DJ, O'Connor MR, Lian MM, Deng S, Choi Y, Yeh H, Caton AJ & Markmann JF (2010) Blockade of GITR-GITRL interaction maintains Treg function to prolong allograft survival. *Eur J Immunol* 40, 1369-1374.

58. Nocentini G, Cuzzocrea S, Genovese T, Bianchini R, Mazzon E, Ronchetti S, Esposito E, Rosanna DP, Bramanti P & Riccardi C (2008) Glucocorticoid-induced tumor necrosis factor receptor-related (GITR)-Fc fusion protein inhibits GITR triggering and protects from the inflammatory response after spinal cord injury. *Mol Pharmacol* 73, 1610-1621.

59. You S, Poulton L, Cobbold S, Liu CP, Rosenzweig M, Ringler D, Lee WH, Segovia B, Bach JF, Waldmann H & Chatenoud L (2009) Key role of the GITR/GITRLigand pathway in the development of murine autoimmune diabetes: a potential therapeutic target. *PLoS One* 4, e7848.

60. Boursalian TE, McEarchern JA, Law CL, & Grewal IS (2009) Targeting CD70 for human therapeutic use. *Adv Exp Med Biol* 647, 108-119.

61. Agarwal A & Newell KA (2008) The role of positive costimulatory molecules in transplantation and tolerance. *Curr Opin Organ Transplant* 13, 366-372.

62. Denoeud J & Moser M (2010) Role of CD27/CD70 pathway of activation in immunity and tolerance. *J Leukoc Biol*. (e-published)

63. Roberts DJ, Franklin NA, Kingeter LM, Yagita H, Tutt AL, Glennie MJ & Bullock TN (2010) Control of established melanoma by CD27 stimulation

is associated with enhanced effector function and persistence, and reduced PD-1 expression of tumor infiltrating CD8(+) T cells. *J Immunother* 33, 769-779.

64. McEarchern JA, Oflazoglu E, Francisco L, McDonagh CF, Gordon KA, Stone I, Klussman K, Turcott E, van Rooijen N, Carter P, Grewal IS, Wahl AF & Law CL (2007) Engineered anti-CD70 antibody with multiple effector functions exhibits in vitro and in vivo antitumor activities. *Blood* 109, 1185-1192.

65. Oflazoglu E, Boursalian TE, Zeng W, Edwards AC, Duniho S, McEarchern JA, Law CL, Gerber HP & Grewal IS (2009) Blocking of CD27-CD70 pathway by anti-CD70 antibody ameliorates joint disease in murine collagen-induced arthritis. *J Immunol* 183, 3770-3777.

66. Yanagisawa S, Takeichi N, Kaneyama T, Yagita H, Taniguchi S, Kim BS & Koh CS (2010) Effects of anti-CD70 mAb on Theiler's murine encephalomyelitis virus-induced demyelinating disease. *Brain Res* 1317, 236-245.

67. Wang H, McCann FE, Gordan JD, Wu X, Raab M, Malik TH, Davis DM & Rudd CE (2004) ADAP-SLP-76 binding differentially regulates supramolecular activation cluster (SMAC) formation relative to T cell-APC conjugation. *J Exp Med* 200, 1063-1074.

68. Keystone E, Fleischmann R, Emery P, Furst DE, van Vollenhoven R, Bathon J, Dougados M, Baldassare A, Ferraccioli G, Chubick A, Udell J, Cravets MW, Agarwal S, Cooper S & Magrini F (2007) Safety and efficacy of

additional courses of rituximab in patients with active rheumatoid arthritis: an open-label extension analysis. *Arthritis Rheum* 56, 3896-3908.

69. Browning JL (2008) Inhibition of the lymphotoxin pathway as a therapy for autoimmune disease. *Immunol Rev* 223, 202-220.

70. Tamada K, Shimozaki K, Chapoval AI, Zhu G, Sica G, Flies D, Boone T, Hsu H, Fu YX, Nagata S, Ni J & Chen L (2000) Modulation of T-cell-mediated immunity in tumor and graft-versus-host disease models through the LIGHT co-stimulatory pathway. *Nat Med* 6, 283-289.

71. Xu Y, Flies AS, Flies DB, Zhu G, Anand S, Flies SJ, Xu H, Anders RA, Hancock WW, Chen L & Tamada K (2007) Selective targeting of the LIGHT-HVEM costimulatory system for the treatment of graft-versus-host disease. *Blood* 109, 4097-4104.

72. Ye Q, Fraser CC, Gao W, Wang L, Busfield SJ, Wang C, Qiu Y, Coyle AJ, Gutierrez-Ramos JC & Hancock WW (2002) Modulation of LIGHT-HVEM costimulation prolongs cardiac allograft survival. *J Exp Med* 195, 795-800.

73. Melero I, Murillo O, Dubrot J, Hervas-Stubbs S, & Perez-Gracia JL (2008) Multi-layered action mechanisms of CD137 (4-1BB)-targeted immunotherapies. *Trends Pharmacol Sci* 29, 383-390.

74. Lynch DH (2008) The promise of 4-1BB (CD137)-mediated immunomodulation and the immunotherapy of cancer. *Immunol Rev* 222, 277-286.

75. Imai Y, Shimaoka M, & Kurokawa M (2010) Essential roles of VLA-4 in the hematopoietic system. *Int J Hematol* 91, 569-575.

76. Ascierto PA, Simeone E, Sznol M, Fu YX, & Melero I (2010) Clinical Experiences With Anti-CD137 and Anti-PD1 Therapeutic Antibodies. *Semin Oncol* 37, 508-516.

77. Qin L, Guan HG, Zhou XJ, Yin J, Lan J & Qian HX (2010) Blockade of 4-1BB/4-1BB ligand interactions prevents acute rejection in rat liver transplantation. *Chin Med J* 123, 212-215.

78. Coyle PK (2010) The role of natalizumab in the treatment of multiple sclerosis. *Am J Manag Care* 16, S164-170.

79. Evans R, Patzak I, Svensson L, De Filippo K, Jones K, McDowall A & Hogg N (2009) Integrins in immunity. *J Cell Sci* 122, 215-225.

80. Stengel FM, Petri V, Campbell GA, Dorantes GL, López M, Galimberti RL, Valdez RP, de Arruda LF, Guerra MA, Chouela EN & Licu D (2009) Control of Moderate-to-Severe Plaque Psoriasis with Efalizumab: 24-Week, Open-Label, Phase IIIb/IV Latin American Study Results. *Arch Drug Inf* 2, 71-78.

81. Yacyshyn B, Chey WY, Wedel MK, Yu RZ, Paul D & Chuang E (2007) A randomized, double-masked, placebo-controlled study of alicaforsen, an antisense inhibitor of intercellular adhesion molecule 1, for the treatment of subjects with active Crohn's disease. *Clin Gastroenterol Hepatol* 5, 215-220.

82. del Zoppo GJ (2010) Acute anti-inflammatory approaches to ischemic stroke. *Ann N Y Acad Sci* 1207,143-148.

83. Paul LC, Davidoff A, Benediktsson H, & Issekutz T (1996) Anti-integrin (LFA-1, VLA-4, and Mac-1) antibody treatment and acute cardiac graft rejection in the rat. *Transpl Int* 9, 420-425.

84. Vincenti F (2008) Costimulation blockade in autoimmunity and transplantation. *J Allergy Clin Immunol* 121, 299-306.

85. Ruperto N, Lovell DJ, Li T, Sztajnbok F, Goldenstein-Schainberg C, Scheinberg M, Penades IC, Fischbach M, Alcala JO, Hashkes PJ, Hom C, Jung L, Lepore L, Oliveira S, Wallace C, Alessio M,Quartier P, Cortis E, Eberhard A, Simonini G, Lemelle I, Chalom EC, Sigal LH, Block A, Covucci A, Nys M, Martini A & Giannini EH (2010) Abatacept improves health-related quality of life, pain, sleep quality, and daily participation in subjects with juvenile idiopathic arthritis. *Arthritis Care Res (Hoboken)* 62, 1542-1551.

86. Walker UA, Courvoisier DS, Dudler J, Aeberli D, von Kempis J, Scherer A & Finckh A (2010) Do new biologics meet the unmet medical need in rheumatoid arthritis? Safety and efficacy of abatacept following B-cell depletion. *Rheumatology (Oxford)*. (e-published)

87. Larsen CP, Pearson TC, Adams AB, Tso P, Shirasugi N, Strobert E, Anderson D, Cowan S, Price K, Naemura J, Emswiler J, Greene J, Turk LA, Bajorath J, Townsend R, Hagerty D, Linsley PS & Peach RJ (2005) Rational development of LEA29Y (belatacept), a high-affinity variant of CTLA4-Ig with potent immunosuppressive properties. *Am J Transplant* 5, 443-453.

88. Ansari MJ, Salama AD, Chitnis T, Smith RN, Yagita H, Akiba H, Yamazaki T, Azuma M, Iwai H, Khoury SJ, Auchincloss H Jr & Sayegh MH (2003) The programmed death-1 (PD-1) pathway regulates autoimmune diabetes in nonobese diabetic (NOD) mice. *J Exp Med* 198, 63-69.

89. Folkl A & Bienzle D (2010) Structure and function of programmed death (PD) molecules. *Vet Immunol Immunopathol* 134, 33-38.

90. Ishida Y, Agata Y, Shibahara K, & Honjo T (1992) Induced expression of PD-1, a novel member of the immunoglobulin gene superfamily, upon programmed cell death. *EMBO J* 11, 3887-3895.

91. Agata Y, Kawasaki A, Nishimura H, Ishida Y, Tsubata T, Yagita H & Honjo T (1996) Expression of the PD-1 antigen on the surface of stimulated mouse T and B lymphocytes. *Int Immunol* 8, 765-772.

92. Freeman GJ, Long AJ, Iwai Y, Bourque K, Chernova T, Nishimura H, Fitz LJ, Malenkovich N, Okazaki T, Byrne MC, Horton HF, Fouser L, Carter L, Ling V, Bowman MR, Carreno BM, Collins M, Wood CR & Honjo T (2000) Engagement of the PD-1 immunoinhibitory receptor by a novel B7 family member leads to negative regulation of lymphocyte activation. *J Exp Med* 192, 1027-1034.

93. Latchman Y, Wood CR, Chernova T, Chaudhary D, Borde M, Chernova I, Iwai Y, Long AJ, Brown JA, Nunes R, Greenfield EA, Bourque K, Boussiotis VA, Carter LL, Carreno BM, Malenkovich N, Nishimura H, Okazaki T, Honjo T, Sharpe AH & Freeman GJ (2001) PD-L2 is a second ligand for PD-1 and inhibits T cell activation. *Nat Immunol* 2, 261-268.

94. Nurieva RI, Liu X, & Dong C (2009) Yin-Yang of costimulation: crucial controls of immune tolerance and function. *Immunol Rev* 229, 88-100.

95. Sharpe A (2005) Costimulation and regulation of autoimmunity and tolerance. *J Pediatr Gastroenterol Nutr* 40, S20-21.

96. Dong C, Juedes AE, Temann UA, Shresta S, Allison JP, Ruddle NH & Flavell RA (2001) ICOS co-stimulatory receptor is essential for T-cell activation and function. *Nature* 409, 97-101.

97. Ansari MJ, Fiorina P, Dada S, Guleria I, Ueno T, Yuan X, Trikudanathan S, Smith RN, Freeman G & Sayegh MH (2008) Role of ICOS pathway in autoimmune and alloimmune responses in NOD mice. *Clin Immunol* 126, 140-147.

98. Derré L, Rivals JP, Jandus C, Pastor S, Rimoldi D, Romero P, Michielin O, Olive D & Speiser DE (2010) BTLA mediates inhibition of human tumor-specific CD8+ T cells that can be partially reversed by vaccination. *J Clin Invest* 120, 157-167.

99. Ford ML & Larsen CP (2009) Translating costimulation blockade to the clinic: lessons learned from three pathways. *Immunol Rev* 229, 294-306.

100. Simnick AJ, Valencia CA, Liu R, & Chilkoti A (2010) Morphing low-affinity ligands into high-avidity nanoparticles by thermally triggered self-assembly of a genetically encoded polymer. *ACS Nano* 4, 2217-2227.

101. Salmaso C, Olive D, Pesce G, & Bagnasco M (2002) Costimulatory molecules and autoimmune thyroid diseases. *Autoimmunity* 35, 159-167.

102. Brandt M, Grotkop C, Steinmann J, & Steinhoff G (2003) Prevention of lung allograft rejection by combined treatment with adhesion molecule antibodies and cyclosporine. *Interact Cardiovasc Thorac Surg* 2, 509-513.

103. Oberholzer J, Kinzer K, & Fiorina P (2010) The anti-LFA-1 trial in islet transplantation. *Am J Transplant* 10, 1725-1726.

104. Posselt AM, Bellin MD, Tavakol M, Szot GL, Frassetto LA, Masharani U, Kerlan RK, Fong L, Vincenti FG, Hering BJ, Bluestone JA & Stock PG (2010) Islet transplantation in type 1 diabetics using an immunosuppressive protocol based on the anti-LFA-1 antibody efalizumab. *Am J Transplant* 10, 1870-1880.

105. Dustin ML, Tseng SY, Varma R, & Campi G (2006) T cell-dendritic cell immunological synapses. *Curr Opin Immunol* 18, 512-516.

106. Wulfing C & Davis MM (1998) A receptor/cytoskeletal movement triggered by costimulation during T cell activation. *Science* 282, 2266-2269.

107. Saito T & Yokosuka T (2006) Immunological synapse and microclusters: the site for recognition and activation of T cells. *Curr Opin Immunol* 18, 305-313.

108. Valitutti S, Muller S, Cella M, Padovan E, & Lanzavecchia A (1995) Serial triggering of many T-cell receptors by a few peptide-MHC complexes. *Nature* 375, 148-151.

109. Bromley SK, Burack WR, Johnson KG, Somersalo K, Sims TN, Sumen C, Davis MM, Shaw AS, Allen PM & Dustin ML (2001) The immunological synapse. *Annu Rev Immunol* 19, 375-396.

110. Yokosuka T & Saito T (2009) Dynamic regulation of T-cell costimulation through TCR-CD28 microclusters. *Immunol Rev* 229, 27-40.

111. Rodriguez-Fernandez JL, Riol-Blanco L, & Delgado-Martin C (2010) What is the function of the dendritic cell side of the immunological synapse? *Sci Signal* 3, re2.

112. Grakoui A, Bromley SK, Sumen C, Davis MM, Shaw AS, Allen PM & Dustin ML (1999) The immunological synapse: a molecular machine controlling T cell activation. *Science* 285, 221-227.

113. Jo EK, Wang H, & Rudd CE (2005) An essential role for SKAP-55 in LFA-1 clustering on T cells that cannot be substituted by SKAP-55R. *J Exp Med* 201, 1733-1739.

114. Teft WA & Madrenas J (2006) The immunological synapse as a novel therapeutic target. *Curr Opin Investig Drugs* 7, 1008-1013.

115. Hartman NC, Nye JA, & Groves JT (2009) Cluster size regulates protein sorting in the immunological synapse. *Proc Natl Acad Sci U S A* 106, 12729-12734.

116. Dustin ML, Chakraborty AK, & Shaw AS (2010) Understanding the structure and function of the immunological synapse. *Cold Spring Harb Perspect Biol* 2, a002311.

117. Dustin ML & Cooper JA (2000) The immunological synapse and the actin cytoskeleton: molecular hardware for T cell signaling. *Nat Immunol* 1, 23-29.

118. Krummel M, Wulfing C, Sumen C, & Davis MM (2000) Thirty-six views of T-cell recognition. *Philos Trans R Soc Lond B Biol Sci* 355, 1071-1076.

119. Varma R, Campi G, Yokosuka T, Saito T, & Dustin ML (2006) T cell receptor-proximal signals are sustained in peripheral microclusters and terminated in the central supramolecular activation cluster. *Immunity* 25, 117-127.

120. Lebedeva T, Dustin ML, & Sykulev Y (2005) ICAM-1 co-stimulates target cells to facilitate antigen presentation. *Curr Opin Immunol* 17, 251-258.

121. Bhatia S, Edidin M, Almo SC, & Nathenson SG (2006) B7-1 and B7-2: similar costimulatory ligands with different biochemical, oligomeric and signaling properties. *Immunol Lett* 104, 70-75.

122. Carman CV & Springer TA (2003) Integrin avidity regulation: are changes in affinity and conformation underemphasized? *Curr Opin Cell Biol* 15, 547-556.

123. Kim M, Carman CV, Yang W, Salas A, & Springer TA (2004) The primacy of affinity over clustering in regulation of adhesiveness of the integrin $\alpha_L\beta_2$. *J Cell Biol* 167, 1241-1253.

124. Hogg N, Laschinger M, Giles K, & McDowall A (2003) T-cell integrins: more than just sticking points. *J Cell Sci* 116, 4695-4705.

125. Shimaoka M & Springer TA (2003) Therapeutic antagonists and conformational regulation of integrin function. *Nat Rev Drug Discov* 2, 703-716.

126. Petros RA & DeSimone JM (2010) Strategies in the design of nanoparticles for therapeutic applications. *Nat Rev Drug Discov* 9, 615-627.

127. Farokhzad OC, Cheng J, Teply BA, Sherifi I, Jon S, Kantoff PW, Richie JP & Langer R (2006) Targeted nanoparticle-aptamer bioconjugates for cancer chemotherapy in vivo. *Proc Natl Acad Sci U S A* 103, 6315-6320.

128. Johnson RN, Kopeckova P, & Kopecek J (2009) Synthesis and evaluation of multivalent branched HPMA copolymer-Fab' conjugates targeted to the B-cell antigen CD20. *Bioconjug Chem* 20, 129-137.

129. Meng H, Chen JY, Mi L, Wang PN, Ge MY, Yue Y & Dai N (2010) Conjugates of folic acids with BSA-coated quantum dots for cancer cell targeting and imaging by single-photon and two-photon excitation. *J Biol Inorg Chem*. (e-published)

130. Han HD, Mangala LS, Lee JW, Shahzad MM, Kim HS, Shen D, Nam EJ, Mora EM, Stone RL, Lu C, Lee SJ, Roh JW, Nick AM, Lopez-Berestein G & Sood AK (2010) Targeted gene silencing using RGD-labeled chitosan nanoparticles. *Clin Cancer Res* 16, 3910-3922.

131. Hong S, Leroueil PR, Majoros IJ, Orr BG, Baker JR Jr & Banaszak Holl MM (2007) The binding avidity of a nanoparticle-based multivalent targeted drug delivery platform. *Chem Biol* 14, 107-115.

132. Stukel JM, Li RC, Maynard HD, & Caplan MR (2010) Two-step synthesis of multivalent cancer-targeting constructs. *Biomacromolecules* 11, 160-167.

133. Shewmake TA, Solis FJ, Gillies RJ, & Caplan MR (2008) Effects of linker length and flexibility on multivalent targeting. *Biomacromolecules* 9, 3057-3064.

134. Rosca EV, Gillies RJ, & Caplan MR (2009) Glioblastoma targeting via integrins is concentration dependent. *Biotechnol Bioeng* 104, 408-417.

135. Muro S, Gajewski C, Koval M, & Muzykantov VR (2005) ICAM-1 recycling in endothelial cells: a novel pathway for sustained intracellular delivery and prolonged effects of drugs. *Blood* 105, 650-658.

Chapter 2

ICAM-1 Targeting of Doxorubicin-Loaded PLGA Nanoparticles to Lung Epithelial Cells

2.1 Introduction

Interaction of leukocyte function associated antigen-1 (LFA-1) and intercellular cell adhesion molecule-1 (ICAM-1) can play a critical role in tumor metastasis and progression.[1-6] ICAM-1 is expressed on a variety of inflammatory and immune effector cells as well as endothelial cells, fibroblasts, and epithelial cells.[7] ICAM-1 is also up-regulated on the surface of a variety of lymphomas, melanomas, renal, pancreatic, bladder and lung carcinomas and/or their local vascular network.[7] The expression of ICAM-1 may be involved in the regulation of tumor susceptibility to the activity of defensive cells. The upregulation of ICAM-1 expression on some types of carcinomas such as melanomas and lung carcinomas may be followed by the extracellular release of soluble ICAM-1 (sICAM-1).[7] The sICAM-1 could interfere with the interaction of surface ICAM-1 and immune cells such as natural killer (NK) cells or lymphocyte activated killer (LAK) cells by competition, leading to the reduction of cancer cell exposure to these protective cells.[7] Shedding of sICAM-1 in the extracellular space has been proposed as one of the mechanisms that tumor cells use to escape cell-mediated cytotoxicity.[7]

A cyclic peptide, cyclo-(1,12)-PenITDGEATDSGC (cLABL), derived from the I-domain of the α_L-subunit of LFA-1 integrin has been shown to impair LFA-1/ICAM-1 interaction by binding to the D_1 domain of ICAM-1. This peptide specifically inhibited homotypic and heterotypic T-cell adhesion to epithelial and endothelial cell monolayers by disrupting the LFA-1/ICAM-1 interaction.[8-12] In addition to its receptor binding characteristics, cLABL displayed receptor mediated

endocytosis, insinuating a possible use as a targeting moiety for intracellular drug delivery.[11] Accordingly, cLABL conjugated nanoparticles were proposed to be a promising anti-cancer drug delivery system targeting ICAM-1.

Recently, monoclonal antibodies have become crucial therapeutic agents against a wide range of cancers. However, autoimmune reactions and short half-lives are often encumbrances for immunotherapy using monoclonal antibodies.[13, 14] Peptides and small molecule inhibitors may offer similar therapeutic interventions by acting as a targeting ligand to proteins on the cell surface.[1] Furthermore, in comparison to monoclonal antibodies, cyclic peptides have been shown to offer improved physicochemical stability and may even improve selectivity to the targeted site.[1, 6]

The utmost ambition of pharmaceutical therapy is to deliver the drug carriers to a specific therapeutic site of action with a triggered or sustained drug release. Advantages of this modality could include a decrease in adverse effects, lower toxicity, an increase in the efficacy of the therapeutic agent and a reduction in the frequency of administration. Polymeric nanoparticles (NP) possess some advantages over other formulations in terms of stability and feasibility of modulating the drug release profile by controlling polymer degradation.[15, 16] In addition, this delivery system permits functional group modification on the nanoparticle surface without compromising the activity of the drug carried.

In this study, cLABL-conjugated poly (DL-lactic-co-glycolic acid) nanoparticles (cLABL-NP) targeting ICAM-1 on A549 lung epithelial cells have

been formulated and characterized. Binding and internalization studies have demonstrated that nanoparticles can be targeted to these epithelial cells via ICAM-1 and can be internalized into the cells rapidly. The cellular internalization was confirmed by utilizing fluorescence markers and microscopy. Interestingly, the results indicated that cLABL-NP trafficked to lysosomes and escaped lysosomal sequestration. Targeting and drug release studies of nanoparticles encapsulating doxorubicin (DOX-NP) suggested that PLGA nanoparticles targeted by cLABL localized this drug within A549 cells to offer sustained release. The IC_{50} of nanoparticles encapsulating doxorubicin, both conjugated and not conjugated with peptide compared to that of free doxorubicin HCl were reported. Ultimately, cLABL-nanoparticles may be aerosolized to provide a targeted anti-cancer drug delivery system directly to the pulmonary epithelium.

2.2 Materials and Methods

Materials

Poly(DL-lactic-coglycolic acid) (50:50) with terminal carboxylate group (PLGA, inherent viscosity 0.22 dL/g, Mw ~ 20 kDa and 0.67dL/g, Mw ~90 kDa) was purchased from LACTEL Absorbable Polymers International (Pelham, AL, USA). Pluronic®F-127, Texas Red Dextran (10,000 Mw, lysine fixable) and 4',6-diamidino-2-phenylindole, dilactate (DAPI, dilactate) were purchased from Invitrogen Molecular Probes, Inc. (Carlsbad, CA, USA). 1-Ethyl-3-[3-dimethylaminopropyl]carbodiimide hydrochloride (EDC) and *N*-hydroxysulfosuccinimide (sulfo-NHS) were purchased from Thermo Fisher Scientific

Inc. (Rockford, IL, USA) Coumarin-6 was obtained from Polysciences, Inc. (Warrington, PA, USA). Doxorubicin HCl for injection was provided by Novaplus (Irving, TX, USA). Dialysis membrane (MWCO 100,000) was purchased from Spectrum laboratory Products Inc. (Rancho Dominguez, CA, USA). F-12K medium and A549 cell line were obtained from American Type Culture Collection (Manassas, VA, USA). Recombinant, Human, Tumor Necrosis Factor-α (TNF-α) was purchased from Promega (Madison, WI, USA). Human Interferon gamma was purchased from Roche Diagnostics Corporation (Indianapolis, IN, USA), 3,3′,5,5′-Tetramethylbenzidine (TMB) was obtained from Sigma (St. Louis, MO, USA). Monoclonal anti-human CD54 (ICAM-1) Domain D1 was purchased from Ancell (Bayport, MN, USA) and Horseradish Peroxidase-Conjugated Goat Anti-Mouse IgG was obtained from Cayman Chemical (Ann Arbor, MI, USA). CellTiter 96® AQ_{ueous} Non-Radioactive Cell Proliferation Assay (MTS) was purchased from Promega (Madison, WI, USA)

Methods

Pluronic®F-127 functional group modification

Terminal hydroxyl groups on Pluronic®F-127-OH were converted to carboxyl groups according to the following procedure (16). Pluronic®F-127-OH (2 g)was dissolved in tetrahydrofuran (THF, 60 ml). Then 4-dimethylaminopyridine (DMAP, 98 mg), triethylamine (108 μl) and succinic anhydride (800 mg) were added. The mixture was stirred for 48 hr at room temperature. The solution was dried by rotary evaporation, and, was then dissolved in carbon tetrachloride (30 ml).Theexcess succinic anhydride

was removed by filtration. The Pluronic®F-127-COOH was purified by precipitation with ice-cold diethylether. The product was identified by ^{1}H NMR sepctroscopy (Bruker AVANCE 400 MHz spectrometer) and FTIR spectroscopy (ABB Bomem MB series).

Preparation of PLGA nanoparticles encapsulating coumarin-6

Nanoparticles encapsulating a fluorescence marker, coumarin-6, were formulated using a solvent displacement method.[15] In brief, PLGA, inherent viscosity 0.22 dl/g or 0.67 dl/g) was dissolved in trifluoroethanol (TFE, 18 mg/ml) containing coumarin-6 (95 μg). The solution was slowly transferred to a water phase containing surfactant; 0.1% Pluronic®F-127-COOH (35 ml) under mild stirring (250 rpm). The nanoparticles were spontaneously formed due to the rapid removal of TFE. Excess surfactant was removed by dialysis against a 0.2% mannitol solution for 48 hr.

Preparation of PLGA nanoparticles encapsulating doxorubicin

Doxorubicin HCl for injection (2 mg/ml) was lyophilized and neutralized using triethylamine (108 μmol). The non-aqueous form of doxorubicin was extracted using methylene chloride and evaporated.[17] In brief, PLGA (0.22 dl/g or 0.67 dl/g) in acetone solution (18 mg/ml) was mixed with 1.8 mg of the purified doxorubicin. The solution was infused (17.5 ml/hr) into 10 ml of 0.1% Pluronic®F-127-COOH (250 rpm) to allow the formation of nanoparticles encapsulating doxorubicin (DOX-NP). Nanoparticles were collected by centrifugation (15,000 rpm, 40 min) and washed three times. The nanoparticles encapsulating doxorubicin conjugated with cLABL (cLABL-DOX-NP) was prepared using the method described above. The

encapsulation efficiency was determined by centrifugation (13,000 rpm, 40 min) of the DOX-NP or cLABL-DOX-NP suspension (200 μl) by collecting the pellet and dissolving in DMSO (200 μl). Doxorubicin content was analyzed by fluorescence spectroscopy (Spectramax M5, ex: 500 nm, em: 600 nm).

Conjugation of cLABL peptide to PLGA-nanoparticles

A Pluronic®F-127-COOH coated PLGA nanoparticles (1.5 mg/ml) suspension was buffered using 2-(*N*-morpholino)ethanesulfonic acid (MES) pH 6.5. Nanoparticles were then incubated with 100 mM 1-Ethyl-3-[3-dimethylaminopropyl]carbodiimide hydrochloride (EDC) and 50 mM *N*-hydroxysulfosuccinimide (sulfo-NHS) for 15 min.[18]The activated carboxyl terminus of Pluronic® F127-COOH on the surface of nanoparticles was allowed to react with the amino terminus of the cLABL peptide (80 μM) at least 6 hr at room temperature. Conjugated NP were collected by centrifugation (10,000 rpm, 10 min) and washed three times with purified water. Size and charge of NP and cLABL-NP were characterized using dynamic light scattering (ZetaPALS, Brookhaven instrument Inc.). The amount of free cLABL after the reaction was quantified by gradient reversed phase HPLC (SHIMADZU) using a C_{18} column. The HPLC consisted of SCL-10A SHIMADZU system controller, LC-10AT VP SHIMADZU liquid chromatograph, SIL-10A XL SHIMADZU autoinjecter set at 10 μl injection volume, DGU-14A SHIMADZU degasser, sample cooler, and SPD-10A SHIMADZU UV-Vis detector (220 nm). The HPLC-UV system was controlled by a personal computer equipped with SHIMADZU class VP Software. All separations were carried out using a Vydac® HPLC column Protein and Peptide C_{18}

column. Gradient elution was carried out at constant flow of 1 ml/min, from 100% A to 0% A (corresponding to 0% B to 100% B) for 15 min, followed by an isocratic elution at 100% B for 3 min. Mobile phase compositions were (A) acetronitrile-water (5:95) with 0.1% TFA (B) acetonitrile–water (90:10, v/v) with 0.1% trifluoroacetic acid (TFA). At the end of each analysis, the cartridge was re-equilibrated at 1 ml/min flow rate for 13 min with A. The density of peptide on the surface of nanoparticles was calculated from the total surface area assuming a normal Guassian particle size distribution.

Drug release study of nanoparticles encapsulating doxorubicin

The release of doxorubicin from cLABL-DOX-NP or DOX-NP was investigated using 0.1M acetate buffer pH 4 and phosphate buffer pH 7.4 as dissolution media. One milliliter of DOX-NP (4 mg/ml) or five hundred microliters of cLABL-DOX-NP (4 mg/ml) were placed in the dialysis membrane (MwCO 10,000) immersed in 100 ml and 50 ml of buffer solution, respectively and were shaken at 100 rpm, 37°C.[19] At predetermined time points, the dialysate was sampled and the amount of released doxorubicin was determined using fluorescence spectroscopy (ex; 500 nm, em; 600 nm).

Cytotoxicity assay

The CellTiter 96® AQ_{ueous} Non-Radioactive Cell Proliferation Assay[(a)] is a colorimetric method used to determine the viability of cells in this cytotoxicity study. ICAM-1 up-regulated A549 cells (80,000 cells/ml) were incubated with cLABL-DOX-NP or DOX-NP for 3 hr and then were washed three times with PBS. Cells

were incubated in cell culture medium for 20 hr to allow the sustained release of the drug. For a control experiment, cells were incubated with doxorubicin HCl for 20 hr. After incubation, cells were washed three times with PBS. The solution composed of tetrazolium compound [3-(4,5-dimethylthiazol-2-yl)-5-(3-carboxymethoxyphenyl)-2-(4-sulfophenyl)-2H-tetrazolium, MTS and an electron coupling reagent (phenazine methosulfate; PMS) (20 μl) was added into each well containing 100 μl of cell culture medium. The plate was then incubated at 37°C, 5%CO_2 for 4 hr. The quantity of formazan product was determined by the amount of 490 nm absorbance.

Determination of ICAM-1 expression on A549 cells using Enzymed-Linked Immunosorbent Assay (ELISA)

A549 carcinomic human alveolar basal epithelial cells were cultured in F12K medium with 10% fetal bovine serum (FBS) and 1% Penicillin-Streptomycin (10,000 U/ml) 37°C, 5% CO_2. Cell monolayers were incubated with TNF-α (1,000 U/ml) or IFN-γ (100 U/ml) for 48 hr to activate the up-regulation of ICAM-1 on the cell surface.[20]ICAM-1 expression was measured using an indirect ELISA. A549 cells (8 x 10^5 cells/ml) were seeded in a 96 well-plate. Cells were fixed by using 2% formaldehyde in PBS (100 μl/well) and incubated at room temperature for 1 hr. Cells were washed with PBS (200 μl/well) and then non-specific adsorption was blocked by incubating with 1% BSA in PBS (120 μl/well) for 30 min at room temperature. After washing with PBS, monoclonal anti-human CD54 (ICAM-1) domain D1 (120μl/well) was added and incubated 1 hr at 37ºC. Goat anti-mouse IgG HRP (100 μl/well) was then added after washing with PBS and incubated for 1 hr at 37ºC. Cells

were washed three times with PBS and incubated with 3,3',5,5' tetramethylbenzidine as the substrate for 15 min at room temperature. The enzyme-substrate reaction was stopped by adding 1 N sulfuric acid. The absorbance was obtained by UV spectroscopy (Spectramax M5; λ_{max} 450 nm)

Binding and Uptake of Nanoparticles by A549 cells

A549 cell monolayers were incubated with TNF-α (1,000 U/ml) for 48 hr to over express ICAM-1 receptors. Cells were then washed three times with serum free F12K and then incubated with nanoparticles (with or without cLABL conjugated) suspended in serum free medium (0.5 mg/ml). Cells were incubated with nanoparticles for different time intervals to observe the uptake kinetics of particles. After incubation, cells were washed three times with ice-cold PBS and lysed with 0.5% Triton X-100 in 0.2 M NaOH.[21] cLABL-NP and NP associated with the cells were detected and compared using a fluorescence plate reader (Spectramax M5; ex: 450 nm, em: 500 nm).[22]

Inhibition of cLABL-NP binding to ICAM-1

Various concentrations of free cLABL peptide or anti-ICAM-1 mAbs were incubated with activated A549 cells for 30 min, 37ºC, 5% CO_2. Cells were then washed three times with serum free media and incubated with cLABL-NP or nanopartilces without peptide for 1 hr at the same condition. Cells were washed three times with ice-cold PBS, lysed with 0.5% Triton X-100 in 0.2 M NaOH. cLABL-NP and NP content bound to the cell surface or internalized into the cells were determined and compared by fluorescence spectroscopy (Spectramax M5; ex: 450 nm, em: 500 nm).

Intracellular trafficking of cLABL-NP to lysosomes

ICAM-1 on A549 cells were activated using (1,000 U/ml) TNF-α for 48 hr. Lysosomes were labeled with Texas Red dextran (10,000 Mw, lysine fixable) to indicate the location of lysosomes. Texas red dextran prepared in serum free F12K (1 mg/ml) was incubated with activated A549 cells for 2 hr. Cells were then washed with serum free media for three times and further incubated with serum free media for up to 12 hr in order to chase the red fluorescent dye to localize in lysosomes.[23, 24] Cells were then incubated in the presence of cLABL-NP or NP containing the green fluorophore, coumarin-6, for 10 min. Cells were washed three times and incubated with serum free medium for each time point. After washing with ice-cold PBS, cells were fixed with 4% formaldehyde solution. Fluorescence emissions of nanoparticles and lysosomes were observed using FITC and rhodamine filter sets, respectively (Nikon Eclipse 80i microscope equipped for epifluorescence). Micrographs were captured using an Orca ER camera (Hamamatsu, Inc., Bridgewater, NJ). Colocalizations of nanoparticles and lysosomes were analyzed by Metamorph, version 6.2 (Universal Imaging Corp., West Chester, PA)

Intracellular trafficking of doxorubicin and nanoparticles encapsulating doxorubicin

TNF-α activated A549 cells were incubated with free doxorubicin (0.5 mg/ml) or doxorubicin encapsulated in nanoparticles conjugated with cLABL (cLABL-DOX-NP) or without cLABL (DOX-NP) (3.8 mg/ml) for 1 hr (for 1 hr observation) and 3 hr (for 3 hr, 8 hr and 24 hr observation). Cells were then washed three times with ice-

cold PBS and incubated with media with serum for each time period (8 hr and 24 hr). Cells were fixed with 4% paraformaldehyde. Nuclei were labeled with DAPI dilactate (blue) (300 nM, ex: 358 nm, em: 461 nm) for 5 min at 37ºC, 5%CO_2. Micrographs were taken using the Nikon Eclipse microscope.

For some studies, nanoparticles encapsulating doxorubicin contained the fluorophore, coumarin-6, to indicate the location of particles in the cells. cLABL-DOX-NP and DOX-NP encapsulating coumarin-6 were incubated with cells for each time period (15 min, 30 min, 1 hr and 3 hr). Cells were washed three times with ice-cold PBS and fixed with 4% paraformaldehyde. Nuclei were labeled with DAPI dilactate (blue) (300 nM, ex: 358 nm, em: 461 nm) for 5 min at 37ºC, 5%CO_2. Micrographs were taken using the Nikon Eclipse microscope.

Statistical analysis

Statistical evaluation of data was performed using an analysis of variance (one-way ANOVA). Newman–Keuls was used as a post-hoc test to assess the significance of differences. To compare the significance of the difference between the means of two groups, the *t*-test was performed; in all cases, a value of $p < 0.05$ was accepted as significant.

2.3 Results and Discussion

Preparation of Carboxylated Pluronic® F-127

The hydroxyl groups of Pluronic® F-127, $HO(C_2H_4O)_{100}(C_3H_6O)_{65}(C_2H_4O)_{100}H$, were converted to carboxyl groups to facilitate the conjugation reaction of this surfactant

with the terminal amine of cLABL peptide.[25] The ^{1}H NMR spectrum displayed the absorption of methylene protons adjacent to the succinic moiety at δ = 4.1 ppm and the proton of the carboxylic acid at δ = 12 ppm (Figure 1).[16] The COOH formation was confirmed by FTIR spectroscopy. The FTIR spectrum showed a strong C=O stretching absorption at 1,720 cm^{-1} and a very broad, strong absorption at 3,500 cm^{-1}, which indicated the appearance of the hydroxyl of carboxylic acid (Figure 2). These results confirmed the formation of carboxylated Pluronic® F-127.

Preparation of PLGA nanoparticles encapsulating coumarin-6

PLGA nanoparticles were prepared by a spontaneous solvent displacement method using carboxylated Pluronic® F-127as an anionic surfactant. Dynamic light scattering showed that the size of nanoparticles encapsulating coumarin-6 was approximately 225 nm in diameter with a low polydispersity suggesting a narrow size distribution, and that the zeta potential value was about -45 mV (Table 1). An increase in size and negative charge of nanoparticles after conjugation with cLABL peptide was observed, which was expected due to the pI value of cLABL peptide (pI~3.5). The size and charge of nanoparticles encapsulating coumarin-6 were comparable when either form of PLGA (0.22 dl/g or 0.67 dl/g) was used to formulate nanoparticles. The encapsulation efficiencies of coumarin-6 in both nanoparticles were reported in Table 2. As expected, the encapsulation efficiencies were diminished in both types of PLGA after the conjugation reaction.

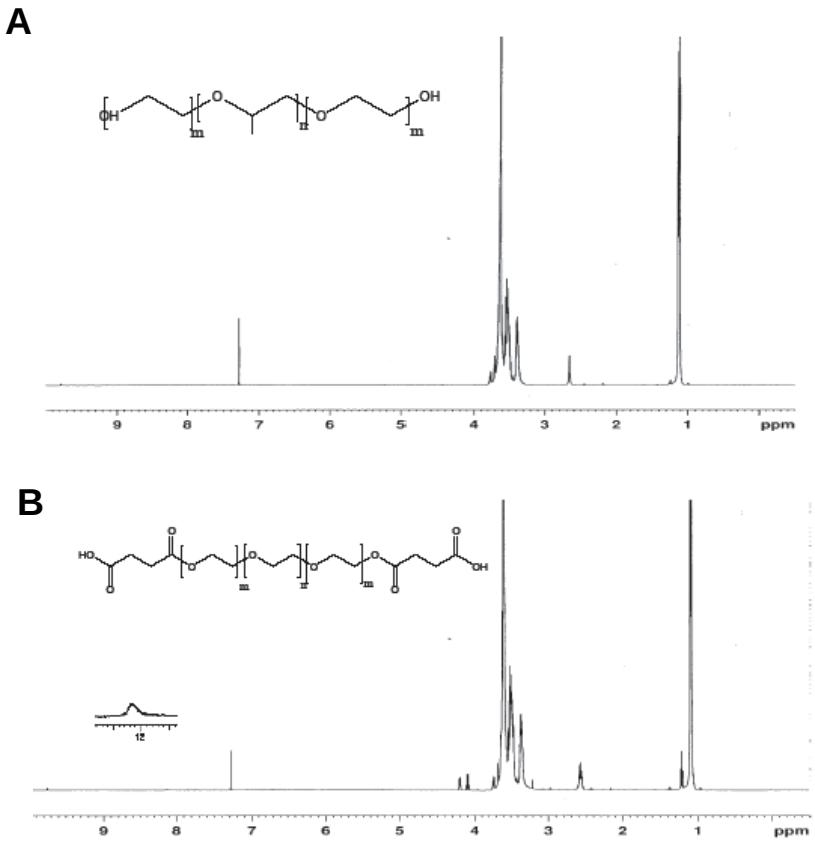

Figure 1 (A) The proton NMR spectrum of Pluronic® F127 (B) Proton NMR spectrum of carboxylated Pluronic® F-127 displaying the absorption of methylene protons adjacent to the succinic moiety at δ = 4.1 ppm and the proton of the carboxylic acid at δ = 12 ppm.

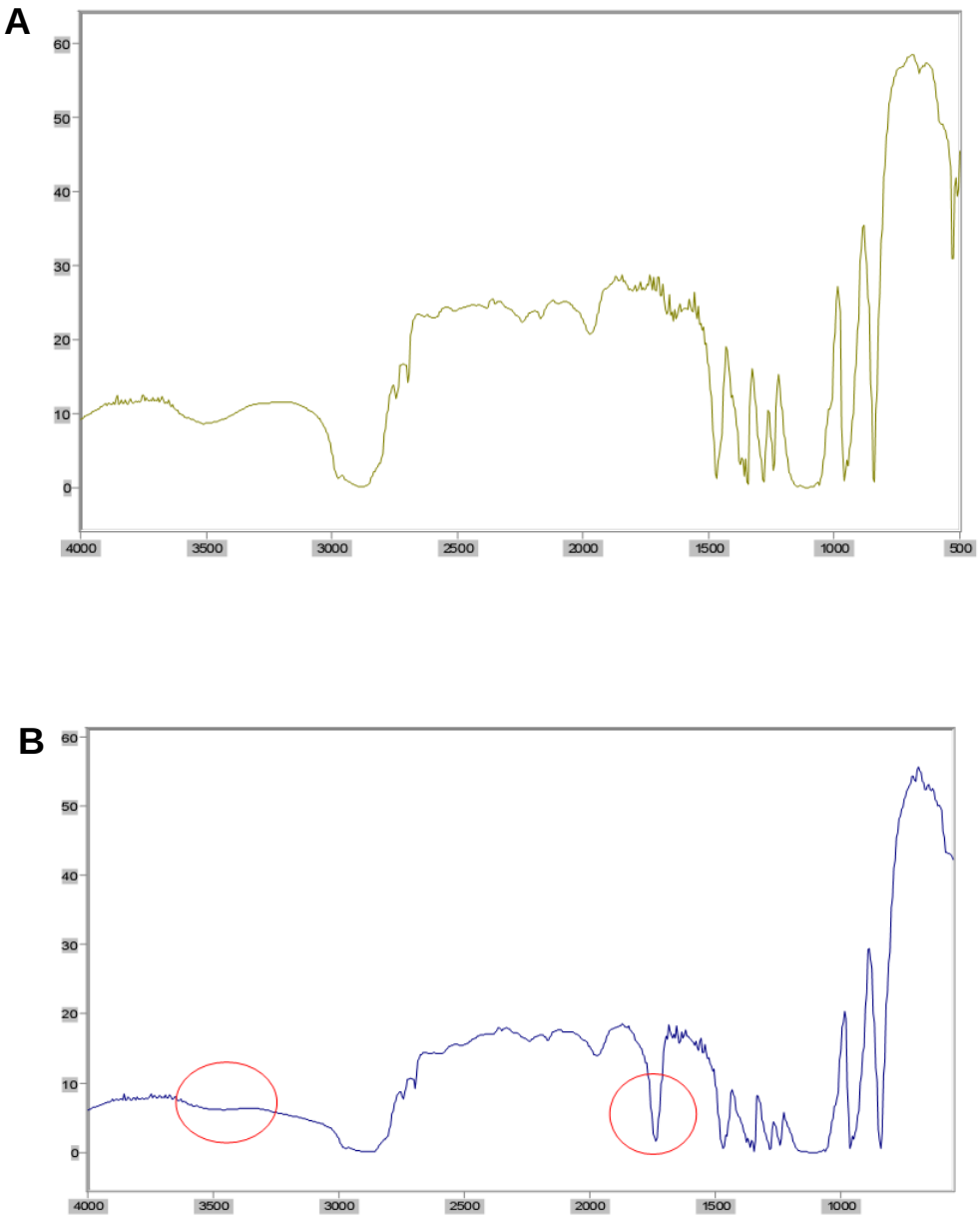

Figure 2 (A) FTIR spectrum of Pluronic® F127. (B) Compared to unmodified Pluronic®, the FTIR spectrum showed a strong C=O stretching absorption at 1,720 cm^{-1} and a very broad, strong absorption at 3,500 cm^{-1} which indicated the appearance of the hydroxyl of carboxylic acid.

Preparation of PLGA nanoparticles encapsulating doxorubicin

A variety of mAbs have been identified for immunotherapy against a wide range of cancers.[26] Peptides that can target the immunoglobulin receptor offer a simple alternative to mAbs. The cLABL peptide itself has a therapeutic effect, however, potency may be improved by using this ligand to target drug loaded nanoparticles. Nanocarriers often exhibit various benefits such as prolonged circulation and tumor localization via the enhanced permeability and retention effect.[17] Doxorubicin, one of the most widely used anti-cancer drugs, was incorporated in nanoparticles in this study.

Nanoparticles encapsulating doxorubicin was prepared and characterized in this study. The size and charge of doxorubicin loaded nanoparticles increased after conjugation with the cLABL peptide (Table 1). The encapsulation efficiency of doxorubicin in nanoparticles was acceptable at 41 ± 4.8 % and 51 ± 7.6% when PLGA Mw~20 KDa and ~90 KDa were used to formulate nanoparticles, respectively (Table 2). After the conjugation reaction, the encapsulation efficiency was reduced by ~54 and ~47% when PLGA Mw~20 KDa and ~90 KDa w ere reacted with cLABL, respectively. However, other studies have suggested that the encapsulation efficiency may be increased by an ester linkage of the carboxylic acid end group of PLGA and the hydroxyl group of doxorubicin, which results in retention of doxorubicin during the nanoparticle preparation procedure.[27] Ultimately, doxorubicin serves as a convenient fluorescent marker for these studies and more hydrophobic drugs would likely offer improved encapsulation efficiencies.

Table 1 Nanoparticle properties prepared from PLGA 0.22 and 0.67 dl/g at specified formulation points

	Coumarin6-NP		**cLABL-coumarin6-NP**		**DOX-NP**		**cLABL-DOX-NP**	
PLGA Inherent - viscosity (dl/g)	**0.22**	**0.67**	**0.22**	**0.67**	**0.22**	**0.67**	**0.22**	**0.67**
Effective diameter (nm)	224 ± 2.7	226 ± 4.5	243 ± 6.6	241 ± 0.8	264 ± 7.8	280 ± 15.4	303 ± 3.6	286 ± 10.3
Polydispersity	0.11 ± 0.03	0.10 ± 0.05	0.05 ± 0.01	0.07 ± 0.04	0.14 ± 0.07	0.19 ± 0.01	0.15 ± 0.01	0.19 ± 0.09
Zeta potential value (mV)	-47 ± 3.1	-45 ± 2.8	-49 ± 3.8	-59 ± 2.8	-29 ± 0.4	-38 ± 3.0	-43 ± 0.6	-45 ± 3.2

Values are representative of three determinations (mean ± S.D.)

Table 2 Encapsulation efficiency (%) of coumarin-6 and doxorubicin in nanoparticles

	Encapsulation efficiency (%)			
	Coumarin6-NP	**cLABL-coumarin6-NP**	**DOX-NP**	**cLABL-DOX-NP**
PLGA 0.22 dl/g	51 ± 1.2	33 ± 5.0	41 ± 4.8	19 ± 2.1
PLGA 0.67dl/g	60 ± 2.4	37 ± 1.3	51 ± 7.6	27 ± 5.4

Values are representative of three determinations (mean ± S.D.)

Table 3 Density of cLABL on the surface of PLGA nanoparticles

	Size (nm)	**Total surface area (m^2/g of PLGA)**	**Surface cLABL (pmol/cm^2)[a]**
PLGA 0.22 dl/g	243	18.4	55 ± 0.8
PLGA 0.67dl/g	241	18.6	51 ± 2.1

Values are representative of three determinations (mean ± S.D.)

Conjugation of cLABL peptide on the surface of nanoparticles

The efficiency of the coupling reaction between the amino group of cLABL and the carboxyl of Pluronic® F-127-COOH coated on nanoparticles was determined. The amounts of free cLABL were analyzed (prior to and after the reaction) by reversed phase HPLC. The peptide density on the surface of nanoparticles encapsulating coumarin-6 was calculated from the total surface area assuming a normal Guassian particle size distribution.[28] The density of peptide on both types of nanoparticle surfaces (0.22 dl/g and 0.67 dl/g) were comparable (Table 3). The calculation showed a higher density of cLABL conjugated compared to previous studies.[28]which conjugated the peptide with polyethylene glycol (PEG)-modified poly(ethylene-alt-maleic acid) on the nanoparticle surface. This may be due to the more available carboxyl groups of Pluronic®-COOH coated on the nanoparticle surface. Therefore, the use of modified Pluronic® may reduce the steps of the conjugation reaction, and also increase the density of peptide conjugated.[28]

***In vitro* drug release study of nanoparticles encapsulating doxorubicin**

Generally the release of doxorubicin from the drug carriers was pH dependent probably due to the increase in solubility of doxorubicin at mildly acidic pH.[29, 30] The release of the drug at pH 4 and 7.4 were determined for doxorubicin encapsulated in cLABL-NP and untargeted NP. These pH values were selected to represent extracellular and lysosomal pH values. The drug release from PLGA nanoparticles was determined using PLGA inherent viscosity 0.67 dl/g in acetate buffer at pH 4 and phosphate buffer at pH 7.4. The release of doxorubicin from cLABL-DOX-NP

followed a biphasic profile regardless of pH (Figure 3). The release profile was characterized by a rapid release in the initial stage. The release of doxorubicin began with an initial burst of 35 ± 1.7% and 34 ± 2.8% from cLABL-DOX-NP at pH 4 and 7.4, respectively, in the first three hours of the study. Drug burst may result from the large surface to volume ratio of nanoparticles and from rapid loss of drug via diffusion through the polymer matrix at or near the particle surface. The initial burst phase was followed by slow and sustained release. The slower phase likely resulted from continued diffusion through the PLGA matrix.[31]

A higher amount of doxorubicin was released from unmodified PLGA nanoparticles at pH 4 compared to at pH 7.4. The release profile of the drug from NP without peptide showed a greater initial burst at pH 4 and pH 7.4 in a comparison to the conjugated peptide, i.e., 76 ± 4.4% vs 35 ± 1.7% and 53 ± 2.7% vs 34 ± 2.8%, respectively, in first three hours. The rapid release at the initial state may be due to the high aqueous solubility of the protonated form of doxorubicin at the glycosidic amine in a low pH medium.[29, 30] Interestingly, doxorubicin was released from cLABL-NP in a higher amount in higher pH medium (pH 7.4) compared with medium pH 4 as shown in Fig. 8 The more increasing release of doxorubicin from cLABL-DOX-NP in higher basic pH may have resulted from the agglomeration of the nanoparticles during the release study at pH 4. At higher pH, cLABL has higher negatively charge compared to at more acidic pH (pI~3.5). The high amount of doxorubicin released at this pH should be considered for drugs delivered by this nanoparticle formulation. The cLABL-NP would need to rapidly localize to the lung epithelium expressing ICAM-1 to avoid premature drug release supporting the

pulmonary delivery as a choice of the route of administration. Furthermore, selection of more hydrophobic chemotherapeutic agents may be appropriate.

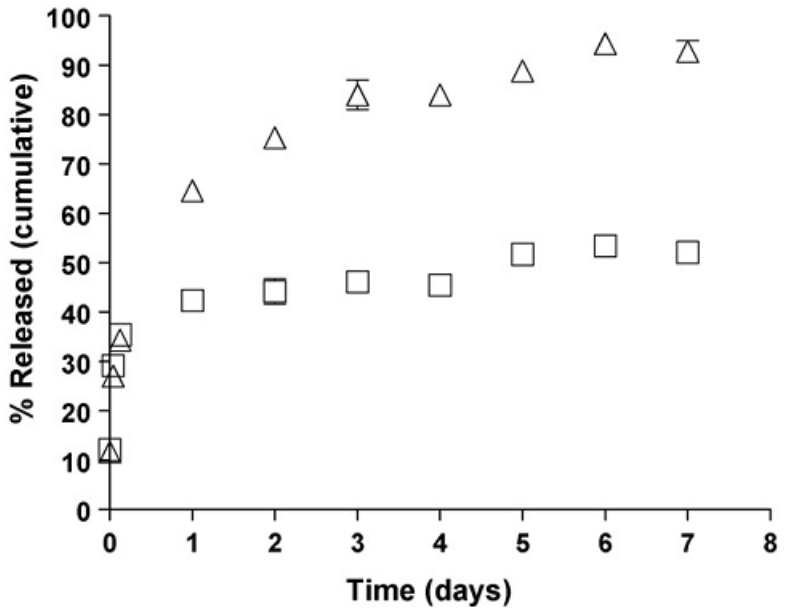

Figure 3 The release of doxorubicin from cLABL-NP began with an initial burst of 35.2±1.7% and 34.1±2.8% at pH 4 (□) and pH 7.4 (△), respectively, in the first 3 h of the study. Data are presented as mean ± S.D. (n = 3).

Cytotoxicity assay

The cytotoxicity of doxorubicin HCl, cLABL-DOX-NP and DOX-NP to A549 cells was evaluated by using MTS assay. The IC_{50} value of free doxorubicin, doxorubicin released from cLABL-NP and doxorubicin released from unconjugated NP was 60, 30 and 53 μg/ml, respectively. The cytotoxicity of doxorubicin released from nanoparticles was comparable to that of free doxorubicin. The concentrations of doxorubicin in nanoparticles were calculated from the drug loading adjusted by the encapsulation efficiency. The relative IC_{50} value of doxorubicin from each

formulation suggested that the activity of drug encapsulated in nanoparticles were not affected by the encapsulation and conjugation reaction. The IC_{50} values of cLABL-DOX-NP and DOX-NP were 3.1 and 3.3 mg/ml, respectively. PLGA NP without doxorubicin did not show any cytotoxicity up to 10 mg/mL (data not shown) suggesting that the doxorubicin is slowly released from these non-cytotoxic carriers. Modification of PLGA NPs with cLABL díd not negatively affect the cell viability

Uptake and Internalization of Nanoparticles

Pro-inflammatory cytokines such as TNF-α have previously been shown to upregulate the expression of ICAM-1.[20] Incubating A549 cells with TNF-α (1,000 U/ml) or IFN-γ (100 U/ml) resulted in about 5 fold and 4 fold increase of ICAM-1, respectively, as determined by ELISA (Figure 4). This result confirmed the overexpressed of ICAM-1 and validated the use of this cell line as an inflammatory epithelial cell model. The binding and uptake of cLABL-NP to A549 cells were found to be significantly more rapid compared to untargeted NP. The increasing fluorescence intensity demonstrated the increasing amount of nanoparticles bound or taken up by cells (Figure 5). In the presence of cLABL-NP, the fluorescence intensity was 2.3 fold higher compared to the control nanoparticles after 5 min of incubation. The difference in the uptake extent diminished when the incubation time increased. This result may indicate saturation of ICAM-1 receptors. In addition, A549 cells have been shown to endocytose nanoparticles extensively, which may explain the significant uptake of unlabeled nanoparticles.[32]

A blocking study demonstrated the inhibition of cLABL-NP binding to ICAM-1 by free cLABL and anti-ICAM-1 mAbs. The depletion of fluorescence intensity showed that the binding of cLABL-NP to ICAM-1 was impeded when free cLABL was incubated with cells first (Figure 6A) suggesting a specific binding of cLABL-NP to ICAM-1 on A549 cells.[33]In addition, a decrease in fluorescent intensity was shown when anti-ICAM-1 was pre-incubated with the cells; however, the difference was not statistically significant (Figure 6B).

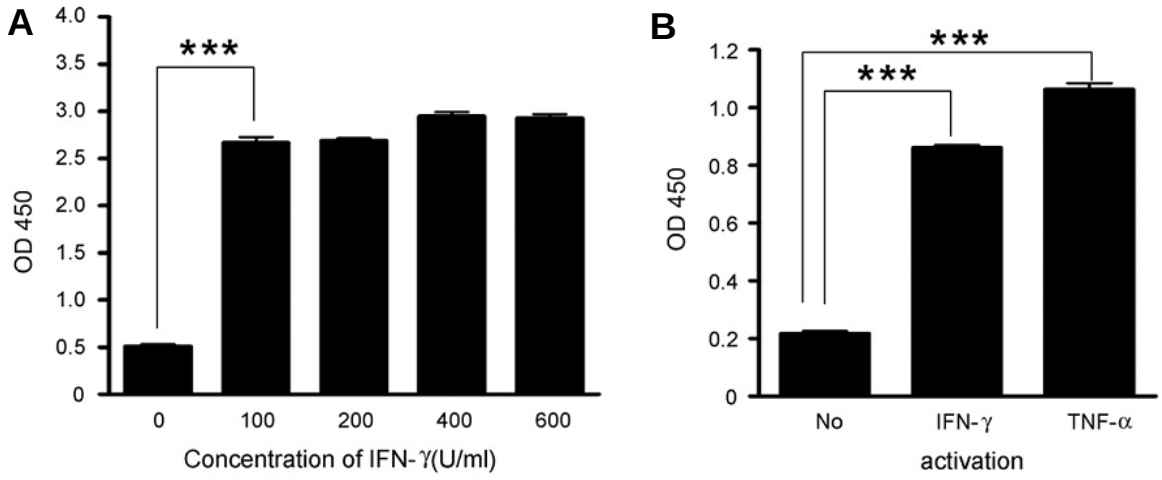

Figure 4 (A) Effect of IFN-γ on A549 ICAM-1 expression. Confluent monolayers of A549 cells were incubated 48 hr with IFN-γ (0-600 U/ml), and ICAM-1 expression was determined by ELISA. Data were presented as mean ± S.D. (*n*=3). (B) Expression of ICAM-1 activated by TNF-α (1000 U/ml) was significantly higher

than IFN-γ (100 U/ml) and non-activated A549 cells. Data are presented as mean ± S.D. (n = 3). *** indicates $p<0.001$.

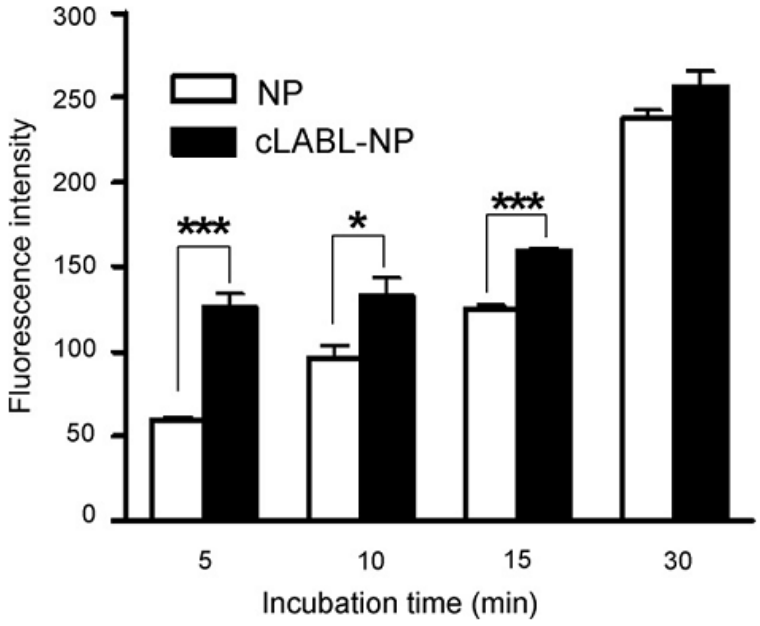

Figure 5 Fluorescent intensity of cLABL-NP was significantly higher than untargeted NP for short incubation periods. Cells were incubated with nanoparticles (0.5 mg/ml) for different time intervals to observe the uptake particles. Cell lysates were analyzed by fluorescence spectroscopy. Data are presented as mean ± S.D. (n = 3). ***$p<0.001$ and *$p<0.05$.

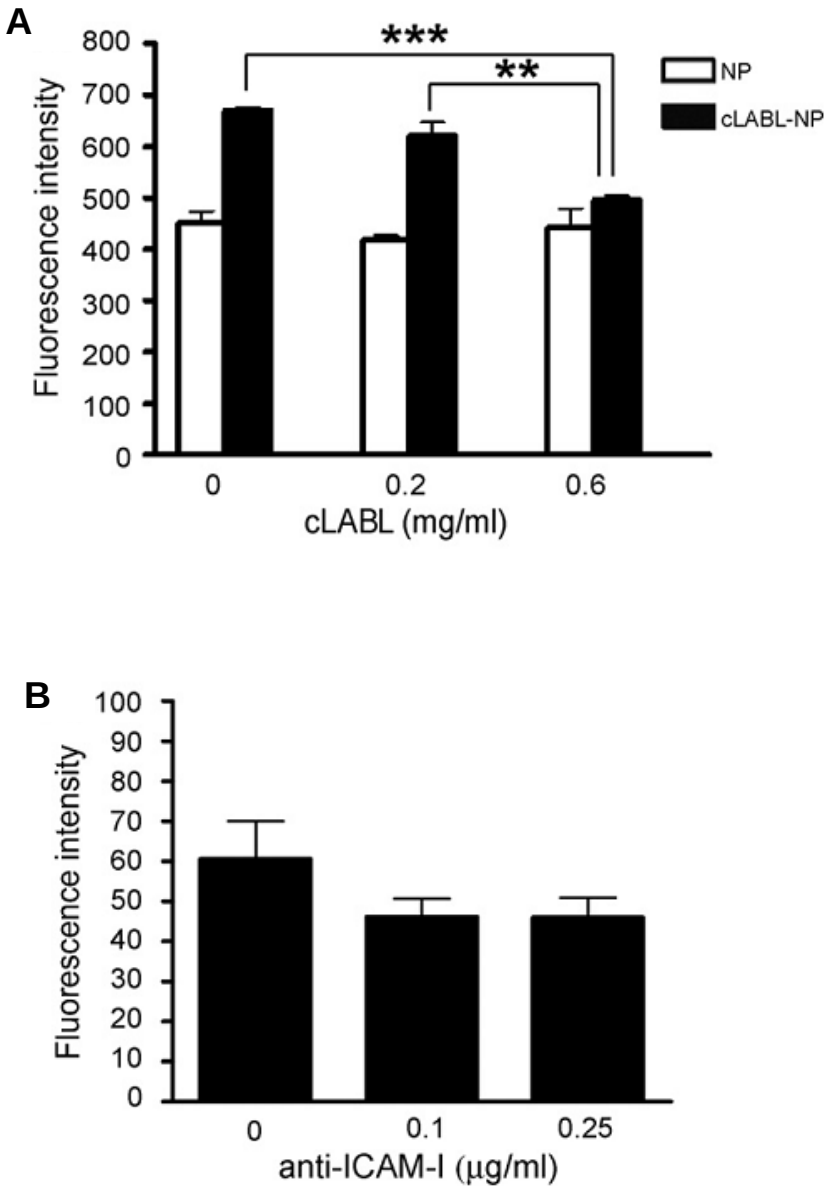

Figure 6 (A) The depletion of fluorescence intensity showed the inhibition of cLABL to the binding and internalization of cLABL-NP. Free cLABL peptide was incubated with cells for 30 min. Cell were then washed and incubated with nanoparticles for 1 hr. Cell lysates were analyzed by fluorescence spectroscopy. (B) Anti-ICAM-1 pre-incubated with cells reduced the fluorescent intensity but the difference was not statistically significant. Cells were treated with anti-ICAM-1 for 30 min, and then

incubated with nanoparticles for 1 hr. Cell lysates were analyzed by fluorescence spectroscopy. Data are presented as mean ± S.D. (n = 3). ***p<0.001 and **p<0.01.

Intracellular trafficking of cLABL-NP to lysosomes

The cLABL-NPs were observed to rapidly internalize into A549 cells after the 15 min incubation period. This rapid internalization of ICAM-1 targeting nanoparticles agreed with internalization of nanocarriers targeted using anti-ICAM-1 monoclonal antibodies studied by Muro et al (15-30 min).[34] The binding and internalization of cLABL-NP were likely induced by the multimeric nature of ICAM-1 ligands (cLABL) on the nanoparticle surface.[34] In this study, cLABL-NPs were observed to accumulate in lysosomes at 1 hr after binding to the cell surface. Subsequently, the colocalization of cLABL-NP with lysosomes steadily decreased until no colocalization was observed at 24 hr (Figure 7).

The intracellular trafficking kinetics of cLABL-NP may have advantages in comparison to unconjugated NP or free drug. Muro et al. report that the cLABL-NP spend more time in the early endosomes as described in the trafficking study of anti-ICAM-1 nanoparticles into HUVECs.[34] The result in this study revealed that internalized cLABL-NP may traffic away from lysosomes. The removal of cLABL-NP, from lysosomes was probably not due to disruption of the lysosomes because there was no change in the distribution of Texas Red conjugated dextran during 24 hr of incubation observed in this study.[35] Overall, the results suggested that the lysosomal degradation of cLABL-NP may be less pronounced by this intracellular trafficking pathway. The therapeutic activity of cytotoxic drugs may also be

prolonged by avoiding enzymatic degradation in the lysosomes by lysosomal sequestration.

Untargeted nanoparticles merged with lysosomes at 2 hr after incubation but to a lower extent compared to ICAM-1 targeted NPs (Figure 8). This result suggested that nanoparticles without peptide may be taken up more slowly than targeted NP which agrees with the result of our uptake study described above. The accumulation of untargeted NPs was also not observed at a later time point of incubation. A mechanism of escape of PLGA-NP has been proposed previously by the fact that PLGA-NP may undergo charge neutralization during trafficking.[35] The removal of particle charge was suggested to mediate membrane association leading to the escape of nanoparticles.[35]

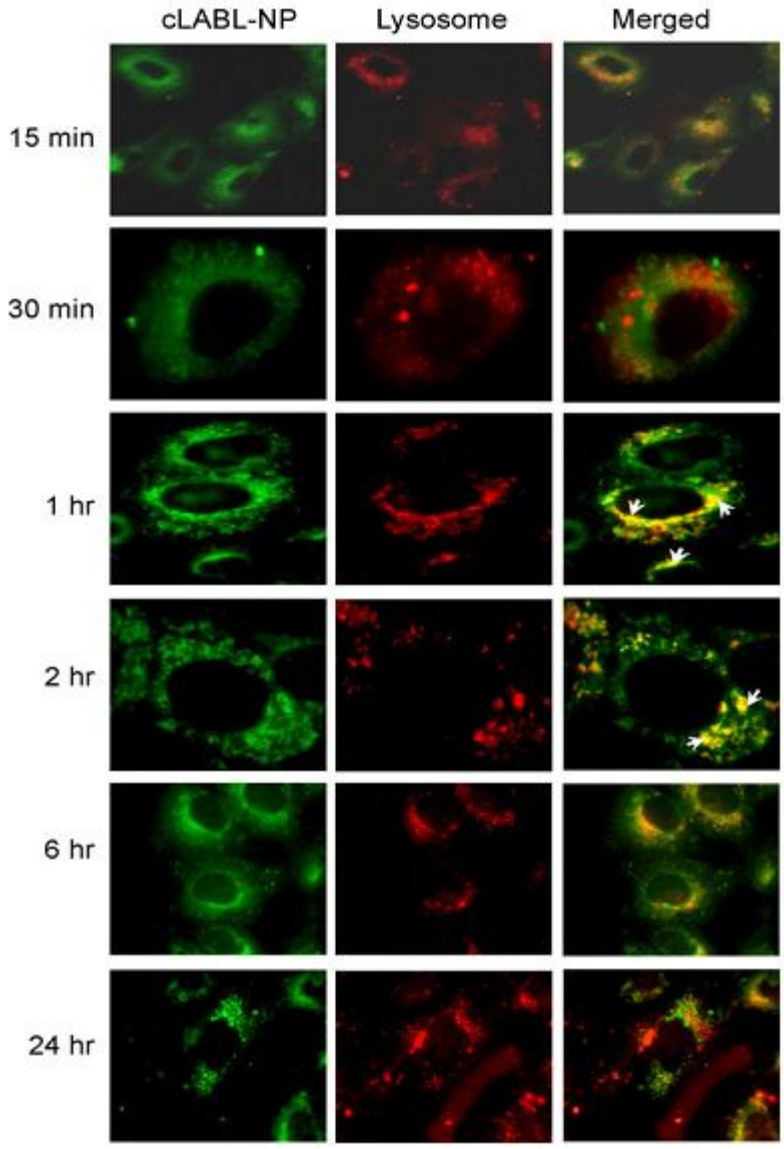

Figure 7 Localization of cLABL-NP with lysosomes (red) was observed at 1 hr after incubation with cells. The extent of colocalization decreased thereafter. Cells were incubated in the presence of cLABL-NP for 10 min, washed and incubated with serum-free medium for each time point. Selected colocalizartions of NP and lysosomes are indicated by the white arrows.

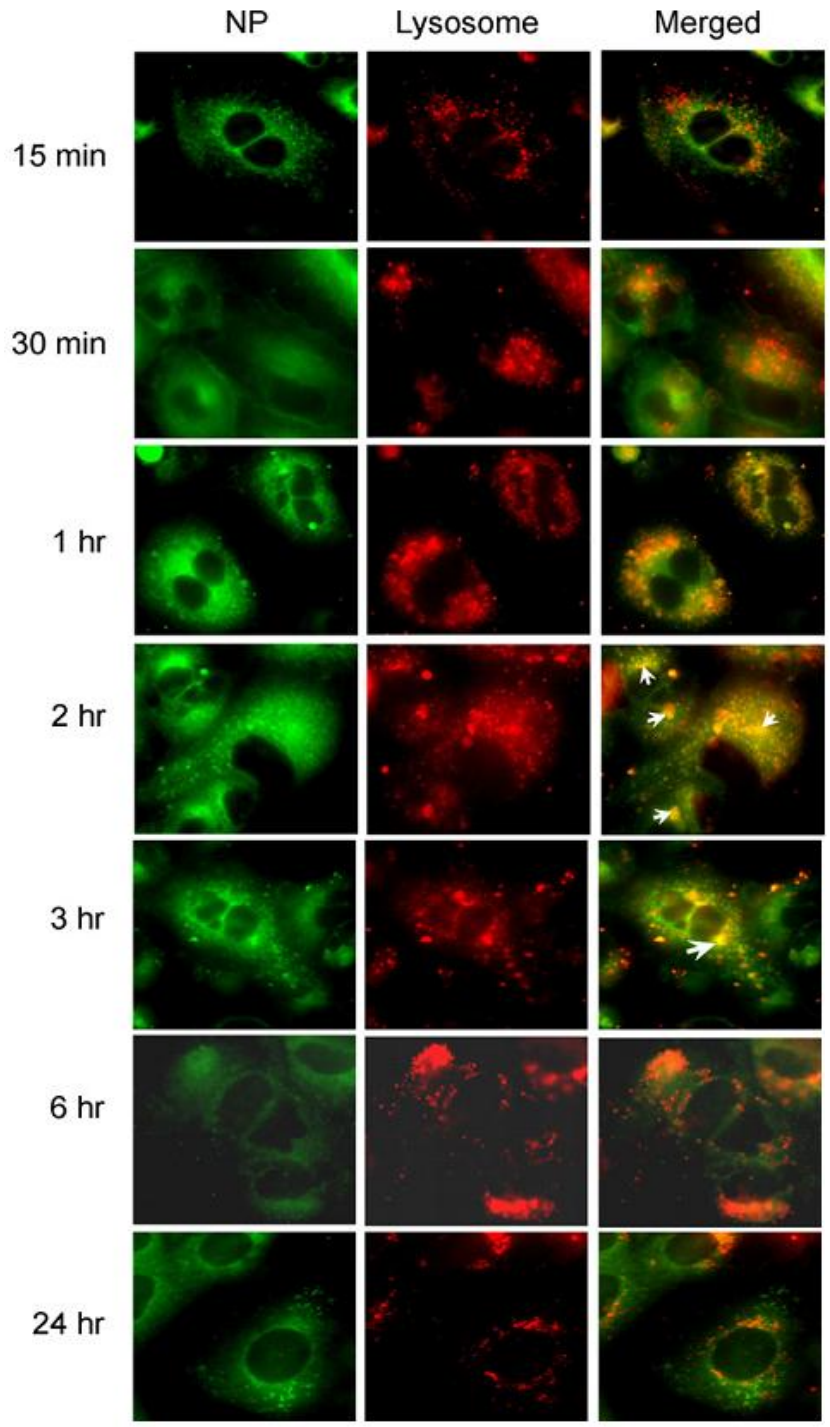

Figure 8 Colocalization of untargeted NP with lysosomes was greatly decreased compared to ICAM-1 targeted NP. Selected colocalizations of NP and lysosomes are indicated by the white arrows.

Intracellular trafficking of doxorubicin and cLABL-NP encapsulating doxorubicin

The cLABL-DOX-NP and DOX-NP were incubated with A549 cells to study intracellular trafficking. Intracellular localization of free doxorubicin, cLABL-DOX-NP and DOX-NP were investigated using fluorescence microscopy. Free doxorubicin, which is fluorescent (red), was used as a control. The nuclei of cells were stained with the blue fluorescence dye, DAPI. The photographs of cLABL-DOX-NP, DOX-NP and free doxorubicin were combined with the stained nuclei to observe the colocalization of the doxorubicin and the nuclei. The merged micrographs showed that free doxorubicin displayed rapid colocalization with the nuclei of A549 cells (in 1 hr) as expected (Figure 9A). Cells exposed to cLABL-DOX-NP exhibited a small degree of colocalization of doxorubicin and nuclei in some cells during the first hour of the study (Figure 9B). This result suggested that a small amount of doxorubicin may be released and localized in the nuclei as indicated by the faint purple color in the nuclei. The colocalization of the drug and the nuclei shown from the color combination was further observed until 24 hr. In contrast, this colocalization of doxorubicin and the nuclei was observed at later time (3 hr) for the untargeted NP (Figure 9C). Doxorubicin was also observed to localize within the nuclei until 24 hrs. In a comparison to free doxorubicin, doxorubicin encapsulated in nanoparticles was slowly released and localized in the nuclei more gradually after cellular uptake. This result provided evidence to the capability of nanoparticles to offer targeted, intracellular delivery of this cytotoxic drug and suggested the prolonged retention of doxorubicin and sustained release of drug from nanoparticles.

Also, the yellow dots in overlaid pictures of cLABL-NP or NP (green) and doxorubicin (red) confirmed the retention of doxorubicin in nanoparticles encapsulating coumarin (green) (Figure 10A and B). The colocalization of dye and drug suggested that the images show the uptake of nanoparticles containing drug and not released drug.

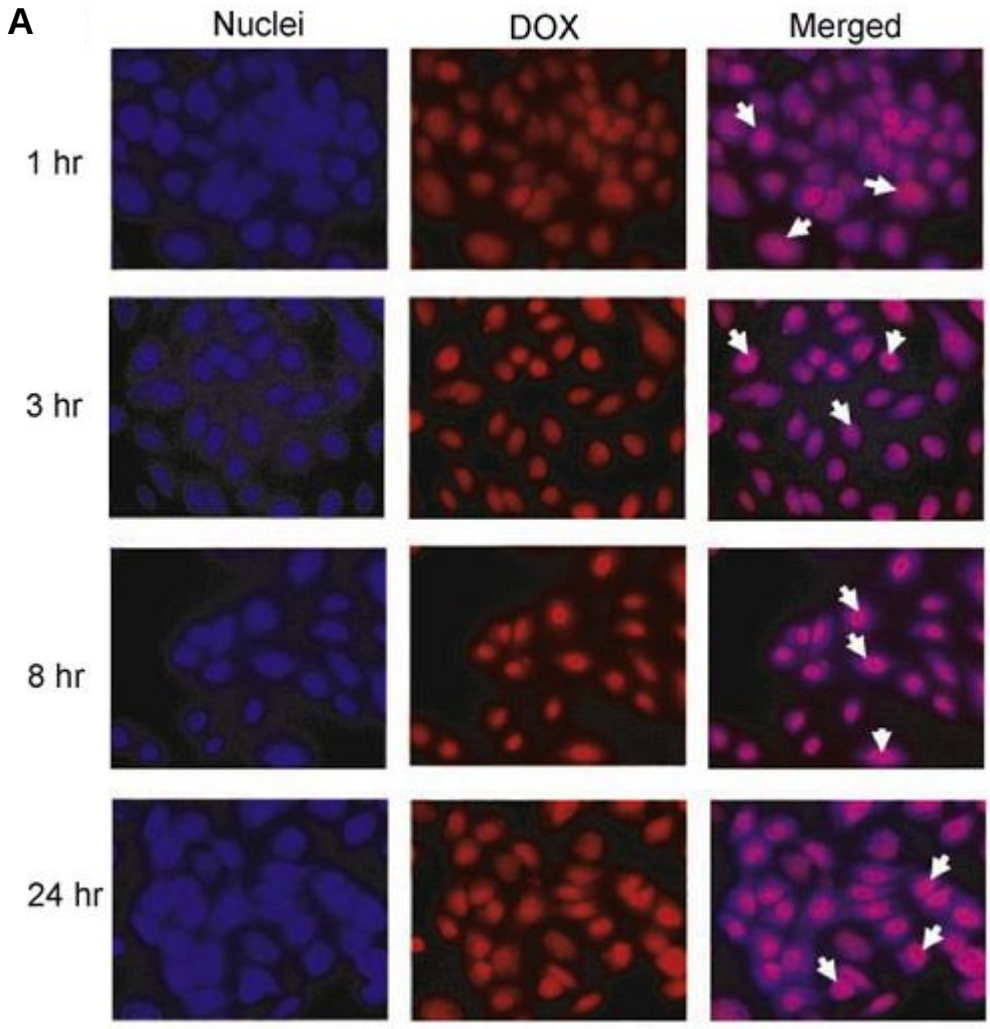

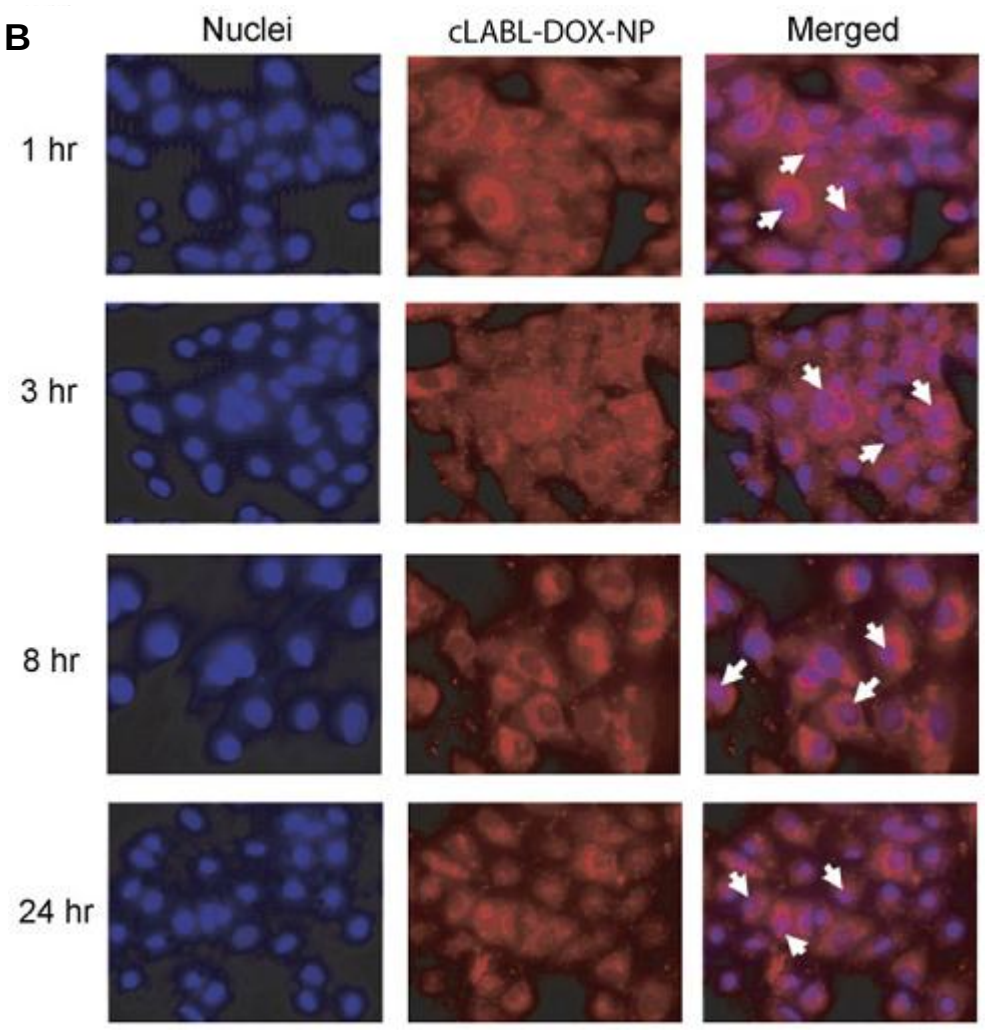
B
Nuclei
cLABL-DOX-NP
Merged
1 hr
3 hr
8 hr
24 hr

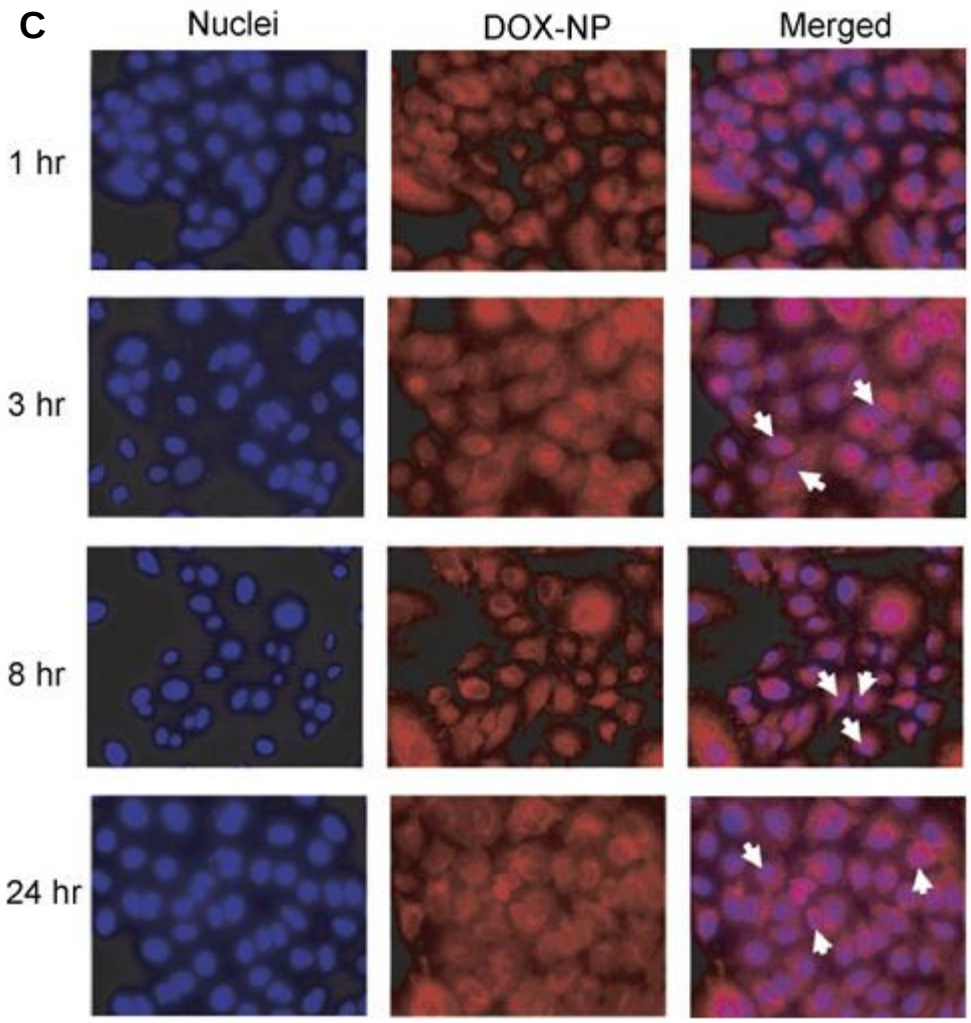

Figure 9 (A) The colocalization of doxorubicin HCl and the nuclei was observed at 1 hr after incubation of the drug with cells. (B) The colocalization of doxorubicin released from cLABL-DOX-NP was observed at 1 hr but with a less extent compared to free drug. (C) The released doxorubicin from untargeted NP localized in the nuclei was observed at 3 hrs. The white arrow indicates the colocalization.

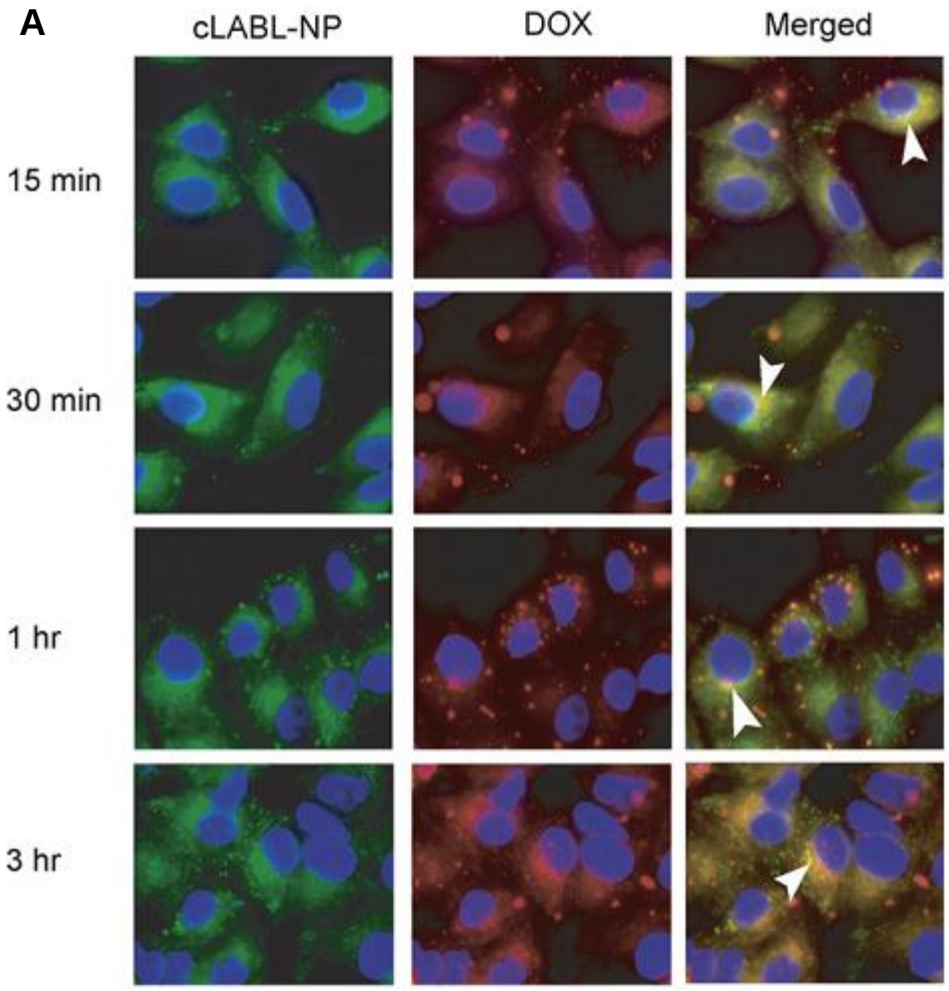
A
cLABL-NP
DOX
Merged
15 min
30 min
1 hr
3 hr

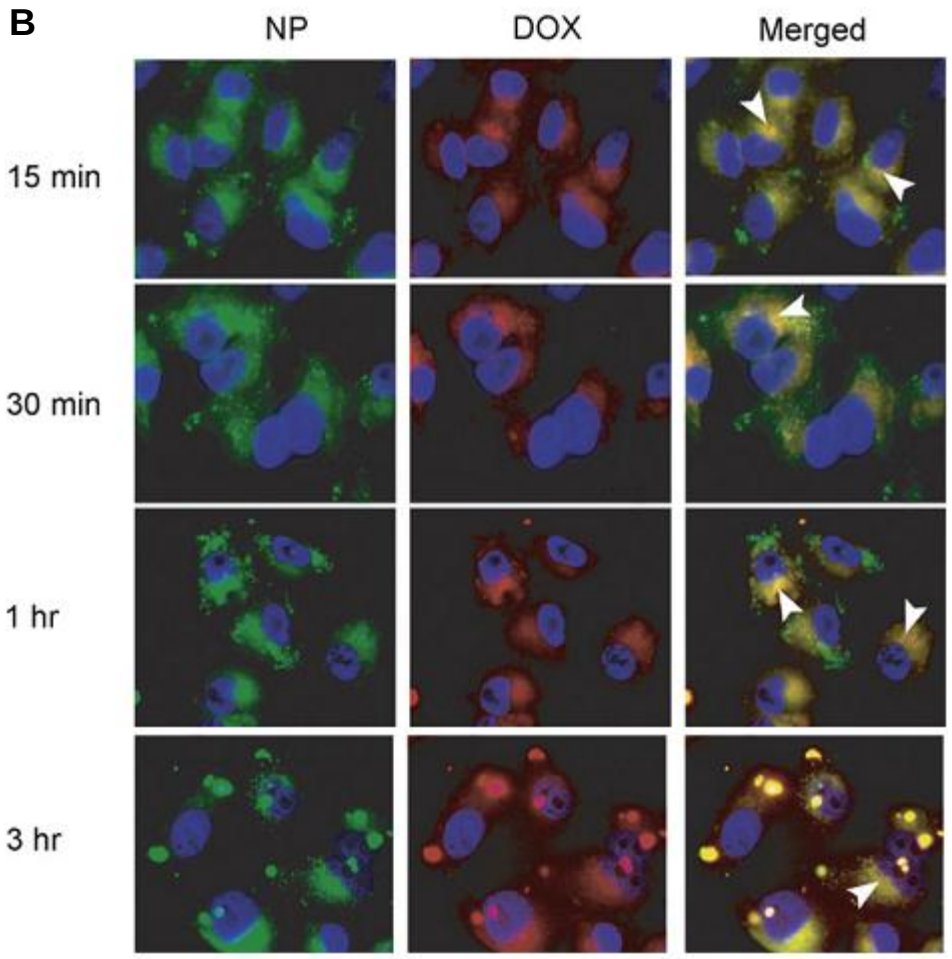

Figure 10 (A) Colocalization of doxorubicin co-encapsulated with coumarin-6 in cLABL-DOX-NP. (B) Colocalization of doxorubicin co-encapsulated with coumarin-6 in DOX-NP. The white arrow indicates the colocalization of coumarin-6 and doxorubicin.

2.4 Conclusion

This work has aimed to further develop the role of cLABL as a means of targeting PLGA NP to a molecular marker, ICAM-1, associated with inflammatory diseases and cancer. Targeted nanoparticles are of increasing interest because they may allow a reduction of adverse side effects and increase the efficacy of a drug by localizing it to the desired site of action. PLGA has advantages over other polymers due to its biodegradability, biocompatibility and approval by the FDA. Besides, PLGA NPs have provided controlled drug release in several studies, which lowered observed side effects.[15, 17, 35, 36] Here, PLGA nanoparticles targeting the immunologically active receptor, ICAM-1, were formulated by attaching the cLABL peptide to the nanoparticle surface. The cLABL-NP displayed specific binding to ICAM-1 compared to non-targeted NP. The cLABL-NPs were also more rapidly taken into A549 lung epithelial cells induced to overexpress ICAM-1. Intracellular trafficking studies showed that cLABL-NP accumulated in lysosomes for 1 hr and then left after 3 hr. Conversely, untargeted NP accumulated in lysosomes more slowly (2 hr), and also left at a later time point. cLABL-NP encapsulating doxorubicin also accumulated quickly in A549 cells. Drug release studies indicated that the cLABL-NP formulated with a high Mw PLGA exhibited sustained drug release that depended on pH. Finally, the cytotoxicity study of cLABL-NP and NP compared to free doxorubicin HCl showed similar IC_{50} values suggesting that the activity of the drug released from nanoparticles was retained. These studies verified that cLABL can target nanoparticles to lung epithelial cells to deliver chemotherapeutics and provide

controlled release drug delivery. The effectiveness of targeted delivery *in vivo* must be inquired in future studies.

References

1. Yusuf-Makagiansar H, Anderson ME, Yakovleva TV, Murray JS, & Siahaan TJ (2002) Inhibition of LFA-1/ICAM-1 and VLA-4/VCAM-1 as a therapeutic approach to inflammation and autoimmune diseases. *Med Res Rev,* 22,146-167.

2. Hopkins AM, Baird AW, & Nusrat A (2004) ICAM-1: targeted docking for exogenous as well as endogenous ligands. *Adv Drug Deliv Rev,* 56, 763-778.

3. Wojcikiewicz EP, Zhang X, Chen A, & Moy VT (2003) Contributions of molecular binding events and cellular compliance to the modulation of leukocyte adhesion. *J Cell Sci,* 116, 2531-2539.

4. McDowall A, Leitinger B, Stanley P, Bates PA, Randi AM & Hogg N (1998) The I domain of integrin leukocyte function-associated antigen-1 is involved in a conformational change leading to high affinity binding to ligand intercellular adhesion molecule 1 (ICAM-1). *J Biol Chem,* 273, 27396-27403.

5. Dunehoo AL, Anderson M, Majumdar S, Kobayashi N, Berkland C & Siahaan TJ (2006) Cell adhesion molecules for targeted drug delivery. *J Pharm Sci,* 95, 1856-1872.

6. Yusuf-Makagiansar H, Makagiansar IT, Hu Y, & Siahaan TJ (2001) Synergistic inhibitory activity of alpha- and beta-LFA-1 peptides on LFA-1/ICAM-1 interaction. *Peptides,* 22, 1955-1962.

7. Melis M, Spatafora M, Melodia A, Pace E, Gjomarkaj M, Merendino AM & Bonsignore G (1996) ICAM-1 expression by lung cancer cell lines: effects of upregulation by cytokines on the interaction with LAK cells. *Eur Respir J,* 9, 1831-1838.

8. Anderson ME & Siahaan TJ (2003) Mechanism of binding and internalization of ICAM-1-derived cyclic peptides by LFA-1 on the surface of T cells: a potential method for targeted drug delivery. *Pharm Res,* 20, 1523-1532.

9. Anderson ME, Yakovleva T, Hu Y, & Siahaan TJ (2004) Inhibition of ICAM-1/LFA-1-mediated heterotypic T-cell adhesion to epithelial cells: design of ICAM-1 cyclic peptides. *Bioorg Med Chem Lett,* 14, 1399-1402.

10. Anderson ME & Siahaan TJ (2003) Targeting ICAM-1/LFA-1 interaction for controlling autoimmune diseases: designing peptide and small molecule inhibitors. *Peptides,* 24, 487-501.

11. Yusuf-Makagiansar H & Siahaan TJ (2001) Binding and internalization of an LFA-1-derived cyclic peptide by ICAM receptors on activated lymphocyte: a potential ligand for drug targeting to ICAM-1-expressing cells. *Pharm Res,* 18, 329-335.

12. Yusuf-Makagiansar H, Yakovleva TV, Tejo BA, Jones K, Hu Y, Verkhivker GM, Audus KL & Siahaan TJ (2007) Sequence recognition of alpha-LFA-1-derived peptides by ICAM-1 cell receptors: inhibitors of T-cell adhesion. *Chem Biol Drug Des*, 70, 237-246.

13. Tibbetts SA, Seetharama Jois D, Siahaan TJ, Benedict SH, & Chan MA (2000) Linear and cyclic LFA-1 and ICAM-1 peptides inhibit T cell adhesion and function. *Peptides,* 21, 1161-1167.

14. Huang M, Matthews K, Siahaan TJ, & Kevil CG (2005) Alpha L-integrin I domain cyclic peptide antagonist selectively inhibits T cell adhesion to pancreatic islet microvascular endothelium. *Am J Physiol Gastrointest Liver Physiol* , 288, G67-73.

15. Avgoustakis K (2004) Pegylated poly(lactide) and poly(lactide-co-glycolide) nanoparticles: preparation, properties and possible applications in drug delivery. *Curr Drug Deliv*, 1, 321-333.

16. Guerrouache M, Karakasyan, C., Gaillet, C., Canva, M., Millot, M.C (2006) Immobilization of a functionalized poly(ethylene glycol) onto b-cyclodextrin-coated surfaces by formation of inclusion complexes: application to the coupling of proteins. *J Applied Polym Sci*, 100, 2362-2370.

17. Kim J, Park S, Lee JE, Jin SM, Lee JH, Lee IS, Yang I, Kim JS, Kim SK, Cho MH & Hyeon T (2006) Designed fabrication of multifunctional magnetic gold nanoshells and their application to magnetic resonance imaging and photothermal therapy. *Angew Chem Int Ed Engl*, 45, 7754-7758.

18. Cheng J, Teply BA, Sherifi I, Sung J, Luther G, Gu FX, Levy-Nissenbaum E, Radovic-Moreno AF, Langer R & Farokhzad OC (2007) Formulation of functionalized PLGA-PEG nanoparticles for in vivo targeted drug delivery. *Biomaterials,* 28, 869-876.

19. Missirlis D, Kawamura R, Tirelli N, & Hubbell JA (2006) Doxorubicin encapsulation and diffusional release from stable, polymeric, hydrogel nanoparticles. *Eur J Pharm Sci,* 29, 120-129.

20. Konno S, Grindle KA, Lee WM, Schroth MK, Mosser AG, Brockman-Schneider RA, Busse WW & Gern JE (2002) Interferon-gamma enhances rhinovirus-induced RANTES secretion by airway epithelial cells. *Am J Respir Cell Mol Biol,* 26, 594-601.

21. Davda J & Labhasetwar V (2002) Characterization of nanoparticle uptake by endothelial cells. *Int J Pharm,* 233, 51-59.

22. Koefod RS, Mann, K.R (1991) Common emissive intermediates in the thermal and photochemical reactions of nonemissive cyclopentadienylruthenium (II) complexes of coumarin laser dyes. *Inorg. Chem,* 30, 221-228.

23. Hirota Y, Masuyama N, Kuronita T, Fujita H, Himeno M & Tanaka Y (2004) Analysis of post-lysosomal compartments. *Biochem Biophys Res Commun,* 314, 306-312.

24. Duvvuri M & Krise JP (2005) A novel assay reveals that weakly basic model compounds concentrate in lysosomes to an extent greater than pH-partitioning theory would predict. *Mol Pharm,* 2, 440-448.

25. Kabanov AV & Alakhov VY (2002) Pluronic block copolymers in drug delivery: from micellar nanocontainers to biological response modifiers. *Crit Rev Ther Drug Carrier Syst,* 19, 1-72.

26. Kurosawa G, Akahori Y, Morita M, Sumitomo M, Sato N, Muramatsu C, Eguchi K, Matsuda K, Takasaki A, Tanaka M, Iba Y, Hamada-Tsutsumi S, Ukai Y, Shiraishi M, Suzuki K, Kurosawa M,Fujiyama S, Takahashi N, Kato R, Mizoguchi Y, Shamoto M, Tsuda H, Sugiura M, Hattori Y, Miyakawa S, Shiroki R, Hoshinaga K, Hayashi N, Sugioka A & Kurosawa Y (2008) Comprehensive screening for antigens overexpressed on carcinomas via isolation of human mAbs that may be therapeutic. *Proc Natl Acad Sci,* 105, 7287-7292.

27. Yoo HS, Lee KH, Oh JE, & Park TG (2000) In vitro and in vivo anti-tumor activities of nanoparticles based on doxorubicin-PLGA conjugates. *J Control Release*, 68, 419-431.

28. Zhang N, Chittasupho C, Duangrat C, Siahaan TJ, & Berkland C (2008) PLGA nanoparticle--peptide conjugate effectively targets intercellular cell-adhesion molecule-1. *Bioconjug Chem,* 19, 145-152.

29. Gillies ER & Frechet JM (2005) pH-Responsive copolymer assemblies for controlled release of doxorubicin. *Bioconjug Chem,* 16, 361-368.

30. Kataoka K, Matsumoto T, Yokoyama M, Okano T, Sakurai Y, Fukushima S, Okamoto K & Kwon GS (2000) Doxorubicin-loaded poly(ethylene glycol)-poly(beta-benzyl-L-aspartate) copolymer micelles: their pharmaceutical characteristics and biological significance. *J Control Release,* 64, 143-153.

31. Holgado MA, Arias JL, Cózar MJ, Alvarez-Fuentes J, Gañán-Calvo AM & Fernández-Arévalo M (2008) Synthesis of lidocaine-loaded PLGA microparticles by flow focusing. Effects on drug loading and release properties. *Int J Pharm,* 358, 27-35.

32. Foster KA, Yazdanian M, & Audus KL (2001) Microparticulate uptake mechanisms of in-vitro cell culture models of the respiratory epithelium. *J Pharm Pharmacol,* 53, 57-66.

33. Muro S, Gajewski C, Koval M, & Muzykantov VR (2005) ICAM-1 recycling in endothelial cells: a novel pathway for sustained intracellular delivery and prolonged effects of drugs. *Blood,* 105, 650-658.

34. Muro S, Cui X, Gajewski C, Murciano JC, Muzykantov VR & Koval M (2003) Slow intracellular trafficking of catalase nanoparticles targeted to ICAM-1 protects endothelial cells from oxidative stress. *Am J Physiol Cell Physiol,* 285, C1339-1347.

35. Panyam J, Zhou WZ, Prabha S, Sahoo SK, & Labhasetwar V (2002) Rapid endo-lysosomal escape of poly(DL-lactide-co-glycolide) nanoparticles: implications for drug and gene delivery. *FASEB J,* 16, 1217-1226.

36. Keegan ME, Falcone, J.L., Leung, T.C., Saltzman, W.M. (2004) Biodegradable microspheres with enhanced capacity for covalently bound surface ligands. *Macromolecules,* 37, 977

Chapter 3

cIBR effectively targets nanoparticles to LFA-1 on acute lymphoblastic T cells

3.1 Introduction

Leukocytes play an important role in disease defense and participate in the adaptive immune response. Under normal conditions, leukocytes circulate between the blood stream and the lymphatic system as non-adherent cells.[1] Upon receiving signals from inflammatory mediators, various cell adhesion molecules are up-regulated and leukocytes are recruited to the vascular endothelium.[1] Leukocytes selectively accumulate at sites of inflammation via this multivalent adhesion mechanism and subsequently migrate into underlying tissues.[2] Several adhesion molecules mediate the process including members of the integrin family and their immunoglobulin (Ig) superfamily ligands.[1, 3] The recruitment of leukocytes from the blood stream to the inflammatory site involves a multistep adhesion cascade (e.g. tethering, rolling, activation and arrest). The integrins playing a major role during arresting and transmigration are LFA-1, $\alpha_4\beta_1$ and $\alpha_4\beta_7$ which bind to members of the immunoglobulin superfamily on endothelium such as ICAM-1.[4] In inflammatory diseases, the extravasation of leukocytes into the inflammed tissues ultimately propagates further inflammation which may lead to a chronic disease state. LFA-1 has emerged as an interesting target for treatment of inflammatory diseases and drug delivery.

LFA-1 is constitutively expressed in a low affinity conformation on the plasma membrane of leukocytes.[5]The ligand binding activity of LFA-1 is tightly regulated. LFA-1 activation results in an increase in the affinity for ligand induced by a conformational change, and clustering of integrins on the cell surface.[4] Rolling leukocytes respond to chemokines on vascular endothelial cells by expressing

specific receptors that transmit intracellular signals through G proteins.[4] Chemokine receptor signaling changes the conformation of LFA-1 from a closed form (low affinity conformation) on the T-cell surface to open form (high affinity conformation) and hence enables T-cells to adhere and then migrate across the vascular wall. LFA-1 clustering is initiated by lateral migration of integrins to form multivalent binding foci, thus strengthening the adhesion.[6]

Leukocytes express molecules from the β_2 integrin subfamily which includes leukocyte function associated antigen-1 (LFA-1, $\alpha_L\beta_2$, CD11a/CD18), MAC-1 (CD11b/CD18) and P150, 95 (CD11c/CD18). These molecules mediate binding to the intercellular adhesion molecule-1 (ICAM-1) Ig superfamily.[2, 3] ICAM-1 (CD54) is the major LFA-1 ligand expressed on endothelial cells, epithelial cells and on antigen presenting cells (APC). ICAM-1 is up-regulated by proinflammatory cytokines such as IL-1, IL-4, IL-6, TNF-α and IFN-γ during inflammation. LFA-1 binds to ICAM-1 via specific interaction between the I domain of LFA-1 and domain 1 (D1) of ICAM-1. Blockade of this molecular interaction using monoclonal antibodies has been shown be efficacious against acute inflammation[7], and autoimmune diseases such as diabetes[8], rheumatoid arthritis [9] and psoriasis[10, 11] in addition to suppressing allograft rejection.[12, 13]

Here, a small peptide antagonist known to allosterically block binding of ICAM-1 to LFA-1 was used as a targeting ligand for nanoparticles.[14] cIBR (cyclo 1,12) Pen-PRGGSVLVTGC-OH is a cyclic peptide derived from D1 of ICAM-1. NMR, docking experiments and competitive inhibition by anti-LFA-1 have shown that the binding site of cIBR is on the I domain of LFA-1.[14-16] cIBR has been

characterized to bind to the L site of the I domain of PMA activated LFA-1.[14] This peptide has been shown to interfere with T cell homotypic and heterotypic adhesion and with mixed lymphocyte reaction.[16-18] Interestingly, cIBR has been reported to be internalized by LFA-1 integrin on the surface of T cells, but not internalized into LFA-1 deficient cell lines[14-15, 19], suggesting that cIBR could be used as a targeting ligand for selective intracellular drug delivery to leukocytes.

LFA-1 mediated adhesion is mediated by integrin clustering in addition to the activation of this receptor. Although the mechanism of clustering remains to be clarified[6], receptor clustering appears to be the consequence of an initial high affinity interaction of LFA-1 with multivalent ICAM-1.[5-6] Multivalent interactions of multiple ligands on nanoparticles can increase the binding avidity by orders of magnitude.[20] In this study, cIBR peptide was conjugated to the surface of nanoparticles to mimic the clustering of ICAM-1 and hence increase the avidity of binding to LFA-1 on T-cells. cIBR conjugated nanoparticles (cIBR-NPs) bound to LFA-1 on T-cells (Molt-3) more rapidly and to a greater extent compared to untargeted nanoparticles. In addition, cIBR-NPs were shown to block the adhesion of Molt-3 cells to A549 lung epithelial cells. These findings suggest a potential dual therapeutic mechanism for cIBR-NPs to control inflammatory diseases by blocking leukocyte adhesion and by targeting the delivery of drugs (e.g. anti-inflammatory agents).

3.2 Materials and methods

Materials

cIBR peptide (Cyclo(1,12)-Pen-PRGGSVLVTGC-OH) (Mw 1,174.5) was synthesized on a Pioneer peptide synthesizer (PerSeptive Biosystems, CA). Poly(DL-lactic-co-glycolic acid) (50:50) with terminal carboxyl group (PLGA, inherent viscosity 0.67dL/g, Mw ~90 kDa) was purchased from LACTEL Absorbable Polymers International (Pelham, AL, USA). Pluronic®F-127, Texas Red Dextran (10,000 kDa, lysine fixable) and 2',7'-bis-(2-carboxyethyl)-5-(and-6)-carboxyfluorescein, acetoxymethyl ester (BCECF, AM) were purchased from Invitrogen Molecular Probes, Inc. (Carlsbad, CA, USA). Coumarin-6 was obtained from Polysciences, Inc. (Warrington, PA, USA). Dialysis membrane (MwCO 100,000) was purchased from Spectrum laboratory Products Inc. (Rancho Dominguez, CA, USA). RPMI 1640 medium, A549 cell line and the Molt-3 cell line were obtained from American Type Culture Collection (Manassas, VA, USA). Phorbol 12-myristate 13-acetate (PMA) was purchased from BIOMOL International, L.P. (Plymouth Meeting, PA).

Methods

PLGA nanoparticle preparation and characterization

Nanoparticles encapsulating a fluorescent marker, coumarin-6, were formulated using a solvent displacement method.[21] In brief, PLGA was dissolved in acetone (18 mg/ml) containing coumarin-6 (50 μg/ml). The solution was slowly transferred to a water phase containing 0.1% Pluronic®F-127-COOH (25 ml) under mild stirring (300 RPM). Terminal hydroxyl groups on Pluronic®F-127 were converted to carboxyl groups according to a reported procedure.[22-23] The nanoparticles spontaneously

formed due to the rapid removal of acetone. Excess surfactant was removed by dialysis against a 0.2% mannitol solution for 48 hrs.

A series of PLGA nanoparticles encapsulating coumarin-6 were formulated according to the above procedure. For the preparation of nanoparticles coated with various ratios of carboxylic acid functional group of Pluroinic F127 surfactant, 0%, 25%, 50% and 100% of 0.1% Pluronic®-COOH solution were mixed with 100%, 75%, 50% and 0% of 0.1% Pluronic®-OH solution, respectively.

Conjugation of cIBR peptide to PLGA-nanoparticles

Pluronic®F-127-COOH coated PLGA nanoparticles (2.2 mg/ml) were buffered using 2-(*N*-morpholino)ethanesulfonic acid (MES; pH 6.5). Nanoparticles were then incubated with 100 mM 1-Ethyl-3-[3-dimethylaminopropyl]carbodiimide hydrochloride (EDC) and 50 mM *N*-hydroxysulfosuccinimide (sulfo-NHS) for 15 min.[23]The activated carboxyl terminus of Pluronic® F127-COOH on the surface of nanoparticles was allowed to react with the amino terminus of the cIBR peptide (170 μM) at least 12 hrs at room temperature. Conjugated NPs were collected by centrifugation (16,089 g, 10 min) and washed three times with purified water. The size and charge of NPs and cIBR-NPs were characterized using dynamic light scattering (ZetaPALS, Brookhaven instrument Inc.).

The amount of free cIBR after the reaction was quantified by gradient reversed phase HPLC (SHIMADZU) using a C_{18} column. The HPLC consisted of SCL-10A SHIMADZU system controller, LC-10AT VP SHIMADZU liquid chromatograph, SIL-10A XL SHIMADZU autoinjecter set at 10 μl injection volume,

DGU-14A SHIMADZU degasser, sample cooler, and SPD-10A SHIMADZU UV-Vis detector (220 nm). The HPLC-UV system was controlled by a personal computer equipped with SHIMADZU class VP Software. All separations were carried out using a Vydac® HPLC Protein and Peptide C_{18} column. Gradient elution was carried out at constant flow of 1 ml/min, from 100% A to 0% A (corresponding to 0% B to 100% B) for 15 min, followed by an isocratic elution at 100% B for 3 min. Mobile phase compositions were (A) acetronitrile-water (5:95) with 0.1% TFA and (B) acetonitrile–water (90:10, v/v) with 0.1% trifluoroacetic acid (TFA). At the end of each analysis, the cartridge was re-equilibrated at 1 ml/min flow rate for 13 min with A. The density of peptide on the surface of nanoparticles was calculated from the total surface area assuming a normal Guassian particle size distribution.

Stimulation of LFA-1 by phorbol 12-myristate 13-acetate (PMA)

The Molt-3 cell line (1 x 10^6 cells/ml) was stimulated using 0.4 μM of PMA for 20 hrs. According to previous reports, PMA is able to activate LFA-1 and improve binding to ICAM-1.[24] Cells at the same concentration were not activated and used as a control. Molt-3 cells, with or without PMA stimulation were incubated with anti-LFA-1-FITC (0, 0.05 and 0.1 mg/ml) at 4 ºC for 45 min. Free antibodies were removed by rinsing three times with PBS after centrifugation (595 g, 1.5 min). The fluorescent intensity of cells was analyzed by flow cytometry. In addition, the specificity of anti-LFA-1-FITC was confirmed by incubation with A549 cells, which express ICAM-1 but not LFA-1. A549 were cultured as previously reported.[23] Molt-3 cells co-express LFA-1 and ICAM-1. Both cells were incubated with 0.4 μM of PMA at 37°C for 20 hrs. Anti-LFA-1-FITC (0.05 mg/ml) was incubated with Molt-3 cells

for 45 min at 4°C. Cells were washed three times with PBS and centrifuged (595 g,1.5 min) The fluorescent intensity of Molt-3 cells was determined by using a FACscan flow cytometer. Data analysis was performed using Cell Quest software (BD).

Binding and uptake of cIBR-NPs into Molt-3 cells

The binding and uptake of cIBR-NPs encapsulated fluorescent dye was studied by using flow cytometry. PMA stimulated Molt-3 cells (1 x 10^6 cells/ml) were added in a 96 well-plate (200 μl/well) containing $CaCl_2$ (1.5 mM) and incubated with cIBR-NPs or NPs encapsulating coumarin-6 (2.2 mg/ml, 90 μl) at 37 °C for 5, 15, 20 and 35 min. Cells were then repeatedly centrifuged (460 g, 4°C for 1 min) and washed three times with cold PBS and fixed with 4% paraformaldehyde. The fluorescent intensity of cells was measured using the FACscan flow cytometer. Data analysis was performed using Cell Quest software (BD). To investigate whether the uptake was dependent on the nanoparticle concentration, Molt-3 cells (1 x 10^6 cells/ml, 100 μl) in serum free media were added to a 96 well-plate containing $CaCl_2$ (1.5 mM) followed by incubation with cIBR-NPs (70 μl/well) at 37 °C for 30 min at various concentrations (0.08, 0.16, 0.33, 0.66, 1.31, 2.63, 5.25 and 10.50 mg/ml). Cells were washed three times with cold PBS by centrifugation at 460 g, 4°C for 1 min. The fluorescent intensity of the Molt-3 cells was again determined using the FACscan flow cytometer. Data analysis was performed as before.

The binding and uptake of cIBR-NPs prepared by using various amounts of Pluronic® F127-COOH by Molt-3 cells was observed and compared using flow

cytometry. Molt-3 cell line (2 x 10^6 cells/ml) was stimulated using 0.4 μM of PMA to activate LFA-1 and improve binding to ICAM-1.[24]PMA stimulated Molt-3 cells (2 x 10^6 cells/ml) were added in microcentrifuge tubes (100 μl) containing $CaCl_2$ (1.5 mM) and incubated with NPs or cIBR-NPs possessing various amounts of cIBR peptides (2.7 mg/ml, 100 μl) at 37 °C for 5, 15, 30 and 60 min. Cells were repeatedly centrifuged (460 g, 4°C for 1 min) and washed three times with cold PBS and fixed with 4% paraformaldehyde. The fluorescent intensity of cells was measured using the FACscan flow cytometer.

Inhibition of the binding of cIBR-NPs

cIBR-NPs were hypothesized to bind to the I domain of LFA-1, a binding site of cIBR peptide.[14-16] The binding site of cIBR-NPs was studied by blocking with cIBR. LFA-1 on Molt-3 (4 x 10^4 cells/ml) was stimulated by PMA (0.4 μM) for 20 hrs. Cells were added to a 96-well plate (100 μl) containing $CaCl_2$ (1.5 mM). Free cIBR at various concentrations (0.0, 0.31, 0.63, 1.2 and 2.5 mg/ml, 80 μl) was incubated with cells for 40 min at 4°C to inhibit the binding of cIBR-NPs or NPs to LFA-1. Cells were then incubated with cIBR-NPs or untargeted NPs (2.2 mg/ml, 80 μl) at 4°C for 40 min. Cells were rinsed three times with cold PBS by centrifugation (460 g, 1 min, 4°C), fixed with 4% paraformaldehyde and again analyzed by flow cytometry .

To further investigate whether the binding site of cIBR-NPs is LFA-1 I domain or not, free LFA-1 I domain was used to block the binding of cIBR-NPs to LFA-1 on plasma membrane of Molt-3 cells. The LFA-1 I domain was dissolved in water at various concentrations, 0, 0.31, 0.63 1.25 and 2.50 mg/ml and was mixed

with cIBR-NPs (2.1 mg/ml, 80 μl) at 37 ºC for 1 hr. After incubation, Molt-3 cells (1x 10^6 cells/ml) were added (100 μl) into the mixture and incubated at 37 ºC for 40 min. Cells were pelleted by centrifugation (460 g, 1 min, 4°C) and free cIBR-NPs and the I domain were removed by three centrifugation/washing cycles. Cells were fixed using 4% paraformaldehyde. The binding of cIBR-NPs to the cells was determined from the fluorescent intensity analyzed by flow cytometry using the specified data analysis.

The specificity of I domain in the inhibition of cIBR-NP uptake was investigated by incubating BSA (0, 0.31, 0.63 1.25 and 2.50 mg/ml) with cIBR-NP (2.1 mg/ml, 80 μl) at 37 ºC for 1 hr. After incubation, Molt-3 cells (1x 10^6 cells/ml) were added (100 μl) into the mixture and incubated at 37 ºC for 40 min to allow binding of cIBR-NP to LFA-1 of cells. Free cIBR-NP and BSA were washed three times with PBS. Cells were fixed with 4% paraformaldehyde. The binding of cIBR-NP to the cells was determined from the fluorescent intensity analyzed by flow cytometry.

Temperature effects on the binding and internalization of cIBR-NPs and NPs

The energy-dependent internalization of cIBR-NPs into Molt-3 cells was investigated in this study. Molt-3 cells (1.1 x 10^6 cells/ml) were added to a 96 well plate (100 μl /well) and incubated with serum free medium containing 1.5 mM $CaCl_2$ for 40 min at 4°C and 37°C followed by incubation with cIBR-NPs or NPs (2.2 mg/ml, 90 μl/well) for 5, 15, 25, 35 and 45 min. Cells were then washed three times with PBS and fixed

with 4% paraformaldehyde. The uptake of cIBR-NPs or NPs by cells was determined from the fluorescent intensity analyzed using flow cytometry as before.

Fluorescence microscopy of the uptake of cIBR-NPs by Molt-3 cells

Fluorescence microscopy was performed to compare the extent of binding and uptake of cIBR-NPs and untargeted NPs in Molt-3 cells. Molt-3 cells (1×10^6 cells/ml) were activated by using 0.4 μM PMA for 24 hrs. Cells were then added to an 8-well plate containing $CaCl_2$ (1.5 mM). cIBR-NPs or NPs (2.2 mg/ml) were incubated with the cells for 5, 15, 30 min and 1 hr at 37°C, 5% CO_2. Unbound nanoparticles were removed by washing three times with cold PBS and fixed with 4% paraformaldehyde. Fluorescence micrographs were acquired using the FITC filter set of a Nikon Eclipse 80i microscope equipped for epifluorescence. Micrographs were captured using an Orca ER camera (Hamamatsu, Inc., Bridgewater, NJ) and analyzed by Metamorph, version 6.2 (Universal Imaging Corp., West Chester, PA).

The binding of Molt-3 cells and cIBR-NPs prepared by using surfactant containing different ratios of Pluronic-COOH and Pluronic-OH was also observed by fluorescence microscopy. PMA activated Molt-3 cell line (2×10^6 cells/ml) were incubated with cIBR-NPs bearing different amounts of cIBR peptide (2.7 mg/ml, 300 μl) for 40 min at 37°C. Binding/uptake of cIBR-NPs and NPs with Molt-3 cells was evaluated using fluorescence microscopy (Nikon Eclipse 80i microscope equipped for epifluorescence). All fluorescence microscopy scans were performed using the same settings for the light source power and detector sensitivity, allowing direct comparison of the results obtained for the different incubations.

Lysosomal trafficking of cIBR-NPs in Molt-3 cells

Fluorescence microscopy was utilized to investigate the intracellular fate of cIBR-NPs and untargeted NPs in Molt-3 cells. Molt-3 cells (1×10^6 cells/ml) were activated with 0.4 μM of PMA for 20 hrs. Cells were washed and dispersed in Texas red dextran (Mw 10,000, lysine fixable, 1 mg/ml) in serum free media and incubated for 2 hrs at 37°C, 5% CO_2. Cells were washed three times with serum free medium. Cells were then incubated in serum free media at 37°C, 5% CO_2 for 12 hrs to allow the dye to traffic lysosomes. Cells were then added to an 8 well plate containing $CaCl_2$ (1.5 mM). Then cIBR-NPs or NPs (100 μl, 2.2 mg/ml) were added to cells and incubated for 10 min at 37°C, 5% CO_2. Unbound nanoparticles were removed by washing three times with serum free medium. Cells were then incubated in serum free medium for each time period (30 min, 1 hr, 2 hrs, 3 hrs, 4 hrs, 6 hrs, 8 hrs and 24 hrs.). Cells were washed by centrifugation at 856 g for 1 min and fixed with 4% paraformaldehyde. Fluorescence emissions of nanoparticles and lysosomes were observed using FITC and rhodamine filter sets, respectively (Nikon Eclipse 80i microscope equipped for epifluorescence). Micrographs were captured using an Orca ER camera. Co-localizations of nanoparticles with lysosomes were analyzed by Metamorph, version 6.2.

Inhibition of heterotypic adhesion by cIBR-NPs

cIBR-NPs were hypothesized to bind to LFA-1 of Molt-3 cells, hence blocking the binding of LFA-1 of Molt-3 cells and ICAM-1 of A549 lung epithelial cells. The inhibition of LFA-1 and ICAM-1 adhesion by cIBR-NPs was monitored in this study.

A549 cells (8 x 10^5 cells/ml) were incubated with TNF-α (1,000 U/mL) for 48 hrs to activate the expression of ICAM-1 as reported previously. [23] LFA-1 on Molt-3 cells was activated by 0.4 μM of PMA in serum free medium for 20 hrs. Molt-3 cells were labeled with a fluorescent dye, 2',7'-bis-(2-carboxyethyl)-5-(and-6)-carboxyfluorescein, acetoxymethyl ester (BCECF, AM) (5 μl, 2 mM), in 20 ml of PBS for 15 min at 37°C. Cells were washed three times with PBS and resuspended in 5 ml of PBS (final concentration of cells was 5.5 x 10^5 cells/ml). Molt-3 cells were then transferred to a 96-well plate (200 μl/well) and incubated with various concentrations of cIBR-NPs (0, 0.38, 0.75 and 1.50 mg/ml) at 37°C for 30 min. Molt-3 cells were then transferred to A549 culture on 8 well plates to evaluate the interaction between ICAM-1 on A549 cells and LFA-1 on Molt-3 cells at 37°C, 5% CO_2 for 45 min. After incubation, unbound Molt-3 cells were washed away with cold PBS three times and the culture was fixed with 4% paraformaldehyde. The binding of Molt-3 to A549 cells was quantified by counting the bound Molt-3 in four images taken with the Nikon Eclipse 80i microscope.

Statistical analysis

Statistical evaluation of data was performed using an analysis of variance (one-way ANOVA). Newman–Keuls was used as a post-hoc test to assess the significance of differences. To compare the significance of the difference between the means of two groups, a *t*-test was performed; in all cases, a value of $p < 0.05$ was accepted as significant.

3.3 Results

PLGA nanoparticle preparation and characterization

PLGA nanoparticles were prepared using a solvent displacement method.[23] Nanoparticles were formed from PLGA, which served as a hydrophobic core to encapsulate the poorly water soluble dye, coumarin-6.[23]The diameter of nanoparticles was approximately 200 nm with a low polydispersity suggesting a narrow size distribution. Modified Pluronic® F -127 bearing carboxylic acid termini yielded negatively charged NPs. The zeta potential value was about -23 mV (Table 1). It is probable that the strong negative charge provided some electrostatic stabilization to reduce agglomeration and maintain particle size. Furthermore, free carboxylic acid groups on the modified surfactant allowed conjugation of the targeting peptide.

Conjugation of cIBR peptide to PLGA-nanoparticles

The cIBR peptide was covalently attached to the carboxylic acid end groups of modified Pluronic® F-127 on the nanoparticle surface using carbodiimide chemistry.[23]The conjugation efficiency was determined by quantifying the unconjugated ligand remaining in the reaction medium after nanoparticle separation. The amount of free cIBR peptide measured by RP-HPLC decreased during the reaction (0-20 hrs) (Figure 1A). The peptide density on the surface of nanoparticles after reaction was calculated assuming a normal Guassian particle size distribution (Table 2). [23] The conjugation reaction was also performed in the absence of EDC to observe any possible adsorption (electrostatic or hydrophobic interaction) of cIBR peptide to the nanoparticles. The result showed that the adsorption of peptide was negligible since the amount of unconjugated peptide in the reaction medium analyzed

by RP-HPLC did not decrease when peptide was incubated with nanoparticles without activation of COOH (Figure 1B).

Table 1 Nanoparticle Properties at Specified Formulation Points

	Effective diameter (nm) [Mean ± SD]	**Polydispersity** [Mean ± SD]	**Zeta potential value (mV)** [Mean ± SD]
NP	199 ± 8.0	0.08 ± 0.04	-22.5 ± 1.4
cIBR- NP	248 ± 10	0.08 ± 0.05	-25.7 ± 1.8

Values are representative of three experiments.

Table 2 Density of cIBR on the Surface of PLGA Nanoparticles

	Size (nm)	**Total surface area (m^2/g of PLGA)**	**Surface cIBR (pmol/cm^2)**
cIBR-NP	248	18.1	39.0 ± 9.6

Values are representative of three experiments (mean ± S.D.).

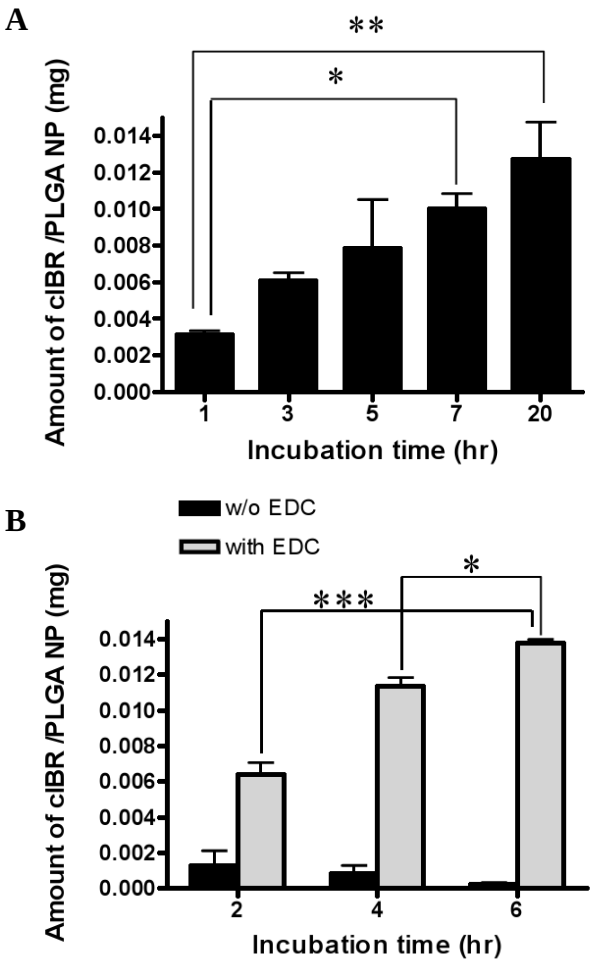

Figure 1 (A) Measurement of cIBR peptide reacted with nanoparticles over the time. The amount of cIBR peptide conjugated on nanoparticle surface increased with incubation time indicating reaction to nanoparticles. (B) The amount of peptide on nanoparticle was constant when the reaction was performed without EDC. Data are presented as mean ± S.D. (n = 3), *** indicates $p< 0.001$, ** indicates $p< 0.01$ and * indicates $p< 0.05$.

The degree of cIBR peptide conjugation to NP surface depends on the density of carboxylic acid groups of surfactant

The density of carboxylic acids coated on NPs was varied by increasing ratio of Pluronic® F127-COOH to Pluronic® F127-OH used as a surfactant in aqueous solution when preparing PLGA nanoparticles. The results from dynamic light scattering and Zeta Pals have shown that the negatively charge of NPs increased with increasing percent of Pluronic® F127-COOH (Figure 2A), whereas the size of nanoparticles were not changed significantly (~170 nm) (Figure 2B). The size and charge of cIBR-NPs prepared from different ratios of Pluronic® F127-COOH were characterized using DLS. The negative charge of the resulting cIBR-NPs increased with increasing ratio of Pluronic® F127-COOH in surfactant solution except for cIBR-NPs prepared from 100% Pluronic® F127-COOH (Figure 2A). cIBR-NPs prepared from 100% Pluronic® F127-COOH had a less negative charge than other formulations probably as a result of charge masking by the cIBR peptide, which has a neutral net charge. Furthermore, the use of different ratios of Pluronic® F127-COOH coated on NPs yielded different amounts of cIBR peptide conjugated on NPs (Figure 3). The amounts of cIBR conjugated on NPs were analyzed by reversed phase HPLC. The results demonstrated that the amount of cIBR on NPs is related to the amounts of carboxylic acid groups. NPs prepared by using 100% of Pluronic® F127-COOH yielded the highest density of cIBR on NP surface, followed by NPs prepared by using 50%, 25% and 0% of Pluronic® F127-COOH, respectively (Figure 3). The results of HPLC demonstrated some extent of cIBR peptide conjugation to NPs prepared from 0% Pluronic® F127-COOH (100% Pluronic® F127-OH). This result suggested that the hydroxyl groups of Pluronic® F127-OH upon activation using EDC

formedan unstable complex, acylisourea, which then complexed with the amino groups of cIBR peptide.[24]

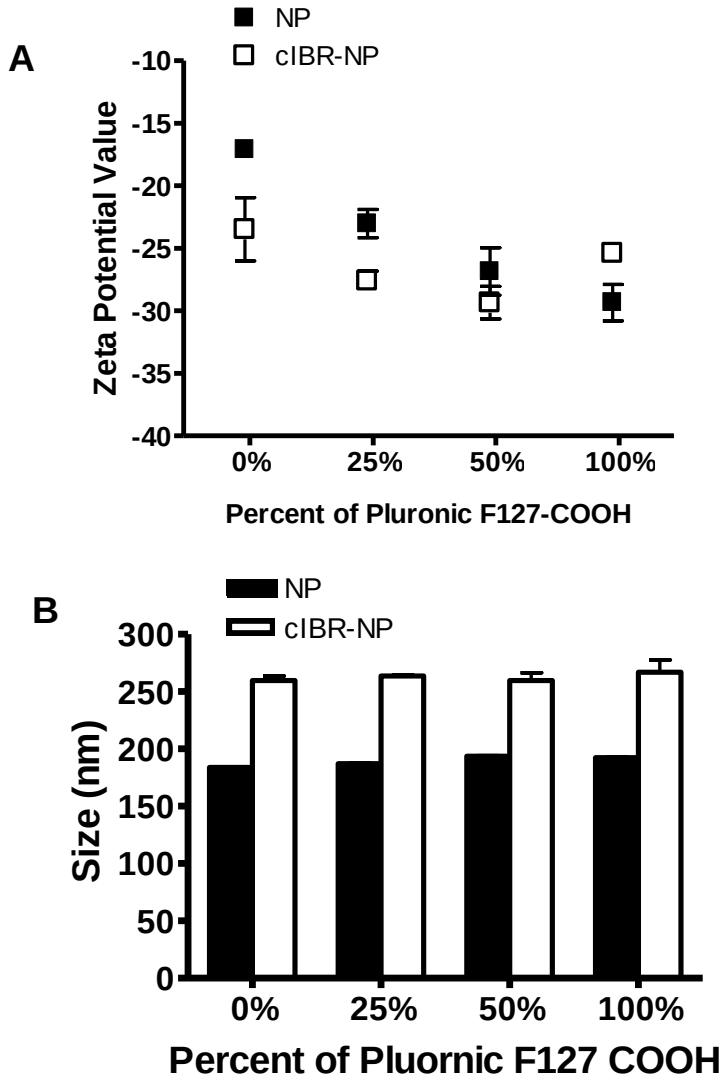

Figure 2 (A) Zeta potential value of NPs and cIBR-NPs (B) size of coumarin loaded PLGA nanoparticles at different percent of Pluronic® F127-COOH used as a surfactant in NP preparation. Data are presented as mean ± S.D. (n = 3).

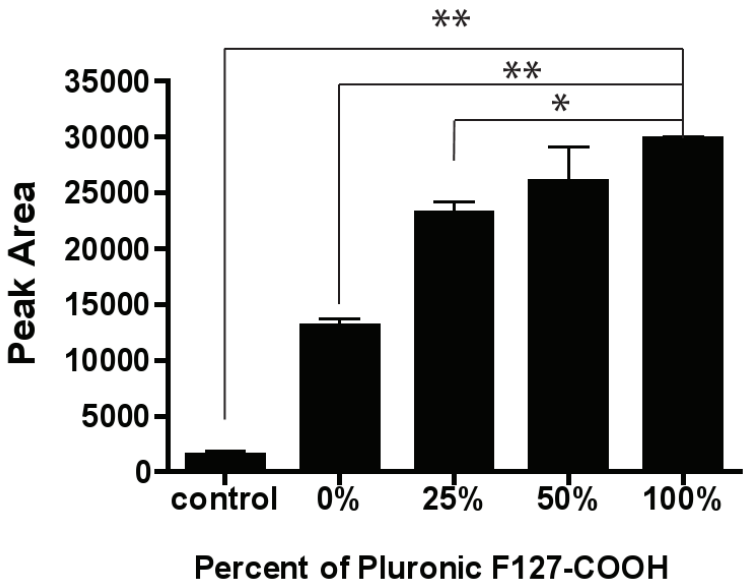

Figure 3 Measurement of cIBR peptide reacted with nanoparticles at different percent of Pluronic® F127-COOH used as a surfactant to prepare NP. The amount of cIBR peptide conjugated on nanoparticle surface increased with percent of Pluronic® F127-COOH indicating the importance of carboxylic acid groups on NP in the conjugation reaction. The amount of cIBR peptide conjugated on NP was very low the absence of EDC in the conjugation reaction (control). Data are presented as mean ± S.D. (n = 3), ** indicates $p< 0.001$ and * indicates $p< 0.05$.

PMA stimulates aggregation of Molt-3 cells

Molt-3 cells were found to aggregate in response to PMA (Figure 4A). Although some homotypic adhesion of Molt-3 cells occurred in the absence of PMA, PMA stimulated Molt-3 cells exhibited much larger cell clusters. In previous reports, PMA was shown to increase the avidity of LFA-1 via *rho*A protein which works as an intracellular transducer of protein kinase C activation leading to integrin activation

and cell aggregation.[25]Immunofluorescence flow cytometry showed that the expression of LFA-1 on Molt-3 cells was not changed when incubated with PMA suggesting that PMA did not induce expression of LFA-1 (Figure 4B). This result was previously observed in other LFA-1 bearing cells.[26]As a control, A549 lung carcinomic epithelial cells, expressing ICAM-1, but not LFA-1 were incubated with PMA and also incubated with anti-LFA-1-FITC. The fluorescent intensity measured by flow cytometry was negligible compared with Molt-3 cells since A549 cells lack LFA-1 (Figure 4C).

cIBR-NPs exhibit interaction with Molt-3 cells

The binding and uptake of cIBR-NPs by Molt-3 cells were monitored using flow cytometry. The interaction of cIBR-NPs and Molt-3 cells was substantially greater than that of untargeted NPs (Figure 5A). Molt-3 cells showed ~5 fold higher fluorescence when incubated with targeted nanoparticles. The fluorescent intensity of Molt-3 cells increased with time for both particle types but to a larger extent for cIBR-NPs. These results suggested that cIBR-NPs bound to Molt-3 cells more quickly and to a greater extent when compared to untargeted NPs. Furthermore, the binding of cIBR-NPs was also concentration dependent; uptake increased with increasing nanoparticle concentration (Figure 5B).

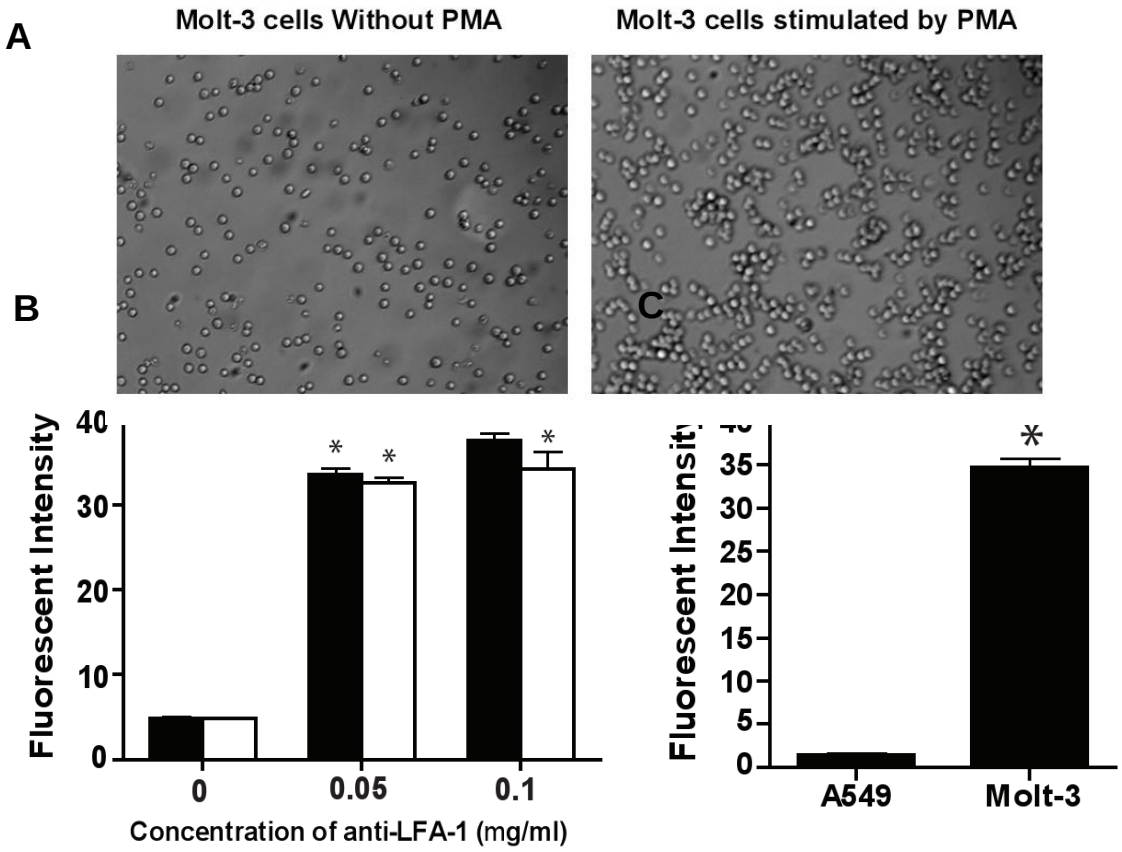

Figure 4 (A) Stimulation of LFA-1 on Molt-3 cells by PMA. Aggregation of PMA stimulated Molt-3 cells was evident compared to unstimulated Molt-3 cells. (B) Binding of anti-LFA-1 to LFA-1 on stimulated and unstimulated LFA1-1. Anti-LFA-1-FITC labeling of LFA-1 revealed that the expression of LFA-1 was unchanged for PMA-stimulated compared to unstimulated Molt-3 cells. (C) Negligible fluorescent intensity of anti-LFA-1-FITC was observed when incubated with cells lacking LFA-1 (A549 cells). Data are presented as mean ± S.D., (n = 3), * indicates $p< 0.001$ compared to 0 mg/ml of anti-LFA-1-FITC.

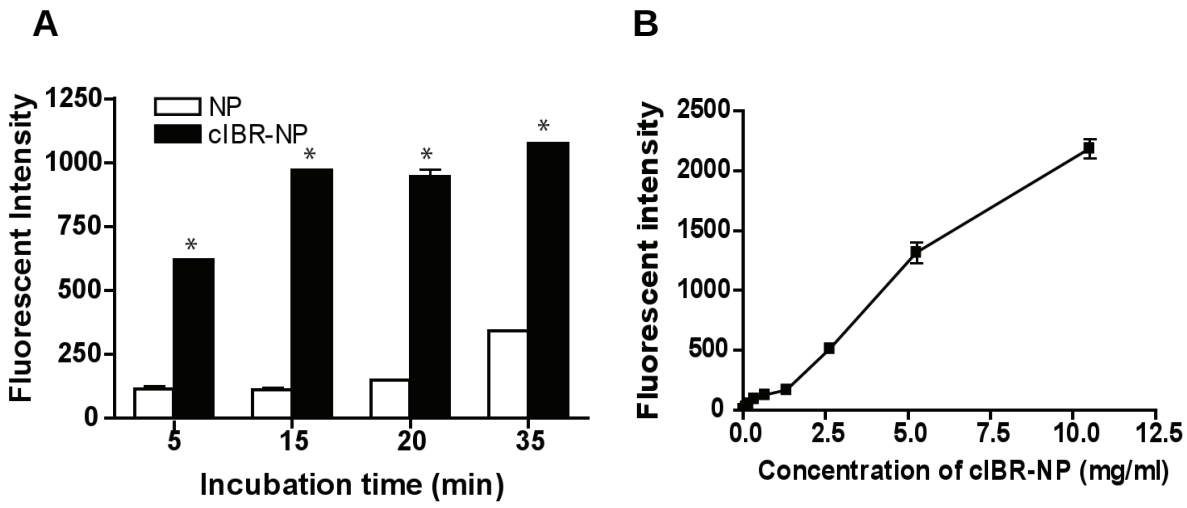

Figure 5 (A) Binding of cIBR-NP to Molt-3 cells. cIBR-NP interaction with Molt-3 cells was significantly greater than untargeted NPs at all time points. The fluorescence of Molt-3 cells incubated with cIBR-NPs increased with time. (B) The dependence of cIBR-NP concentration on the binding to Molt-3 cells. The fluorescence of Molt-3 cells increased as the concentration of cIBR-NPs increased. Data are presented as mean ± S.D. (n = 3), * indicates $p < 0.001$.

Free cIBR and the LFA-1 I domain inhibited the binding of cIBR-NPs to Molt-3 cells

Inhibition of cIBR-NPs was investigated by incubating Molt-3 cells with free cIBR peptide followed by incubation with cIBR-NPs or NPs. The fluorescent intensity of cells incubated with cIBR-NPs decreased significantly compared to cells incubated with untargeted NPs (Figure 6A). Disrupting of the binding of cIBR-NPs to Molt-3 cells by cIBR peptide suggested cIBR-NPs targeted LFA-1. The binding of untargeted NPs was again very low.

To further validate binding specificity, cIBR-NPs were allowed to bind to the I domain of LFA-1 prior to incubation with Molt-3 cells. The I domain was expected to bind to cIBR on targeted NPs and block the binding of targeted NPs to LFA-1 on Molt-3 cells. As the concentration of the LFA-1 I domain increased, the binding of cIBR-NPs correspondingly decreased (Figure 6B). The binding of cIBR-NPs was reduced to ~60% when 2.5 mg/ml of the I domain was used with cIBR-NPs compared to the absence of the I domain whereas there was no significantly reduction of the cIBR-NP binding to Molt-3 cells when BSA was firstly mixed with cIBR-NP (Figure 6C). This result further supported the specific binding of cIBR-NPs to the I domain of LFA-1. Previous reports indicated that cIBR peptide has a PRGG sequence with the β-turn structure of the D_1 of ICAM-1, the binding site of LFA-1.[14-15] Furthermore, Anderson and Siahaan elucidated the binding specificity of cIBR peptide and showed that cIBR-FITC binding to soluble LFA-1 can be competitively inhibited by an anti-CD11a antibody as an indicator of specific binding of cIBR to the I domain of LFA-1.[14]

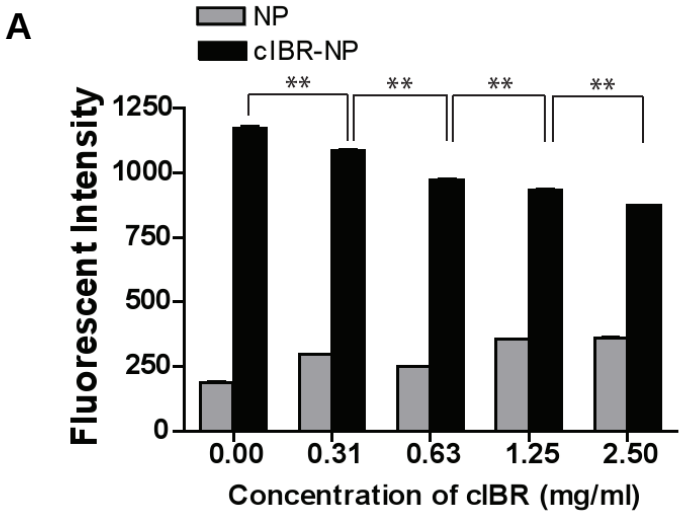

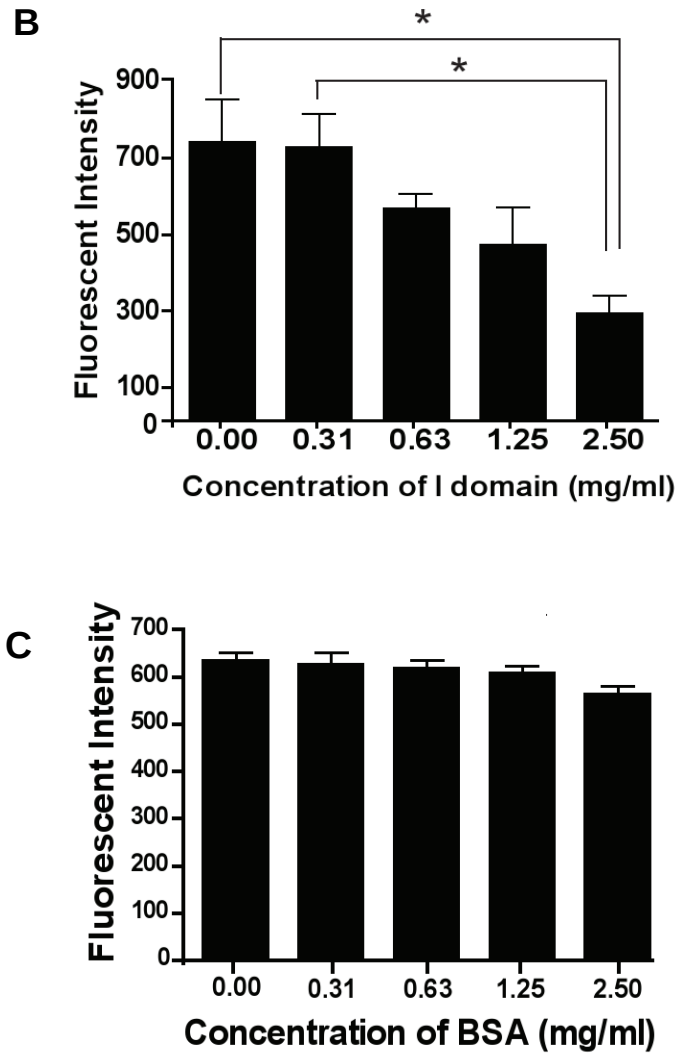

Figure 6 (A) The inhibition of cIBR peptide to the binding of cIBR-NP to Molt-3 cells. The interaction of cIBR-NPs with Molt-3 cells decreased as free cIBR peptide concentration increased suggesting that cIBR competitively inhibits binding to LFA-1 on Molt-3 cells. Data are presented as mean ± S.D. (n = 3), ** indicates $p < 0.001$. (B) The inhibition of LFA-1 I domain to the binding of cIBR-NP to Molt-3 cells. The interaction of cIBR-NPs with Molt-3 cells was also competitively inhibited by the I domain of LFA-1. The I domain was added to the NPs prior to addition of cells. (C)

The uptake of cIBR-NP pretreated with BSA by Molt-3 cells did not significantly decrease in the presence of BSA. Data are presented as mean ± S.E., (n = 3), ** indicates $p< 0.01$ and *indicates $p< 0.05$.

Uptake of cIBR-NPs is temperature dependent

Molt-3 cells were incubated with cIBR-NPs at 4 °C and 37 °C to determine the effect of temperature on the uptake of nanoparticles and to learn whether the mechanism of cIBR-NPs entry into Molt-3 cells was energy dependent. The uptake of cIBR-NPs decreased significantly at 4 °C (Figure 7A), suggesting that cIBR-NPs uptake was indeed energy dependent. Furthermore, the fluorescent intensity of cells incubated with cIBR-NPs at 37 °C increased over time. At low temperature, cIBR-NPs binding was similar to binding at 37 °C; however, the increase in fluorescent intensity occurred more slowly suggesting that endocytosis was slowed at low temperature. The dependence of temperature on the uptake of untargeted nanoparticles was also investigated. The uptake of nanoparticles without peptide was also decreased at low temperature but to a lesser extent (Figure 7B) confirming an energy dependent endocytic process observed previously.[27]

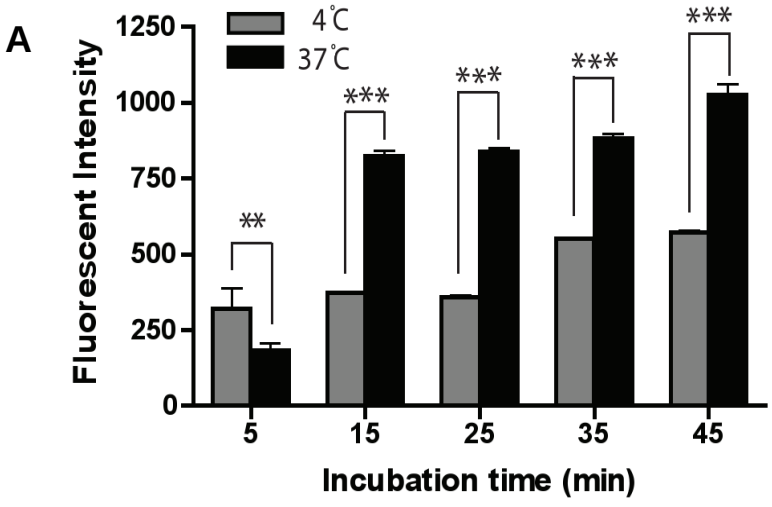

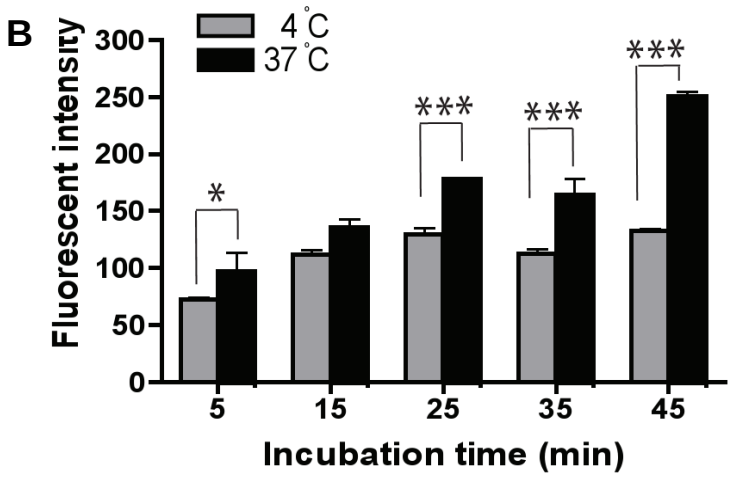

Figure 7 The dependence of temperature on the binding of cIBR-NP to Molt-3 cells. The binding and uptake of (A) cIBR-NPs and (B) NPs were slowed at low temperature (4 °C), which suggested energy dependent endocytosis of nanoparticles. Data are presented as mean ± SD., (n = 3), * indicates $p< 0.05$, ** indicates $p< 0.01$ and *** indicates $p< 0.001$.

Fluorescence microscopy of Molt-3 cells and nanoparticles

The uptake of cIBR-NPs and NPs by Molt-3 cells was examined by fluorescence microscopy. The association of cIBR-NPs and NPs with Molt-3 cells was clearly demonstrated by fluorescence micrographs. The fluorescent intensity of cells incubated with untargeted NPs was far less than cells incubated with targeted NPs (Figure 8). The fluorescent intensity of cells incubated with NPs slowly increased with incubation time and showed the greatest intensity at the longest time, whereas the fluorescent intensity of cells incubated with cIBR-NPs was quite high initially. These results supported the kinetics of cIBR-NPs incubated with Molt-3 cells

determined by flow cytometry. Both suggest the rapid binding and internalization of cIBR-NPs and may suggest receptor saturation.

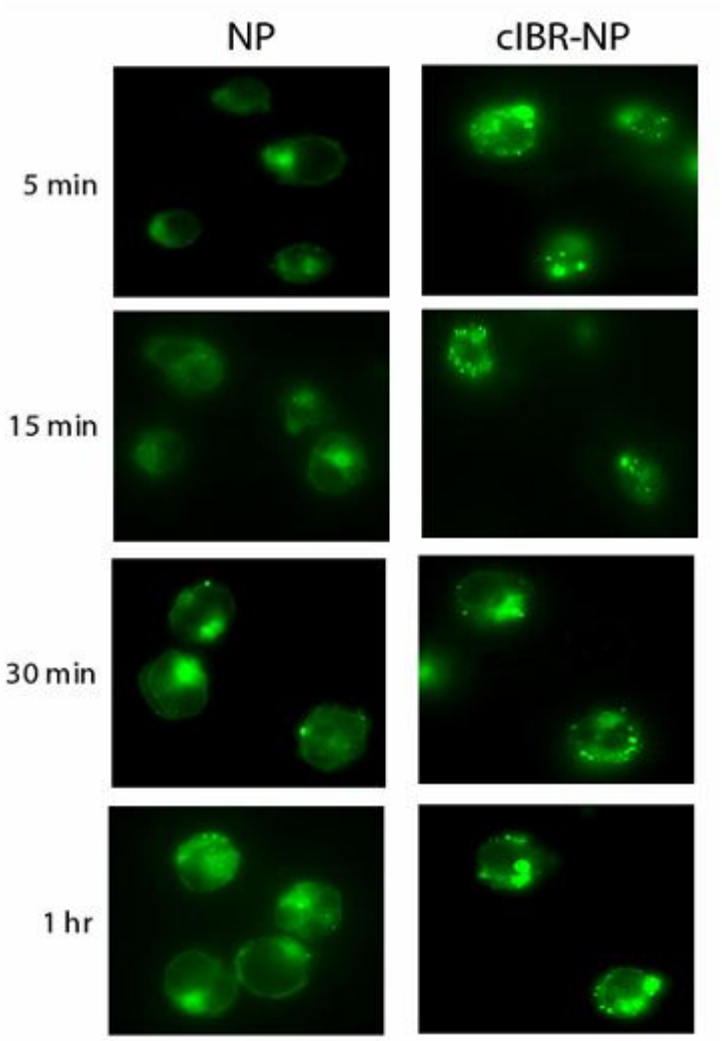

Figure 8 Micrograph of Molt-3 cells incubated with cIBR-NP or NP encapsulating fluorescence dye. Interaction of cIBR-NPs with Molt-3 cells occurred more quickly and to a greater extent compared to untargeted NPs at each incubation time as shown by fluorescence micrographs.

cIBR-NPs prepared by using 100% Pluronic® F127-COOH exhibited the most rapid binding to Molt-3 cell line.

The purpose of this experiment is to quantify the effect of cIBR density on NP surface on the binding of cIBR-NPs to LFA-1 expressing cell line (Molt-3 cells). Nanoparticles with different amounts of cIBR peptide grafted on the surface were incubated with Molt-3 cells to investigate the effect of cIBR density on binding of cIBR-NPs by Molt-3 cells. The flow cytometry data showed that fluorescent intensity of Molt-3 cells incubated with cIBR-NPs prepared from 100% Pluronic® F127-COOH was higher than cells incubated with cIBR-NPs prepared from 50%, 25% and 0% Pluronic® F127-COOH, respectively at all incubation times. Fluorescence intensity of Molt-3 cells incubated for 60 minutes with cIBR-NPs prepared from 100%, 50% and 25% Pluronic® F127-COOH were ~1.7, 1.3 and 1.0 fold greater than cIBR-NPs prepared from 0% Pluornic-COOH, respectively, suggesting the importance of cIBR peptide density in the binding to LFA-1 on Molt- 3 cells (Figure 9A).

cIBR-NPs with different degrees of cIBR peptide conjugated and untargeted NPs binding to LFA-1 expressing cells was also examined on Molt-3 cell lines using fluorescence microscopy. Fluorescence microscopy clearly demonstrated binding of cIBR-NPs to Molt-3 cells. Molt-3 cells incubated with untargeted NPs exhibited low level of green fluorescence, while Molt-3 cells incubated with cIBR-NPs demonstrated higher fluorescence intensity indicating the greater degree of cell association with cIBR-NPs (Figure 9B). Binding of cIBR-NPs was shown to depend on cIBR density on NPs as fluorescence intensities of Molt-3 cells increased upon the

increase in percent of Pluronic® F127-COOH used to prepare NPs. These results indicated that increasing cIBR density on NP mediated by increasing carboxylic acid groups on NP surface are of potential importance in modulating the interaction of cIBR-NPs with LFA-1 expressing cell line.

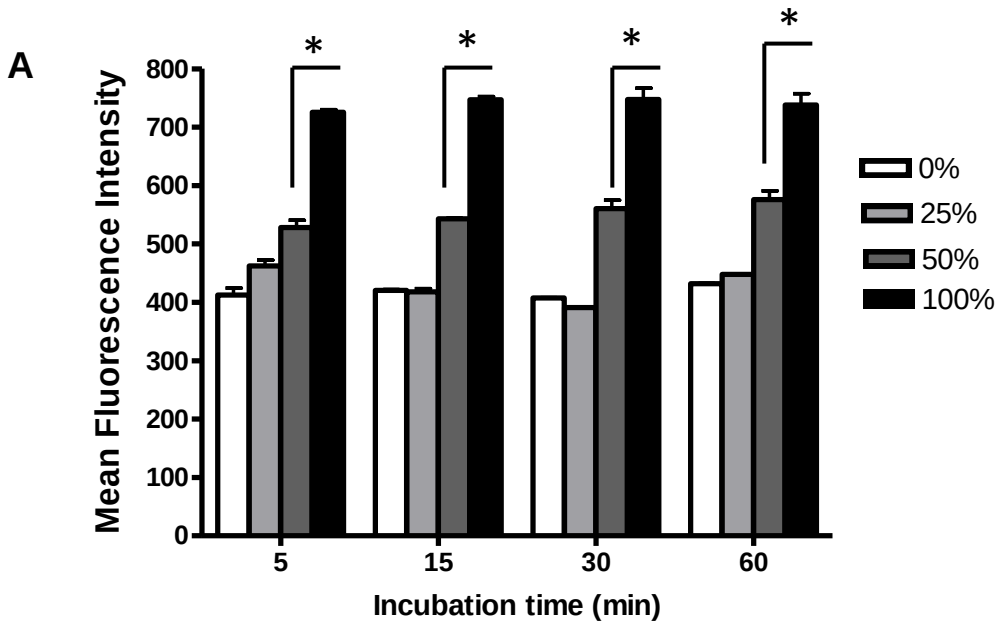

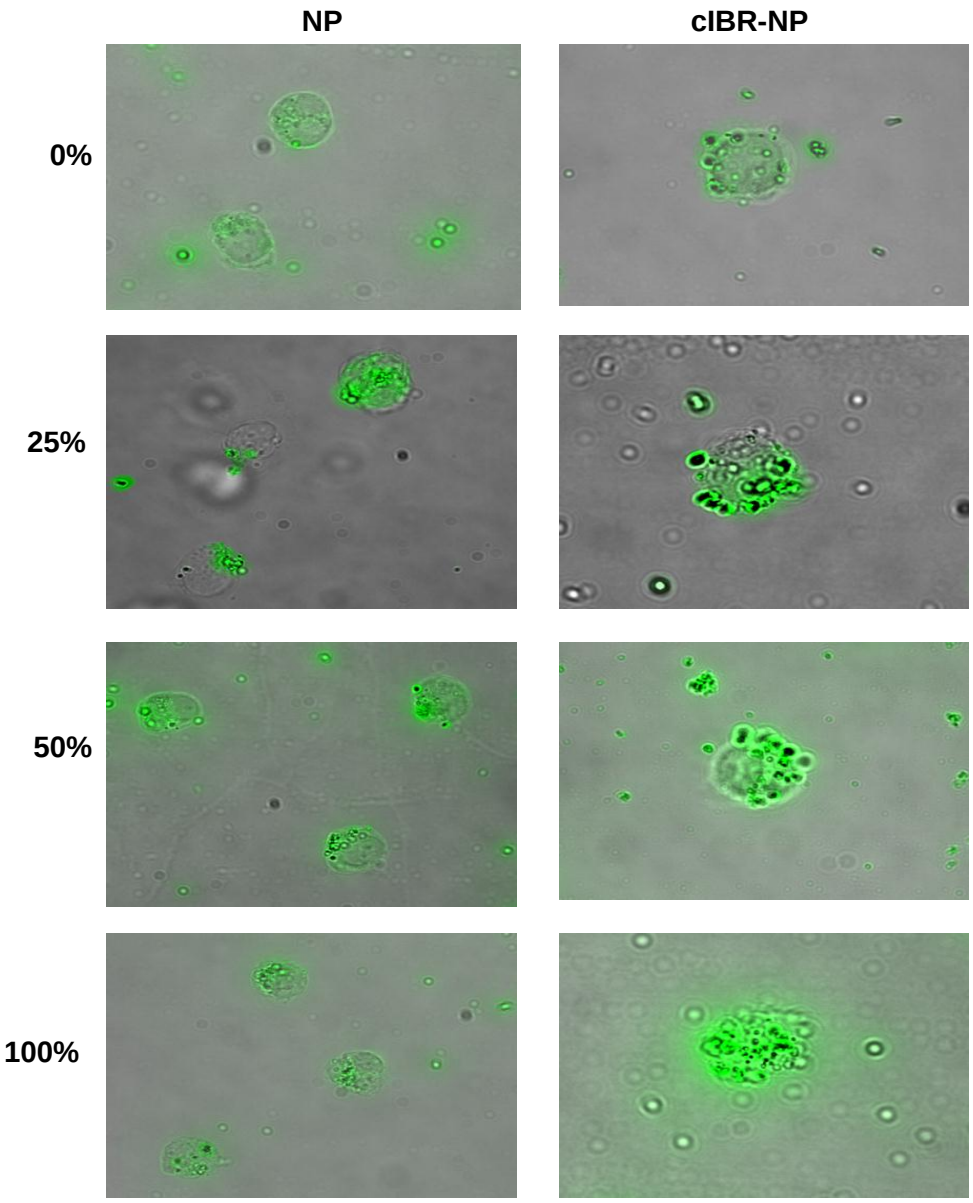

Figure 9 (A)Micrograph of Molt-3 cells incubated with cIBR-NP or NP encapsulating fluorescence dye. Interaction of cIBR-NPs with Molt-3 cells occurred more quickly and to a greater extent compared to untargeted NPs at each incubation time as shown by fluorescence micrographs. (B) Binding of cIBR-NP to Molt-3 cells. The association of cIBR-NP prepared from 100% of Pluronic® F127-COOH with Molt-3 cells was significantly greater than cIBR-NPs prepared from surfactant

containing lower percent of Pluronic® F127-COOH at all time points. Data are presented as mean ± S.D. (n = 3), * indicates $p < 0.001$.

Trafficking of cIBR-NPs to lysosomes

Lysosomes are acidic and contain hydrolytic enzymes where nanoparticles or drugs in nanoparticles may be degraded. To inviestigate whether cIBR-NPs traffick to the lysosomes or not, co-localozation of lysosomes and nanoparticles was monitored. The lysosomal compartments of Molt-3 cells were stained with Texas red-dextran (lysine fixable) to track cIBR-NPs and NPs uptake. Then, cells were treated with cIBR-NPs or NPs encapsulating the green fluorescent dye. The intracellular localization of nanoparticles was tracked at different time points and lysosomal accumulation was indicated by yellow fluorescence in merged images (Figure 10). The co-localization of cIBR-NPs with lysosomal vesicles was not evident over 24 hrs. The co-localization of untargeted NPs with lysosomes was undetectable at 6 hrs and was detected at 24 hrs. These results implied that cIBR-NPs did not traffic to lysosomes but untargeted NPs slowly accumulated in lysosomes.

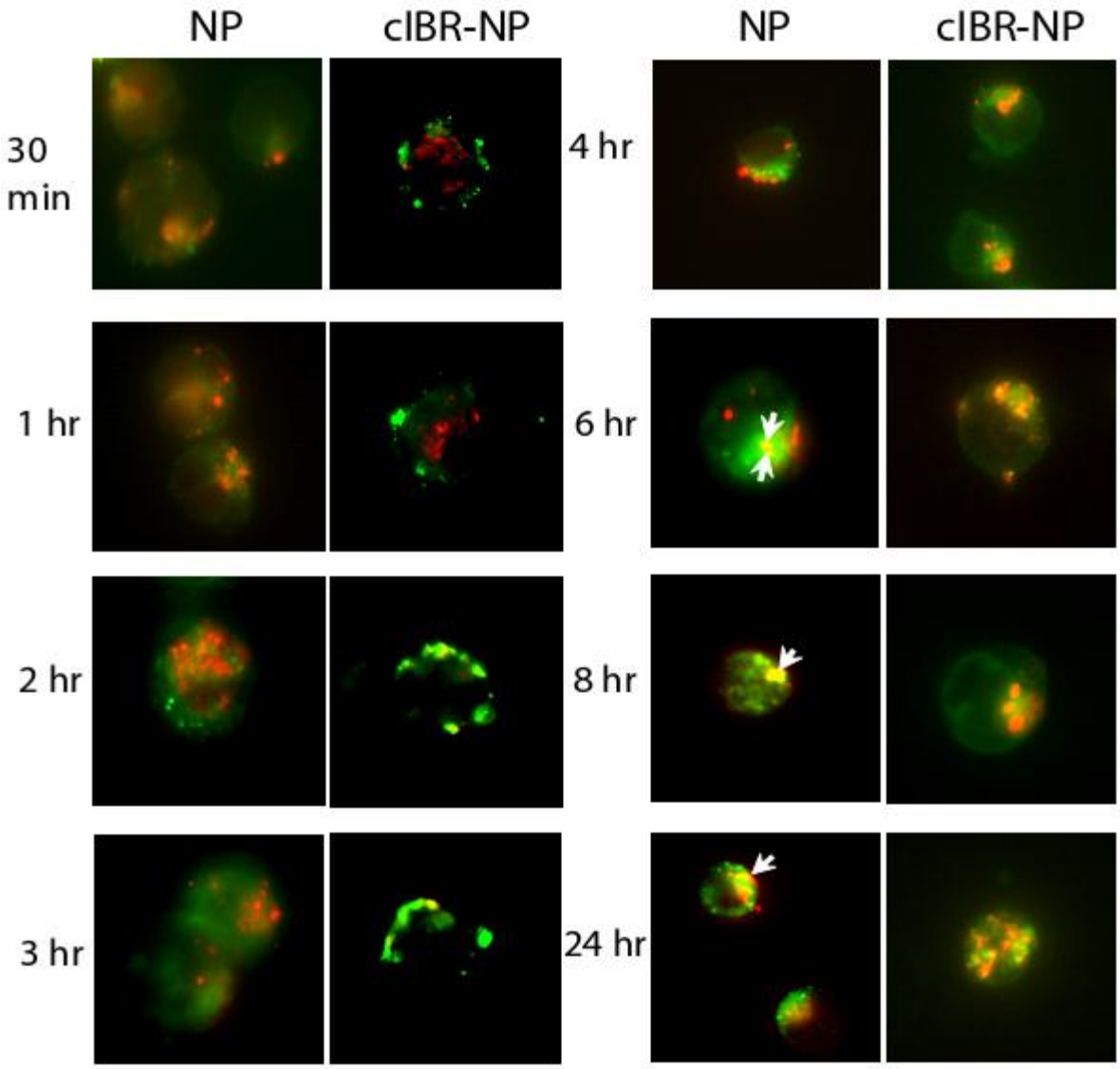

Figure 10 Micrographs of Molt-3 cells incubated with cIBR-NP or NP in the presence of Texas red-dextran. Intracellular trafficking of cIBR-NPs and NPs (green) to lysosomal compartments (red) of Molt-3 cells. The co-localization (yellow fluorescence) of cIBR-NPs with lysosomes was generally not observed over 24 hrs, whereas co-localization of NPs with lysosomes was first observed at 6 hrs and slowly increased over 24 hrs.

cIBR-NPs inhibit the adhesion of Molt-3 cells and lung epithelial cells.

Leukocyte recruitment to endothelial and epithelial tissues requires interaction of LFA-1 and ICAM-1.[14, 28]cIBR peptide alone has been shown to inhibit homotypic and heterotypic cell interactions via binding LFA-1.[17, 19, 29] The interaction of LFA-1 on PMA-stimulated Molt-3 cells and ICAM-1 expressed on lung carcinomic epithelial cells activated with TNF-α resulted in heterotypic cell adhesion and was investigated by fluorescence microscopy. Micrographs allowed quantification of the number of adhered Molt-3 cells (stained with a green fluorescent dye) to A549 cells (Figure 11A). Pretreatment of Molt-3 cells with cIBR-NPs was investigated as a means to inhibit this heterotypic cell adhesion. When PMA-stimulated Molt-3 cells were pre-incubated with cIBR-NPs, significant inhibition was observed (Figure 11B). Pretreatment of Molt-3 cells with cIBR-NPs yielded up to a ~73% decrease in adhered cells suggesting that cIBR-NPs bound to LFA-1 of Molt-3 cells blocked the availability of LFA-1 integrins to bind to ICAM-1 on A549 cells. Furthermore, cIBR-NPs may decrease the availability of LFA-1 on the cell surface via endocytosis of this receptor.[14]The result of this study revealed the potential of cIBR-NPs to inhibit lymphocyte recruitment during inflammatory responses.

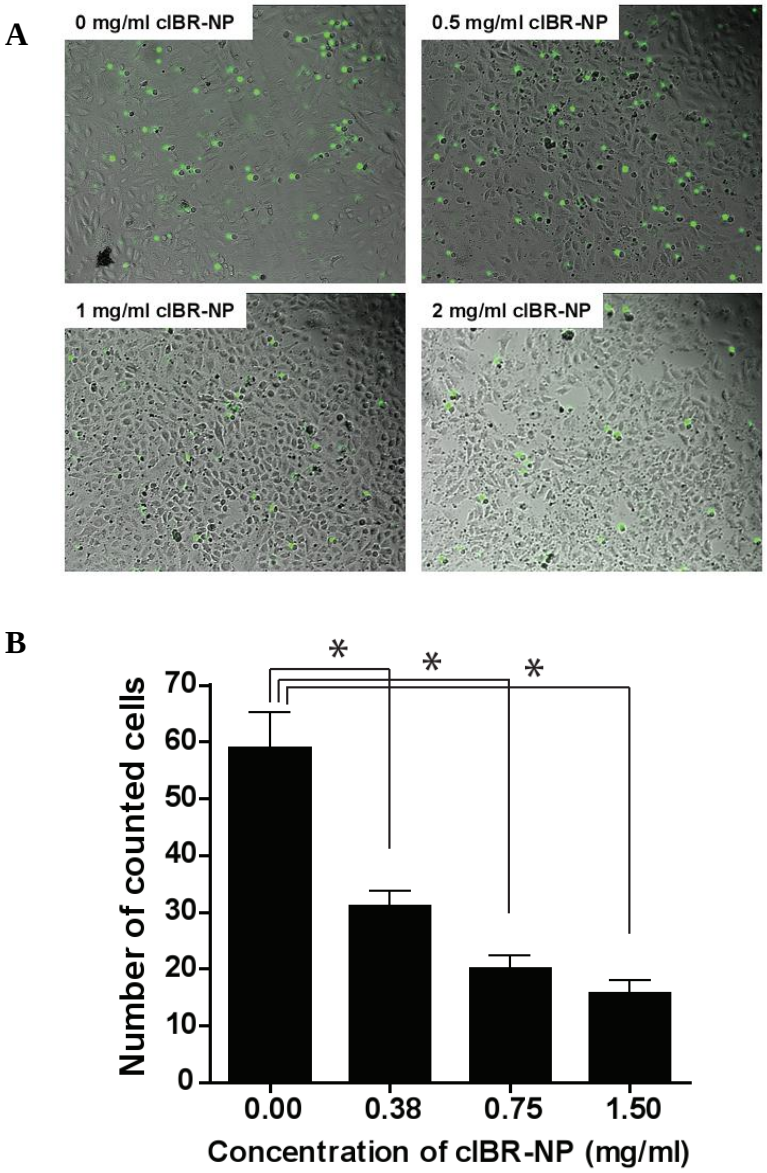

Figure 11 The inhibition of cIBR-NP to the interaction of LFA-1 and ICAM-1 on Molt-3 cells and A549 cells. (A) Optical micrographs of the adhesion of Molt-3 cells (green) to A549 lung epithelial cells at various concentrations of cIBR-NPs. (B) cIBR-NPs inhibited the heterotypic adhesion of Molt-3 cells to A549 cells in a dose dependent manner. Data are presented as mean ± S.D., (n = 3), * indicates $p< 0.001$ compared with 0 mg/ml of cIBR-NPs.

3.4 Discussion

The interaction of LFA-1 and ICAM-1 plays a vital role in leukocyte recruitment and migration across the vasculature during normal leukocyte circulation through lymph nodes and during recruitment in the response to inflammatory signals. LFA-1 also participates in the 'immunological synapse' between T lymphocytes and antigen presenting cells (APC).[6] In recent decades, potential therapeutic agents used to block the binding of LFA-1 to ICAM-1 to treat immunological and inflammatory disorders have focused on monoclonal antibodies and small molecules designed to antagonize interactions between these proteins.[30-31] However, hypersensitivity reactions and unpredictable half-lives are often encumbrances for immunotherapy using monoclonal antibodies.[29, 31, 32] In comparison to monoclonal antibodies, cyclic peptides have been shown to offer improved safety, physicochemical stability and may even improve selectivity to the targeted site.[3, 33]

cIBR, a cyclic peptide derived from domain 1 of ICAM-1, has demonstrated specific binding to isolated LFA-1 and to the surface of T cells.[9, 10] Previous research showed that cIBR conjugated to the fluorescent dye FITC entered cells via endocytosis; however, cIBR conjugated to doxorubicin mainly passively diffused through the cell membrane of HL-60 cells.[29] Passive diffusion of cIBR-doxorubicin may be a result of the increased hydrophobicity of the conjugate, a change in the conformation of the cIBR peptide after conjugation and/or steric hindrance of doxorubicin at the recognition site of the cIBR peptide.[29] Regardless, these findings suggested that the delivery of some drugs may be improved if the drugs were encapsulated.

In the present study, cIBR was conjugated to the surface of PLGA nanoparticles. The physical incorporation of drug in the particle matrix may mask the hydrophobicity of the drug and mitigate potential off-target passive diffusion into cells driven by the poorly water soluble compound. Furthermore, the grafting of cIBR to the end of a long chain surfactant on the nanoparticle surface can reduce steric hindrance at the cIBR binding site which may have occurred in a single drug-peptide conjugate.

The importance of multivalency in the LFA-1/ICAM-1 interaction and the activation of high avidity LFA-1 in some types of LFA-1 expressing cells have been reported.[34] LFA-1 is exclusively expressed on leukocytes but these cells do not adhere to ICAM-1 unless activated (e.g. by PMA).[6, 35] Furthermore, Welder et al have demonstrated that monovalent soluble intercellular cell adhesion molecule-1 (sICAM-1) is unable to bind efficiently to LFA-1 expressed on cells unless it is first rendered multivalent by coupling to polystyrene microspheres, thus, illustrating the importance of multivalency.[36] Pyszniak et al have demonstrated that sICAM-1-coated microspheres specifically bind to activated LFA-1 but not to the low avidity state.[35] The distribution of high avidity LFA-1 on the cell surface was observed to be highly localized on some types of LFA-1 expressing cells, whereas the low avidity state was more evenly distributed. They also reported that only after activation with PMA, isolated splenic T cells and murine T cell hybrodoma T28 bound the sICAM-1 microspheres and the binding was inhibited by anti-LFA-1 mAb. Therefore, utilizing a high density of cIBR ligands on nanoparticles may improve binding efficiency of cIBR-NPs to activated LFA-1 due to multivalent ligand receptor interactions.

In the present study, grafting cIBR peptide to biodegradable PLGA nanoparticles increased selectivity, the rate, and the extent of binding of untargeted nanoparticles and internalization by activated LFA-1 on acute lymphoblastic leukemia T cells (Molt-3). The uptake of targeted nanoparticles was concentration and temperature dependent suggesting receptor-mediated endocytosis. The partial inhibition of nanoparticle uptake at low temperature (4 °C) suggested that the internalization of the cIBR-NPs likely occurred via an energy dependent endocytic pathway.

Lysosomesare acidic intracellular compartments that contain a variety of hydrolytic enzymes. Texas red-dextran is internalized by fluid phase endocytosis and accumulates in lysosomes due to its acid hydrolase-resistant nature.[37]The fate of nanoparticles was investigated by studying the colocalization of nanoparticles and lysosomes via fluorescence microscopy. Virtually no colocalization of cIBR-nanoparticles and lysosomes was observed suggesting that LFA-1 targeted nanoparticles do not traffic to lysosomes. The internalization and recycling of LFA-1 to the plasma membrane has been reported.[38] The exocytosis cycle of several types of integrins has also been shown in polymorphonuclear cells including neutrophils.[38] The recycling process of integins is functional to retrieve these receptors and, as they cleave their ligands, to recycle them as adhesion molecules on the plasma membrane.[38] It is possible that cIBR-NPs bound to LFA-1 may enter this receptor recycling process.[38] Regardless, cIBR-NPs may have advantages over untargeted NPs for drug delivery because they can avoid hydrolytic degradation in lysosomes.

3.5 Conclusion

Targeted drug delivery has emerged as an important strategy to improve the efficacy and reduce the adverse effects of drugs. In the present study, cIBR-NPs were characterized as a potential drug delivery system targeting the receptor, LFA-1 integrin, on leukocytes. cIBR-NPs were bound and internalized by LFA-1 on Molt-3 T-cells much more rapidly and to a greater extent than untargeted nanoparticles. Furthermore, cIBR-NPs bound specifically to LFA-1 on the Molt-3 cell line as confirmed by competitive inhibition assays. cIBR-NPs did not appear to traffic to lysosomal compartments suggesting that encapsulating drugs in this type of NPs may offer some protection from lysosomal degradation. The adhesion between T cells and lung epithelial cells expressing LFA-1 and ICAM-1, respectively was significantly inhibited by cIBR-NPs. These studies suggest the plausibility of using LFA-1 as a target molecule with the potential of a dual therapeutic effect by blocking leukocyte recruitment and targeting immunomodulators or anti-inflammatory drugs to leukocytes.

References

1. Bechard D, Arnaud S, Hamida H, Thibaut G, Anne T, Marc A, Jöel P, Jean-Paul D, André-Bernard T, Philippe L. (2001) Human Endothelial-Cell Specific Molecule-1 Binds Directly to the Integrin CD11a/CD18 (LFA-1) and Blocks Binding to Intercellular AdhesionMolecule-1.*J Immunol*, 167, 3099-3160.
2. Sigal A, Bleijs DA, Grabovsky V, van Vliet SJ, Dwir O, Figdor CG, van Kooyk Y, Alon R. (2000) The LFA-1 Integrin Supports Rolling Adhesions on ICAM-1

Under Physiological Shear Flow in a Permissive Cellular Environment. *J Immunol,* 165, 442-452.

3. Yusuf-Makagiansar H, Anderson M.E, Yakovleva TV, Murray JS, Siahaan TJ. (2002) Inhibition of LFA-1/ICAM-1 and VLA-4/VCAM-1 as a therapeutic approach to inflammation and autoimmune diseases. *Medicinal Research Reviews,* 22, 146-167.
4. Hogg N, Laschinger M, Giles K, McDowall A. (2003) T-cell integrins: more than just sticking points. *Journal of Cell Sciences*, 116, 4695-4705.
5. Sarantos MR, Raychaudhuri S, Lum AFH, Staunton DE, Simon SI. (2005) Leukocyte function-associated antigen 1-mediated adhesion stability is dynamically regulated through affinity and valency during bind formation with intercellular adhesion molecule-1. *JBC*, 280, 28290-28298.
6. Hogg N, Henderson R, Leitinger B, McDowall A, Porter J, Stanley P. (2002) Mechanisms contributing to the activity of integrins on leukocytes. *Immunological reviews*, 186, 164-171.
7. Guerette B, Skuk D, Celestin F, Huard C, Tardif F, Asselin I, Roy B, Goulet M, Roy R, Entman M, Tremblay JP. (1997) Prevention by anti-LFA-1 of acute myoblast death following transplantation.*J Immunol*, 159, 2522.
8. Moriyama H, Yokono K, Amano K, Nagata M, Hasegawa Y, Okamoto N, Tsukamoto K, Miki M, Yoneda R, Yagi N, Tominaga Y, Kikutani H, Hioki K, Okumura K, Yagita H, Kasuga M. (1996) Induction of tolerance in murine autoimmune diabetes by transient blockade of leukocyte function-associated antigen-1/intercellular adhesion molecule-1 pathway**.***J Immunol*, 157, 3737-3743.

9. Kavanaugh AF, Davis LS, Jain RI, Nichols LA, Norris SH, Lipsky PE. (1996) A phase I/II open label study of the safety and efficacy of an anti-ICAM-1 (intercellular adhesion molecule-1; CD54) monoclonal antibody in early rheumatoid arthritis.*J Rheumatol, 23, 1338-1344.*
10. Papp K, Bissonnette R, Krueger JG, Carey W, Gratton D, Gulliver WP, Lui H, Lynde CW, Magee A, Minier D, Ouellet JP, Patel P, Shapiro J, Shear NH, Kramer S, Walicke P, Bauer R, Dedrick RL, Kim SS, White M, Garovoy MR. (2001) The treatment of moderate to severe psoriasis with a new anti-CD11a monoclonal antibody. *Journal of the American Academy of Dermatology*, 45, 665-674.
11. Gottlieb AB, Krueger JG, Wittkowski K, Dedrick R, Walicke PA, Garovoy M. (2002) Psoriasis as a model for T-cell–mediated disease: Immunobiologic and clinical Effects of treatment with multiple doses of Efalizumab, an anti–CD11a antibody. *Arch Dermatol*, 138, 591-600.
12. Isobe M, Yagita H, Okumura K, Ihara A. (1992) Specific acceptance of cardiac allograft after treatment with antibodies to ICAM-1 and LFA-1. *Sciences*, 255, 1125-1127.
13. Harihara Y, Sugawara Y, Inoue K, Kubota K, Bandai Y, Makuuchi M, Miyasaka M. (1996) Dose dependent immunosuppressive effects of antibodies to ICAM-1 and LFA-1 on hepatic allografts.*Transplantation Proceedings*, *28, 1794-1795.*
14. Anderson ME, Tejo BA, Yakovleva T, Siahaan TJ. (2006) Characterization of Binding Properties of ICAM-1 Peptides to LFA-1: Inhibitors of T-cell Adhesion.*Chem Bio Drug Des*, 68, 20-28.

15. Anderson ME, Siahaan TJ. (2003) Mechanism of binding and internalization of ICAM-1-derived cyclic peptides by LFA-1 on the surface of T cells: a potential method for targeted drug delivery. *Pharm Res*, 20, 1523-1532.
16. Zimmerman T, Oyarzabal J, Sebastián ES, Majumdar S, Tejo BA, Siahaan TJ, Blanco FJ. (2007) ICAM-1 peptide inhibitors of T-cell adhesion bind to the allosteric site of LFA-1. An NMR characterization, *Chem. Biol. Drug Design*, 70, 347–353.
17. Tibbetts SA, Seetharama SDJ, Siahaan TJ, Benedict SH, Chan MA. (2000) Linear and cyclic LFA-1 and ICAM-1 peptides inhibit T cell adhesion and function. *Peptides*, 21, 1161-1167.
18. Tibbetts SA, Chirathaworn C, Nakashima M, Seetharama SDJ, Siahaan JT, Marcia AC, Benedict HS. (1999) Peptides derived from icam-1 and lfa-1 modulate t cell adhesion and immune function in a mixed lymphocyte culture1. *Transplantation*, 68, 685-692.
19. Gürsoy RN, Siahaan JT. (1999) Binding and internalization of an ICAM-1 peptide by the surface receptors of T cells. *J Peptides Res*, *53, 414-421*.
20. Hong S, Leroueil PR, Majoros IJ, Orr BG, Baker JR.Jr, Holl MMB. (2007) The binding avidity of a nanoparticle-based multivalent targeted drug delivery platform. *Chemistry and Biology Article*, 14, 107-115.
21. Avgoustakis K. (2004) Pegylated poly(Lactide) and poly(Lactide-Co-Glycolide) nanoparticles:preparation, properties and possible applications in drug delivery. *Current Drug Delivery*, 1, 321-333.

22. Guerrouache M, Karakasyan C, Gaillet C, Canva M, Millot MC. (2006) Immobilization of a functionalized poly(ethylene glycol) onto β-cyclodextrin-coated surfaces by formation of inclusion complexes: application to the coupling of proteins. *J Applied Polym Sci*, 100, 2362-2370.
23. Chittasupho C, Xie S, Baoum A, Yakovleva T, Siahaan JT, Berkland C. (2009) ICAM-1 targeting of doxorubicin-loaded PLGA nanoparticles to lung epithelial cells. *European journal of pharmaceutical sciences*, 37, 141-150.
24. Chiou S, Wu W, (2004) Immobilization of Candida rugosa lipase on chitosan with activation of the hydroxyl groups. *Biomaterials*, 25, 197-204.
25. Tominaga T, Sugie K, Hirata M, Morii N, Fukata J, Uchida A, Imura H, Narumiya S. (1993) Inhibition of PMA-induced, LFA-1-dependent lymphocyte aggregation by ADP ribosylation of the small molecular weight GTP binding protein, rho. *J. Cell Biol*, 120, 1529-1537.
26. Rothlein R, Springer TA. (1986) The requirement for lymphocyte function-associated antigen 1 in homotypic leukocyte adhesion stimulated by phorbol ester. *J. Exp. Med*. 163, 1132 - 1149.
27. Panyam J, Labhasetwar V. (2003) Dynamics of endocytosis and exocytosis of Poly(D,L-lactic-co-glycolide) nanoparticles in vascular smooth muscle cells. *Pharmaceutical Research*, 20, 212-220.
28. Porter JC, Hall A. (2009) Epithelial ICAM-1 and ICAM-2 regulate the egression of human T cells across the bronchial epithelium. *The FASEB journal*, 23, 493-502.

29. Majumdar S, Kobayashi N, Krise JP, Siahaan TJ. (2007) Mechanisms of internalization of an ICAM-1 derived peptide by human leukemic cell line HL-60: Influence of physicochemical properties on targeted drug delivery. *Molecular pharmaceutics*, 4, 749-758.
30. Kelly TA, Jeanfavre DD, McNeil DW, Woska JR.Jr, Reilly PL, Mainolfi EA, Kishimoto KM, Nabozny GH, Zinter R, Bormann B, Rothlein R. (1999) Cutting edge: A small molecule antagonist of LFA-1-mediated cell adhesion. *J of immunol*, 163, 5173-5177.
31. Wofsy D. (1985) Strategies for treating autoimmune disease with monoclonal antibodies. *West J Med*, 143, 804–809.
32. Huang M, Matthews K, Siahaan TJ, Kevil CG. (2005) α_L-Integrin I domain cyclic peptide antagonist selectively inhibits T cell adhesion to pancreatic islet microvascular endothelium. *Am J Physiol Gastrointest Liver Physiol*, 288, G67-G73.
33. Yusuf-Makagiansar H, Makagiansar, IT, Hu Y, Siahaan TJ. (2001) Synergistic inhibitory activity of α- and β-LFA-1 peptides on LFA-1/ICAM-1 interaction. *Peptides, 22, 1995-1962.*
34. Tanaka Y. (1999) Activation of leukocyte function-associated antigen-1 on adult T cell leukemia cells. *Leukemia and lymphoma*, 36, 15-23.
35. Pyszniak AM, Welder CA, Takei F. (1993) Cell surface distribution of high-avidity LFA-1 detected by soluble ICAM-1 coated microspheres. *Journal of Immunology*, 152, 5241.

36. Welder CA, Lee DHS, Takei F. (1993) Inhibition of cell adhesion by microspheres cpated with recombinant soluble ICAM-1. *Journal of Immunology*, 150, 2203-2210.

37. Hirota Y, Masuyama N, Kuronita T, Fujita H, Himeno M, Tanaka Y. (2004) Analysis of post-lysosomal compartments. *Biochemical and biophysical. Research Communications*, 314, 306-312

38. Fabbri M, Meglio SD, Gagliani MC, Consonni E, Molteni R, Bender JR, Tacchetti C, Pardi R. (2005) Dynamic partitioning into lipid rafts controls the endo-exocytic cycle of the αL/β2 integrin, LFA-1, during leukocyte chemotaxis. *Molecular biology of the cell*, 16, 5793-5803.

Chapter 4

Nanoparticles Targeting Dendritic Cell Surface Molecules Effectively

Block T cell Conjugation and Shift Response

4.1 Introduction

Professional antigen presenting cells (APC) such as dendritic cells (DCs) help orchestrate immune responses to foreign antigens by capturing antigen and loading it onto major histocompatibilty complex (MHC) class II. The antigen-primed APC then present the antigen to naïve CD4+T cells which express cognate T cell receptors.[1] The resulting immunological synapse formed between T cells and APCs often initiates signaling events for T cell proliferation and effector function such as cytokine production.[2] Leukocyte function-associated antigen-1 (LFA-1; primarily on T cells) binding to intercellular adhesion molecule 1 (ICAM-1; primarily on DCs) can prolong the immunological synapse and support T cell activation.[3-5] Targeting of these molecules is known to modify T cell activation.[6]

Molecules that mediate cell adhesion or signaling are typically present in large numbers at the cell-cell interface. Several studies have shown that multivalency can enhance the binding of ligands to these types of receptors and shift the response of targeted cells.[7-10] For example, multivalent presentation of anti-CD20 monoclonal antibody fragments can enhance the targeting of B cell antigen CD20.[10] Similarly, multiple copies of peptide ligands on a polymer backbone can improve binding to CD21 on B cells when compared to free ligand.[11]Arrays of RGD peptides on micelles have been consistently found to dramatically enhance binding to $\alpha_v\beta_3$ receptors in contrast to free RGD peptides.[12]

The response of cells targeted by multivalent ligands is often unexpected. Antigen valency has been found to be a key parameter affecting binding to B cells

and cellular response.[13] High valency antigen arrays induced antibody production by B cells, while low valency antigen arrays did not.[13] Multivalent ligands induced calcium influx in a dose dependent manner, whereas the same molar concentration of free ligand did not.[13] Ligand valency also affects the response of leukocytes undergoing rolling adhesion. For example, multivalent L-selectin ligands clustered L-selectin and induced L-selectin shedding, but the corresponding monovalent ligands did not.[14-15]Thus, multivalent ligands can affect cell response in addition to enhancing ligand binding.

The binding of LFA-1 and ICAM-1 is also controlled by changes in avidity resulting from receptor clustering.[16-17] Cell adhesion mediated by ICAM-1 and LFA-1 involves multivalent interaction between these two molecules on opposing cells (APC and T cell). LABL (ITDGEATDSG) is a peptide modeled after the I domain of LFA-1 which is the binding site of ICAM-1. cIBR (cyclo 1,12 Pen-PRGGSVLVTGC) is a cyclic peptide derived from domain 1 of ICAM-1 which binds to the I domain of LFA-1.[18-19] LABL and cIBR peptides inhibit homotypic and heterotypic T cell adhesion as well as mixed lymphocyte reactions.[20-22]

Nanoparticles modified with these peptides (cLABL-NPs and cIBR-NPs) were previously used to specifically target ICAM-1 and LFA-1 expressing cells, respectively.[23-25] NPs targeting these receptors were found to bind cells and rapidly internalize via receptor-mediated endocytosis. In addition, cIBR-NP blocked the adhesion of T cells to lung epithelial cells expressing a high level of ICAM-1.[23] Since the oligomeric states of LFA-1 and ICAM-1 molecules contribute to their ability to regulate T cell responses, it was hypothesized that these nanoparticles may bind with

high avidity to ICAM-1 or LFA-1 on DCs. Such targeted NPs were suspected to be better inhibitors of T cell conjugation to DCs compared to free ligands and a potential tool to alter cell response.

4.2 Materials and Methods

Materials

LABL peptide (ITDGEATDSG, Mw 964.95) and cIBR peptide (cyclo 1,12 Pen-PRGGSVLVTGC, Mw 1174.50) were synthesized on a Pioneer peptide synthesizer (PerSeptive Biosystems, CA). Poly(DL-lactic-co-glycolic acid) (50:50) with terminal carboxyl group (PLGA, inherent viscosity 0.67dL/g, Mw ~90 kDa) was purchased from Lakeshore Biomaterials (Birmingham, AL, USA). Pluronic®F-127 was obtained from BASF Corporation. (Mount Olive, NJ, USA). 1-Ethyl-3-[3-dimethylaminopropyl]carbodiimide hydrochloride (EDC), *N*-hydroxysulfosuccinimide (sulfo-NHS) and 2-β mercaptoethanol were purchased from Thermo Fisher Scientific Inc. (Rockford, IL, USA). Coumarin-6 was purchased from Polysciences, Inc. (Warrington, PA, USA). Dialysis membrane (MwCO 100,000) was purchased from Spectrum laboratory Products Inc. (Rancho Dominguez, CA, USA). RPMI-1640 medium was obtained from Cellgro (Manassas, VA, USA). Tumor Necrosis Factor-α (TNF-α) was purchased from Promega (Madison, WI, USA). Granulocyte Macrophage-Colony Stimulating Factor (GM-CSF) was purchased from Peprotech Inc. (Rocky Hill, NJ, USA). Carboxyfluorescein diacetate succimidyl ester (CFSE) and 5-(and-6)-(((4cloromethyl) enzoyl)amino)tetramethylrhodamine (Orange CMTMR)were purchased from

Invitrogen Corporation, (Carlsbad, CA). Monoclonal anti-human CD54 (ICAM-1) Domain 1 and Monoclonal anti-LFA-1 were purchased from Ancell (Bayport, MN, USA). CellTiter 96® AQ_{ueous} Non-Radioactive Cell Proliferation Assay (MTS) was purchased from Promega (Madison, WI, USA). Ovalbumin was purchased from Sigma (St. Louis, MO). Penicillin, streptomycin and L-glutamine were purchased from Cellgro (Manassas, VA, USA). IL-2 was generously provided by Dr. Christophe Nicot at the University of Kansas Medical Center. B6.129S7-*Rag1*^{tm1Mom}Tg(TcraTcrb)425Cbn mice were purchased from Taconic Farms (Hudson, NY). C57BL/6 wildtype mice were purchased from Jax labs (Bar Harbor, ME).

Methods

Cell culture and isolation

Bone marrow derived dendritic cells were generated from C57BL/6 wildtype mice as described.[26] Briefly, 2 x 10^6 cells were isolated from bone marrow, plated on bacterial Petri dishes and cultured in 10 ml DC media (RPMI-1640, 10% heat inactivated fetal bovine serum, 100 μg/ml penicillin-streptomycin, 50 μM β-mercaptoethanol, 20 ng/ml murine granulocyte macrophage colony stimulating factor (GM-CSF) (R&D), and 2 nM L-glutamine. At 72 hours (Day 3), 10 ml of fresh DC media was added to each dish. On days 6 and 8, 10 ml of supernatant and cells were removed, cells recovered by centrifugation (90 x *g*) and added back to the dish with fresh DC medium. On day 9 non-adherent cells were collected, labeled with (5 μM) 5-(and-6)-carboxyfluorescein diacetate, succinimidyl ester (CFSE) for 10 minutes at

37°C, washed, primed with 50 μg/ml ovalbumin, and matured overnight with 100 ng/ml TNF-α.

On day 10, T cells were isolated from B6.129S7-*Rag1*^{tm1Mom}Tg(TcraTcrb)425Cbnmice spleens by passing spleens through a wire mesh. T cells were purified using a negative selection, mouse T cell enrichment kit according to manufacturers' directions (EasySep).

PLGA nanoparticle preparation and characterization

PLGA nanoparticles and nanoparticles loaded with coumarin-6 were prepared by a solvent displacement method. In brief, PLGA was dissolved in acetone (18 mg/ml) containing coumarin-6 (50 μg/ml). The solution was gently infused into 0.1% Pluronic®F-127-COOH (25 ml) under mild stirring (300 RPM). Terminal hydroxyl groups on Pluronic®F-127 were converted to carboxyl groups according to a reported procedure.[27]The resultant nanoparticle suspension was dialyzed (100,000 MWCO) against a 0.2% mannitol solution for 48 hrs to remove excess surfactant. Particle size and zeta potential of nanoparticles were characterized using dynamic light scattering (ZetaPALS, Brookhaven instrument Inc.).

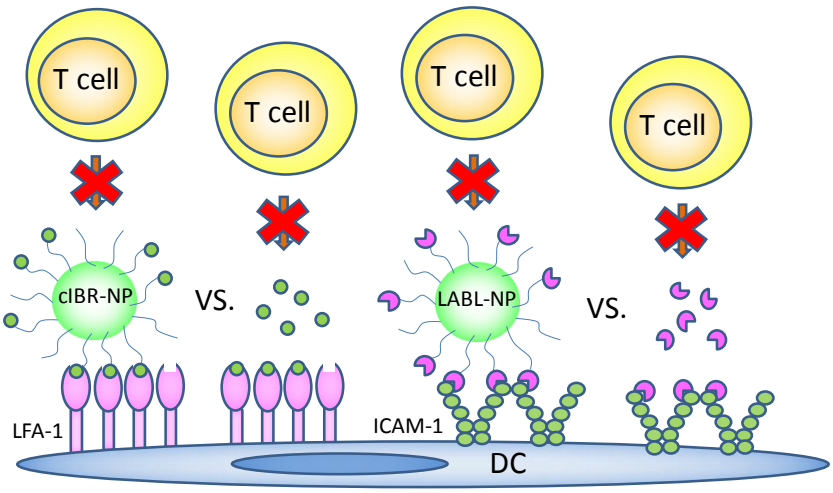

Figure 1 T cell conjugation to DCs maybe blocked by the binding of cIBR-NP to LFA-1 or LABL-NP to ICAM-1 on DCs.

Conjugation of LABL and cIBR peptides to PLGA-nanoparticles

The N-terminus of peptide was covalently linked with the carboxyl groups of Pluronic®F-127-COOH coated on PLGA nanoparticles by carbodiimide chemistry.[23] Specific binding of the LABL and cIBR peptides suggests they are radially pointing away from the particles surface (Figure 1).Nanoparticles (2.2 mg/ml) were buffered using 2-(*N*-morpholino)ethanesulfonic acid (MES; pH 6.5) and incubated with 100 mM 1-Ethyl-3-[3-dimethylaminopropyl]carbodiimide hydrochloride (EDC) and 50 mM *N*-hydroxysulfosuccinimide (sulfo-NHS) for 15 min. EDC was used to react with a carboxyl group on PLGA NPs and formed an amine-reactive O-acylisourea intermediate. Sulfo-NHS was added to stabilize this intermediate, hence increasing the efficiency of coupling reaction. Excess EDC and sulfo-NHS were removed by centrifugation (16,089 g, 10 min). Then, cIBR or LABL peptides (0.4 mg) were added and allowed to react with Pluronic®F-127-COOH on nanoparticles for 12 hrs at

room temperature. Peptide conjugated NPs were collected by centrifugation (16,089 g, 10 min) and washed three times with purified water.

The conjugation efficiency was determined by quantifying the unconjugated ligand remaining in the reaction medium after nanoparticle separation. The peptide density on the surface of nanoparticles after reaction was calculated assuming a normal Guassian particle size distribution.[23, 25]The amount of free peptides in reaction medium was analyzed by gradient reversed phase HPLC (SHIMADZU) using a C_{18} column. The HPLC consisted of SCL-10A SHIMADZU system controller, LC-10AT VP SHIMADZU liquid chromatograph, SIL-10A XL SHIMADZU autoinjecter set at 30 μl injection volume, DGU-14A SHIMADZU degasser, sample cooler, and SPD-10A SHIMADZU UV-Vis detector (220 nm). The HPLC-UV system was controlled by a personal computer equipped with SHIMADZU class VP Software. All separations were carried out using a Vydac® HPLC Protein and Peptide C_{18} column. Gradient elution was carried out to determine the amount of LABL peptide at constant flow of 1 ml/min, from 0% B to 8% B for 5 min, followed by 14.3% B at 17.5 min, 50% at 23 min and 70% B at 24 -35 min. HPLC gradient system was programmed to separate cIBR peptide at constant flow of 1 ml/min, from 25% B for 5 min, 55% B at 25 min and 100%B at 25.1 -30 min. Mobile phase compositions were (A) acetronitrile-water (5:95) with 0.1% TFA and (B) 100% acetonitrile with 0.1% trifluoroacetic acid (TFA).

LFA-1 and ICAM-1 expression on dendritic cells and T cells

The relative expression of LFA-1 and ICAM-1 on T cells and DCs were qualitatively assessed using flow cytometry (FACScan). DCs (4×10^5 cells/ml) were matured with TNF-α (1,000 U/ml) and primed with ovalbumin (OVA) (50 μg/ml) for 24 hrs. DCs were isolated by centrifugation, and incubated 45 minutes on ice with 80 μl of anti-ICAM-1 (0.05 mg/ml) or anti-LFA-1 (0.25 mg/ml) conjugated with FITC at 1:50 dilution. Cells were washed three times and analyzed by flow cytometry.

Splenic C57BL/6-TgN(OT-II.2a)-Rag1 T cells (2.2×10^6 cells/ml) were incubated with 80 μl of anti-ICAM-1-FITC (0.05 mg/ml) or anti-LFA-1-FITC (0.25 mg/ml) on ice for 45 min. Unbound antibodies were removed by rinsing three times with PBS after centrifugation (16,089 g, 2.5 min). The fluorescent intensity of cells was measured by a FACscan flow cytometer. Data analysis was performed using Cell Quest software (BD).

Binding and uptake of LABL-NPs and cIBR-NPs into DCs

The binding and uptake of LABL-NPs and cIBR-NPs encapsulated fluorescent dye was monitored using flow cytometry. DCs (1×10^5 cells/ml) were added and allowed to adhere on a 96 well-plate (200 μl/well) for 24 hr in the presence of TNF-α (1,000 U/ml) and OVA (50 μg/ml). DCs were washed three times with PBS and incubated with NPs, LABL-NPs or cIBR-NPs (2.2 mg/ml, 100 μl) at 37 °C for 15, 30, 45 and 60 min. Cells were washed three times with PBS and trypsinized for 3 min at 37°C. Then DCs were transferred to microcentrifuge tube and washed once with PBS by centrifugation (600 g, 2 min). The fluorescent intensity due to DC uptake of

fluorescent NPs was measured using the FACscan flow cytometer. Data analysis was performed using Cell Quest software (BD).

Fluorescence microscopy of DCs binding/uptake with LABL-NPs or cIBR-NPs

Dendritic cells (1 x 10^6 cells/ml, 300 μl) were added into an 8-well plate and stimulated by TNF-α (1,000 U/ml) and OVA (50 μg/ml) for 24 hrs. Cells were washed with PBS and then incubated with NPs, LABL-NPs or cIBR-NPs (2.2 mg/ml, 300 μl) for 40 min at 37°C. Unbound nanoparticles were removed by washing three times with PBS and cells were fixed with 4% paraformaldehyde. Fluorescence micrographs were acquired using the FITC filter set of a Nikon Eclipse 80i microscope equipped for epifluorescence. Micrographs were captured using an Orca ER camera (Hamamatsu, Inc., Bridgewater, NJ) and analyzed by Metamorph, version 6.2 (Universal Imaging Corp., West Chester, PA). All images were corrected for variations in excitation light intensity.

***In vitro* cellular cytotoxicity of LABL-NPs and cIBR-NPs**

MTS cell viability assays were performed to provide an assessment of the toxicity of LABL-NPs and cIBR-NPs on T cells and TNF-α stimulated and OVA primed DCs. Briefly, T cells (3.2 x 10^6 cells/ml) and DCs (1 x 10^5 cells/ml) were seeded on 96-well plates and incubated with various concentrations of LABL-NPs and cIBR-NPs for 24 hr. A tetrazolium salt MTS was applied and the incubation was continued for additional 4 hrs. MTS was converted by mitocondrial dehydrogenase enzyme in living cells to form a colored formazan product. The absorbance of the formazan product was recorded at 490 nm using a 96-well plate reader (Spectramax M5).

DCs and T cell conjugate formation

DCs (4 x 10^5 cells/ml) were stained by incubating with 5 ml of CFSE in PBS (10 μM) for 10 min at 37 °C in PBS. The staining was quenched by the addition of 25 ml of complete culture medium and incubation at 4°C for 10 min. The remaining dye was washed away by three washes with complete culture medium. T cells were incubated with 10 μl of CMTMR orange fluorescent dye (5 μM) in 10 ml of PBS for 30 min at 37°C. The reaction of the dye was quenched by incubating with complete culture medium for 30 min at 37°C. T cells were washed three times with complete culture medium. Untreated DCs were used as a positive control. Dendritic cells (4 x 10^5 cells/ml) primed with OVA (50 μg/ml) and matured in the presence of TNF-α (1,000 U/ml) were incubated with anti-ICAM-1 (1 μg/ml), anti-LFA-1 (5 μg/ml), NPs (2.2 mg/ml), LABL peptide (0.095, 0.19 and 0.38 mM), LABL-NPs (1.1, 2.2 and 4.4 mg/ml), cIBR peptide (0.012, 0.024 and 0.048 mM) or cIBR-NPs (1.1, 2.2 and 4.4 mg/ml) for 30 min at 37 °C. DCs were washed three times with PBS and incubated with T cells (2 x 10^6 cells/ml) for 2 hr at 37 °C. After incubation, DCs were washed three times with PBS and fixed with 4% paraformaldehyde. Cells were imaged using an Orca ER camera (Hamamatsu, Inc., Bridgewater, NJ) and imaged using Metamorph, version 6.2 (Universal Imaging Corp., West Chester, PA). Dendritic cells and T-cells attached to dendritic cells were measured by using Image J software per condition from all images. The analysis was performed by using color segmentation (RGB channel separation), which was made binary and followed by measurement of the area of R and G channels. Similar threshold limiting was applied

to all images and colors. The results were reported by the percent of ratio of R channel area (corresponds to T cells) to G channel area (corresponds to DC). The percentage of T cell-conjugates was calculated.

$$\% \text{ T cell conjugated to DC} = \frac{\text{Area of T cells binding DCs}}{\text{Area of DCs}} \times 100$$

T cell proliferation assay

Primary T cells isolated from C57BL/6-TgN(OT-II.2a)-Rag1 mice were labeled with carboxyfluorescein succinimidyl ester (CFSE) (5 μM) for 10 min at 37 °C, 5% CO_2 to observe the dye dilution by cell division. The staining was quenched by the addition of 5 volumes of culture medium into T cells and incubated 10 min at 4°C. DCs (4 x 10^5 cells/ml) were matured in the presence of TNF-α (1,000 U/ml) and primed with OVA (50 μg/ml) for 24 hrs in 24-well plate. DCs were treated with anti-ICAM-1 (1 μg/ml), anti-LFA-1 (5 μg/ml), unconjugated NPs (2.2 mg/ml), LABL peptide (0.095, 0.19 and 0.38 mM), LABL-NPs (1.1, 2.2 and 4.4 mg/ml), cIBR peptide (0.012, 0.024 and 0.048 mM) or cIBR-NPs (1.1, 2.2 and 4.4 mg/ml) for 30 min, at 37 °C, 5% CO_2 and washed three times with PBS. T cells (2 x 10^6 cells/ml) in serum free RPMI-1640, IL-2 and 1% penicillin-streptomycin were incubated with DCs 7 days at 37°C, 5% CO_2.T cells collected after 24 hrs (1 day) and 168 hrs (7 days) were centrifuged at 16,089 gfor 2 minutes and fixed with 4% paraformaldehyde. The CFSE dilution was measured by using FACScan flow cytometer. The percent of T cell proliferation was analyzed by calculating the percent of cells with diluted CFSE using FlowJo software.

Quantification of cytokines in cell culture supernatants by ELISA

DCs were matured in the presence of TNF-α (1,000 U/ml) and primed with OVA (50 μg/ml) for 24 hrs in 24-well plate. DCs were treated with anti-ICAM-1 (1 μg/ml), anti-LFA-1 (5 μg/ml), unconjugated NPs (2.2 mg/ml), LABL peptide (0.095, 0.19 and 0.38 mM), LABL-NPs (1.1, 2.2 and 4.4 mg/ml), cIBR peptide (0.012, 0.024 and 0.048 mM) or cIBR-NPs (1.1, 2.2 and 4.4 mg/ml) for 30 min, at 37 °C, 5% CO_2 and washed three times with PBS. T cells (2 x 10^6 cells/ml) in serum free RPMI-1640, IL-2 and 1% penicillin-streptomycin were incubated with DCs 7 days at 37°C, 5% CO_2.Supernatants of cell cultures were collected for cytokine detection. Secreted TNF-α, IL-2, IL6 and IL-17 were measured by ELISA assay (Cytokine Core Lab, Baltimore, Maryland). ELISA was performed in Nunc Maxisorb ELISA strips freshly coated with capture antibody for 16 hours before the assay was performed. Detecting antibody and the streptavidin- peroxidase conjugate were added into standard, all samples and controls. Premixed substrate solution (Neogen) was then added. The plate was read on a Molecular Divices ELISA plate reader. Curve fitting was selected among linear, quadratic and 4-point based on the best regression coefficient using the SoftPro software package.

Statistical analysis

Statistical evaluation of data was performed using an analysis of variance (one-way ANOVA). Newman–Keuls was used as a post-hoc test to assess the significance of differences. To compare the significance of the difference between the means of two

groups, a *t*-test was performed; in all cases, a value of $p < 0.05$ was accepted as significant.

4.3 Results

Characterization of nanoparticles and peptide-conjugated nanoparticles

A variety of targeted and control NPs were synthesized. The size of all PLGA NP formulations was less than 200 nm and NPs possessed a negative zeta potential (Table 1). Low polydispersity values (<0.1) suggested a relatively narrow particle size distribution. LABL and cIBR peptides were successfully conjugated to PLGA-NPs. The zeta potential of LABL-NPs was more negative than unconjugated NPs, presumably due to the LABL peptide having a net charge of -3. cIBR-NPs had a less negative charge than unconjugated NPs. Pluronic® F127-COOH groups were probably masked by the cIBR peptide, which has a net charge of +1. The amounts of LABL and cIBR peptides attached to NPs were determined by quantifying the unconjugated peptide remaining in the medium after the conjugation reaction.[23] LABL was conjugated with a high density, while cIBR density closely matched a previous publication (Table 2). [23]

Relative expression of ICAM-1 and LFA-1 on DCs and T cells

Expression levels of ICAM-1 and LFA-1 on activated bone marrow derived dendritic cells (DCs) matured with TNF-α and primed with OVA were determined using fluorescent anti-ICAM-1 and anti-LFA-1. DCs expressed both ICAM-1 and LFA-1 indicating that either LABL or cIBR could be used to target these adhesion molecules on DCs (Figure 2A). For these studies we used primary CD4+ T cells, which express

an ovalbumin specific T cell receptor (OT-II). Flow cytometry data showed minimal expression of ICAM-1 on primary OT-II T cells but high expression of LFA-1 as expected (Figure 2B). Although NPs were not directly incubated with OT II T cells, the relative expression of these two receptors was provided for reference.

Table 1 Nanoparticle properties of specified formulations*

	NP	**LABL-NP**	**cIBR-NP**
Effective diameter (nm)	154.6 ± 10.0	172.6 ± 2.5	171.9 ± 4.3
Polydispersity	0.026 ± 0.030	0.070 ± 0.039	0.055 ± 0.005
Zeta potential (mV)	-21.4 ± 0.4	-34.7± 2.0	-13.9 ± 0.8

*Values are representative of three experiments (mean ± S.D.).

Table 2 Density of peptides on the surface of nanoparticles*

	Size (nm)	**Total surface area (m^2/g of PLGA)**	**peptide density (pmol/cm^2)**
LABL-NP	172.6	25.9	265.5 ± 78.5
cIBR-NP	171.9	26.1	39.5 ± 3.0

*Values are representative of three experiments (mean ± S.D.)

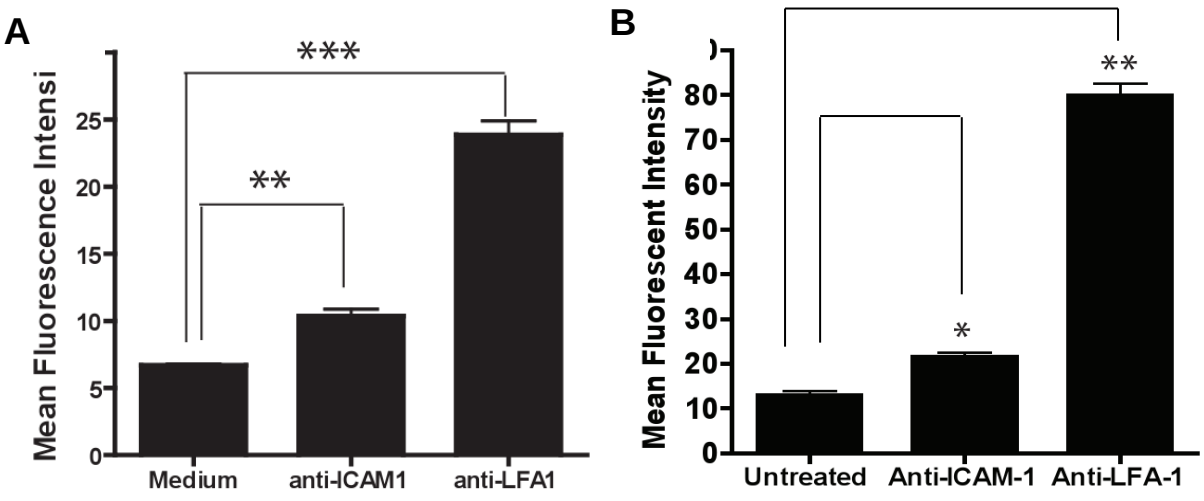

Figure 2 (A) ICAM-1 and LFA-1 expression on dendritic cells and on (B) T cells. OVA-primed DCs and T cells were incubated with anti-ICAM-1 and anti-LFA-1 for 45 min on ice. Cells were washed and analyzed by flow cytometry. ** indicates $p<0.001$ and * indicates $p<0.05$.

Both LABL-NPs and cIBR-NPs exhibited rapid binding to DCs

LABL peptide binds specifically to the domain 1 of ICAM-1, whereas cIBR peptide binds the I domain of LFA-1.[18-19] LABL-NPs, cIBR-NPs and unconjugated NPs were incubated with DCs to investigate the binding by DCs. Immature DCs were stimulated with TNF-α and primed with OVA for 24 hrs prior to addition of NPs. In comparison to untargeted NPs, fluorescent intensities of DCs incubated with LABL-NPs or cIBR-NPs were much higher than cells incubated with untargeted NPs at all incubation times. Fluorescence intensities of DCs incubated 45 minutes with LABL-NPs or cIBR-NPs were ~2 and ~2.3 fold greater than NPs, respectively, indicating

that the interactions of LABL-NPs and cIBR-NPs with DCs occurred more rapidly and to a greater extent compared to untargeted NPs (Figure 3).

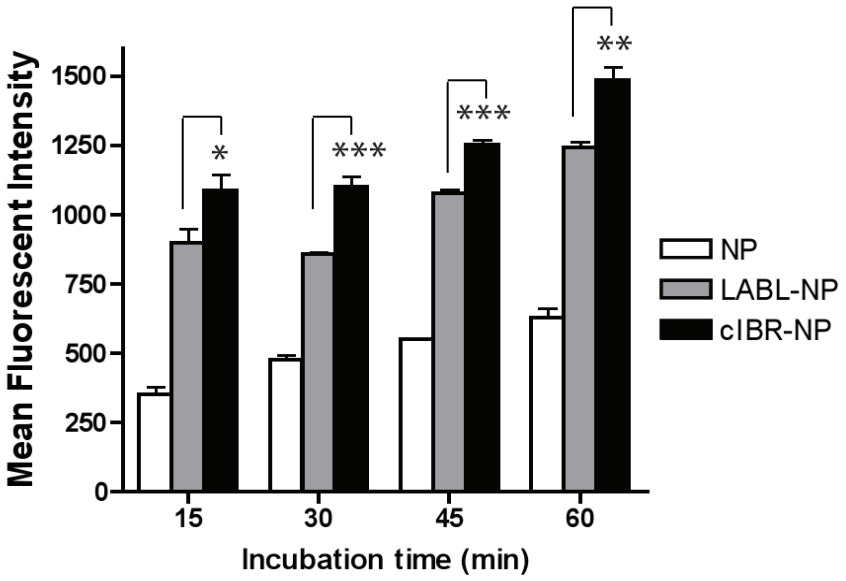

Figure 3 Binding of NPs, LABL-NPs or cIBR-NPs to dendritic cells. NPs, LABL-NPs and cIBR-NPs were incubated with OVA-primed and TNF-α activated DCs for 15, 30, 45 or 60 min at 37 °C and analyzed by flow cytometry. The interaction of cIBR-NPs with dendritic cells was significantlygreater than LABL-NPs and untargeted NPs at all time points. The fluorescence of dendritic cells incubated with each of the NP types increased with time. * indicates $p< 0.05$, ** indicates $p< 0.01$ and *** indicates $p< 0.001$.

Fluorescence microscopy of DCs binding nanoparticles

The binding of NPs, LABL-NPs or cIBR-NPs by DCs was also followed using fluorescence microscopy. Nanoparticle fluorescence rapidly localized to DCs (Figure 4A). Images collected using MetaMorph were analyzed using ImageJ software and

showed ~2 times greater fluorescence intensity of DCs incubated with LABL-NPs compared to untargeted NPs at 40 min (Figure 4B), thus supporting flow cytometry results. DCs treated with cIBR-NPs demonstrated even higher fluorescent intensities. These results indicated that LABL-NPs and cIBR-NPs effectively targeted DCs.

The internalization of LABL-NPs and cIBR-NPs was supported by the punctate fluorescence pattern observed in the micrographs. Similar patterns were also reported for the uptake of untargeted NPs and cLABL-NPs in lung epithelial cells (A549 cells) and endothelial cells (HUVECs) expressing high levels of ICAM-1 in previous reports.[24-25] The punctate pattern of cIBR-NPs appeared slightly more evident than LABL-NPs and untargeted NPs at 40 min of incubation (Figure 4A). These results supported the flow cytometry data.

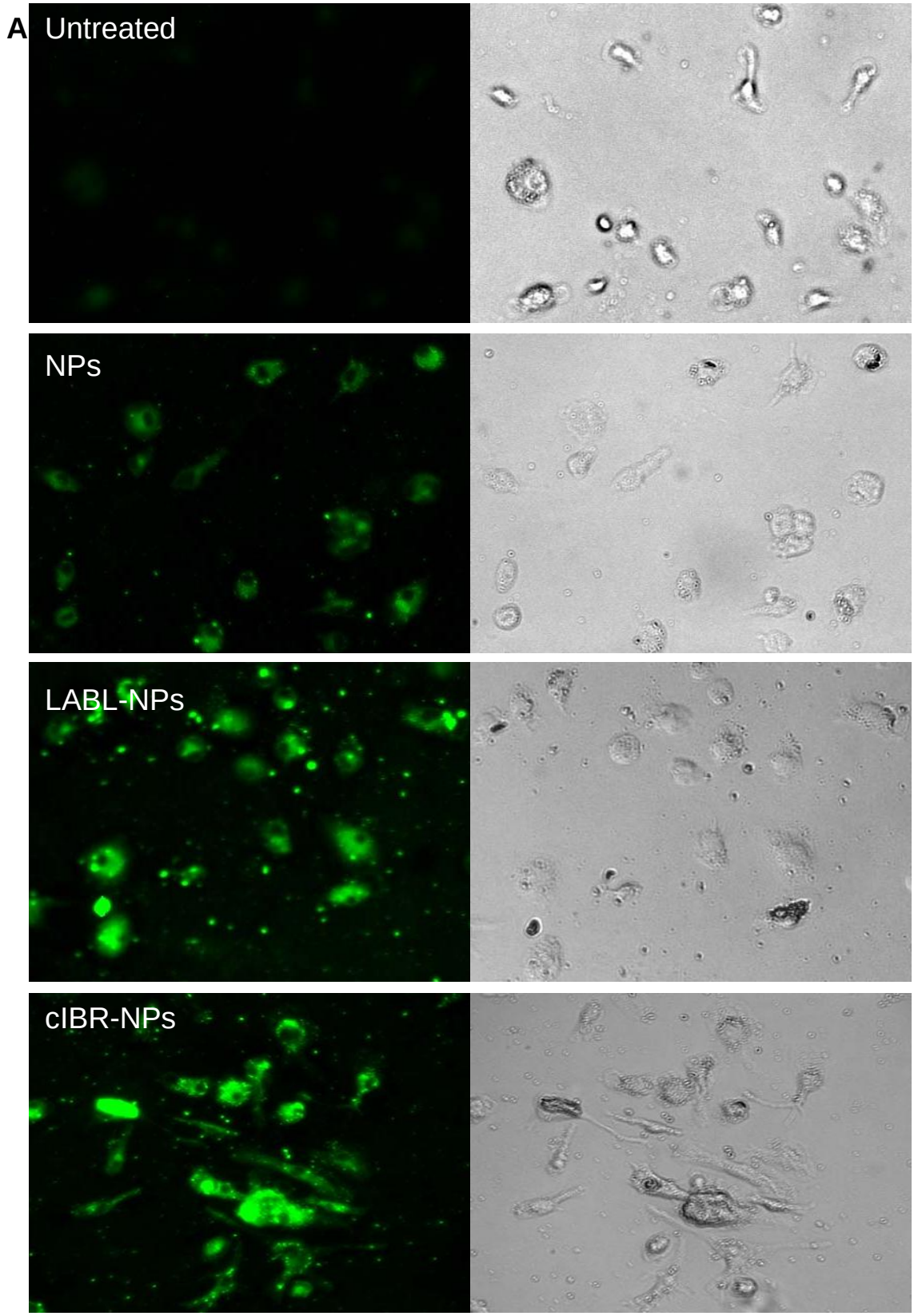
A
Untreated
NPs
LABL-NPs
cIBR-NPs

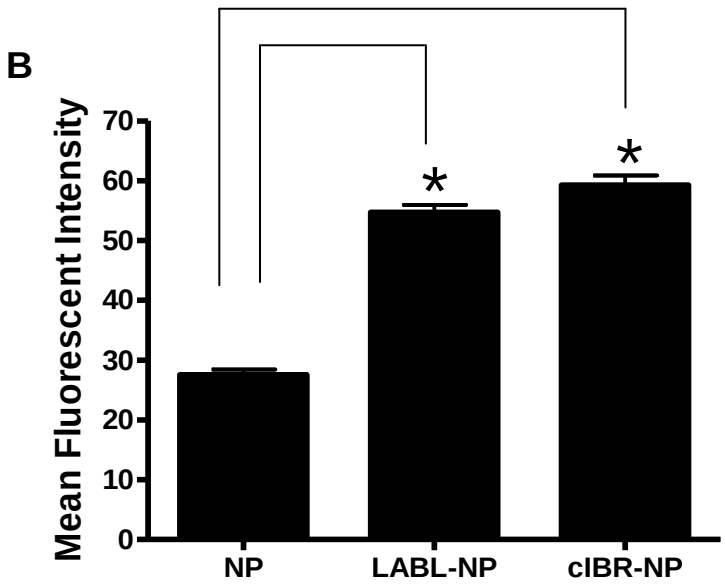

Figure 4 (A) Fluorescent micrographs of DCs in medium (untreated), DCs incubated with untargeted NPs, DCs incubated with LABL-NPs and DCs incubated with cIBR-NPs for 40 min. Punctate fluorescence patterns suggested the accumulation of NPs with the cells (B) Mean fluorescent intensities of DCs incubated with NP, LABL-NP and cIBR-NP were quantified from micrographs using ImageJ software. DCs were stimulated by TNF-α and primed with OVA for 24 hrs prior to the study. DCs were then incubated with NPs, LABL-NPs and cIBR-NPs for 40 min at 37 °C. * indicates $p < 0.001$.

***In vitro* cellular cytotoxicity of LABL-NPs or cIBR-NPs**

Cell viability studies indicated that LABL-NPs and cIBR-NPs were minimally cytotoxic to DCs and T cells. The average cell viability was greater than 95% at all concentrations tested when LABL-NPs and cIBR-NPs were incubated with DCs for 24 hrs (Figure 5A and 5B). For reference, the viability of T cells exposed to LABL-

NPs and cIBR-NPs relative to untreated cells was also evaluated. After 24 hrs of treatment, a decrease in T cell viability was observed at LABL-NPs concentrations higher than 16 mg/ml (IC_{50} = 25.6 mg/ml). The IC_{50} of cIBR-NPs with T cells was 3.4 mg/ml. From our results, we inferred that DCs were highly viable after incubation with these particles for 30 min in the conjugation study. DC cultures were washed to remove any free NPs prior to addition of primary T cells; therefore, T cell cytotoxicity data is only offered for references.

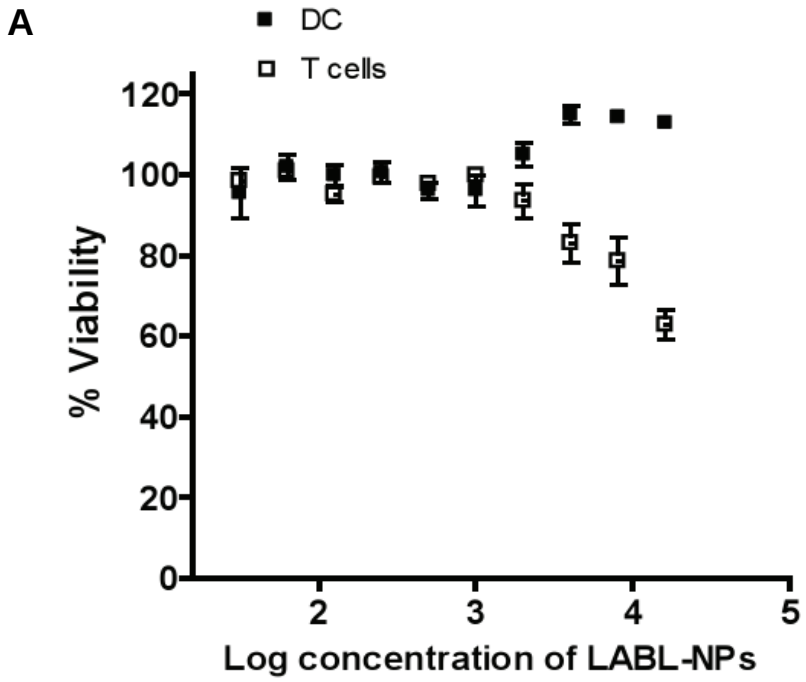

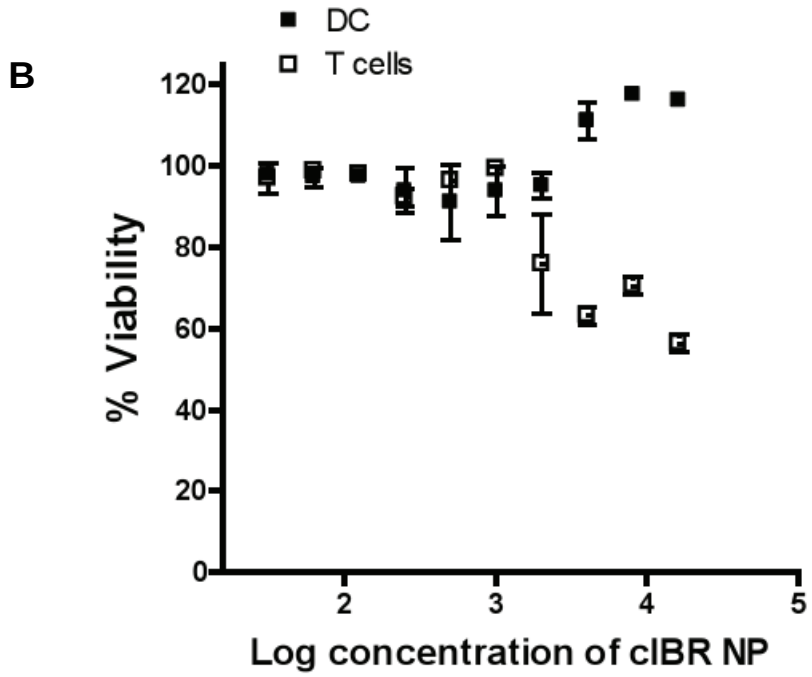

Figure 5 Dendritic cell and T cell viability in the presence of (A) LABL-NPs or (B) cIBR-NPs. LABL-NPs and cIBR-NPs were minimally cytotoxic to DCs and T cells at the concentrations used for ensuing studies.

Peptide-NPs significantly inhibited the conjugation of DCs and T cells.

The induction of cell proliferation and cytokine production in resting T cells requires binding of LFA-1 on T cells and its receptor, ICAM-1 on DCs to allow prolonged signaling.[3-5] The effect of LFA-1/ICAM-1 blockade on conjugate formation between T cells isolated from B6.129S7-*Rag1*^{tm1Mom}Tg(TcraTcrb)425Cbnmice and mature DCs primed with OVA was investigated. LABL-NP blockade of ICAM-1 on DCs led to a substantial decrease in the number of T cells bound to DCs (Figure 6). Pretreatment of DCs with LABL-NPs resulted in up to a 76% decrease in T cell binding to DCs compared to T cells incubated with untreated DCs. From these results, we inferred that LABL-NPs bound ICAM-1 expressed on DCs and blocked

the availability of ICAM-1 to interact with LFA-1 on T cells. The number of T cells interacting with DCs pretreated with cIBR-NPs was decreased up to 78% compared to T cells incubated with untreated DCs. Untargeted NPs decreased the T cell conjugation to DCs by only 23%.

In addition, free peptides were incubated at molar concentrations corresponding to the molar amount of peptides presented on the surface of nanoparticles. Peptide-conjugated nanoparticles blocked the binding of T cells to DCs significantly better than free peptides. Furthermore, inhibition of the T cell conjugation to DCs was further enhanced by increasing LABL-NP or cIBR-NP concentration. These data were also analyzed by counting T cells conjugated to DCs (Figure 6C) and the results were in agreement with the analysis reported here using Image J software.

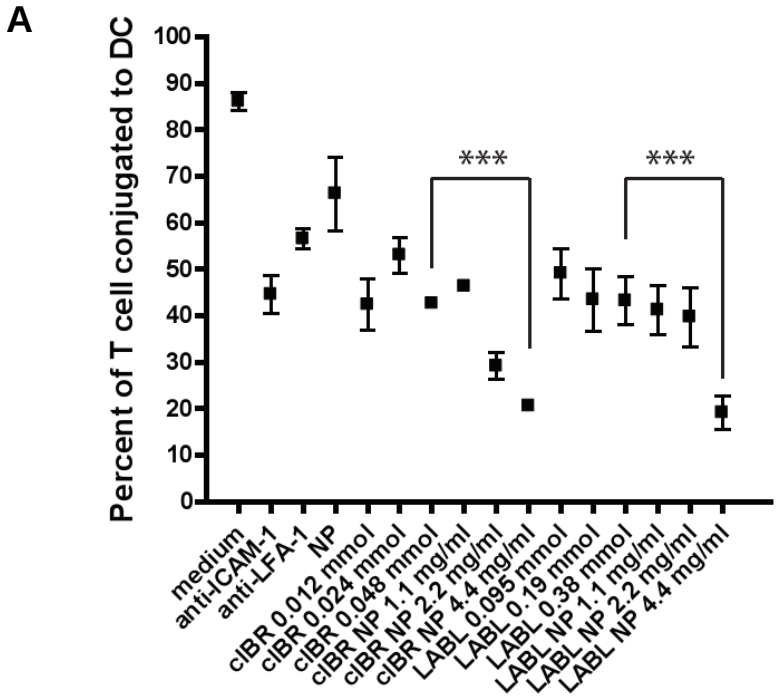

B

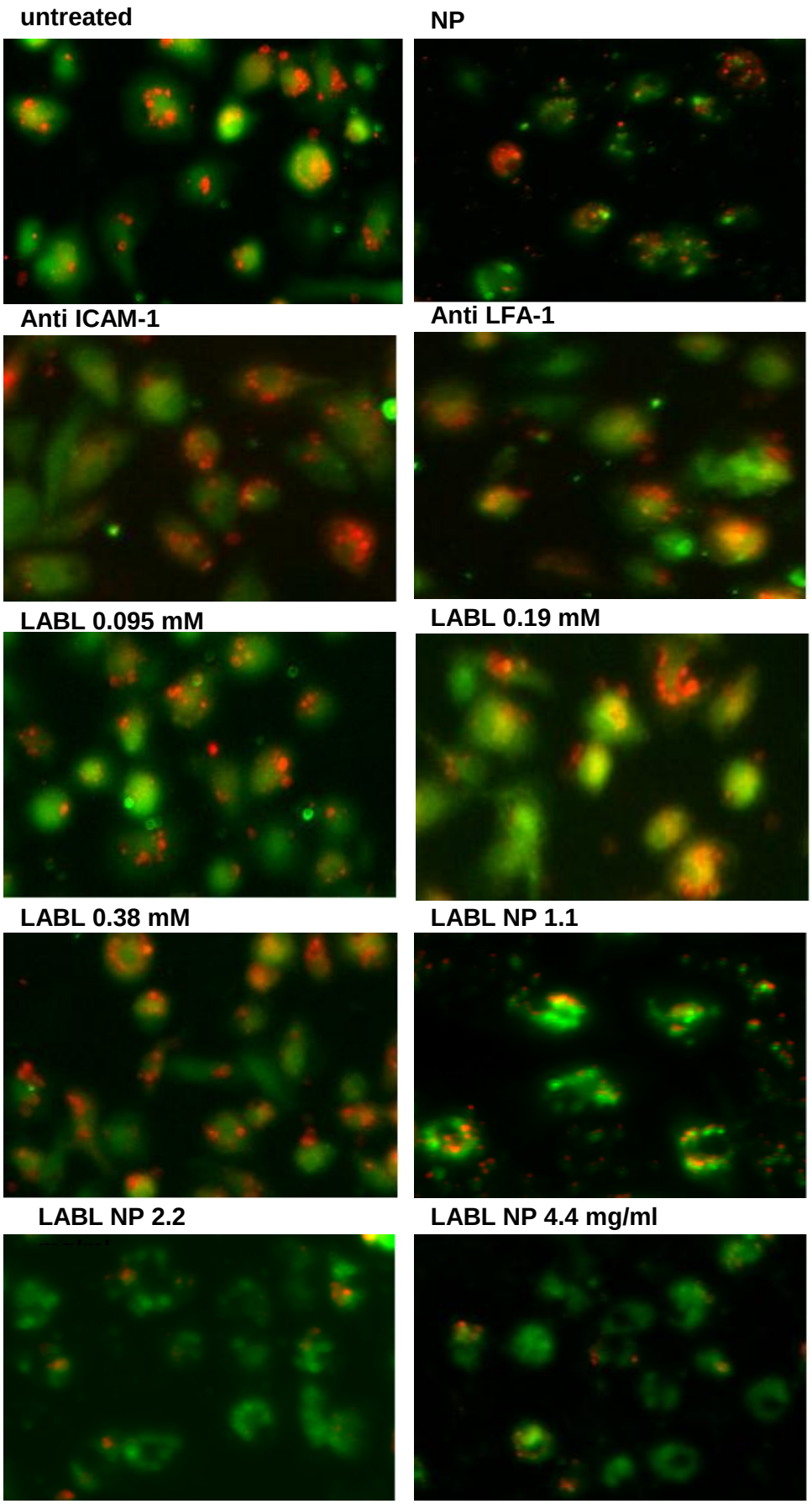
untreated
NP
Anti ICAM-1
Anti LFA-1
LABL 0.095 mM
LABL 0.19 mM
LABL 0.38 mM
LABL NP 1.1
LABL NP 2.2
LABL NP 4.4 mg/ml

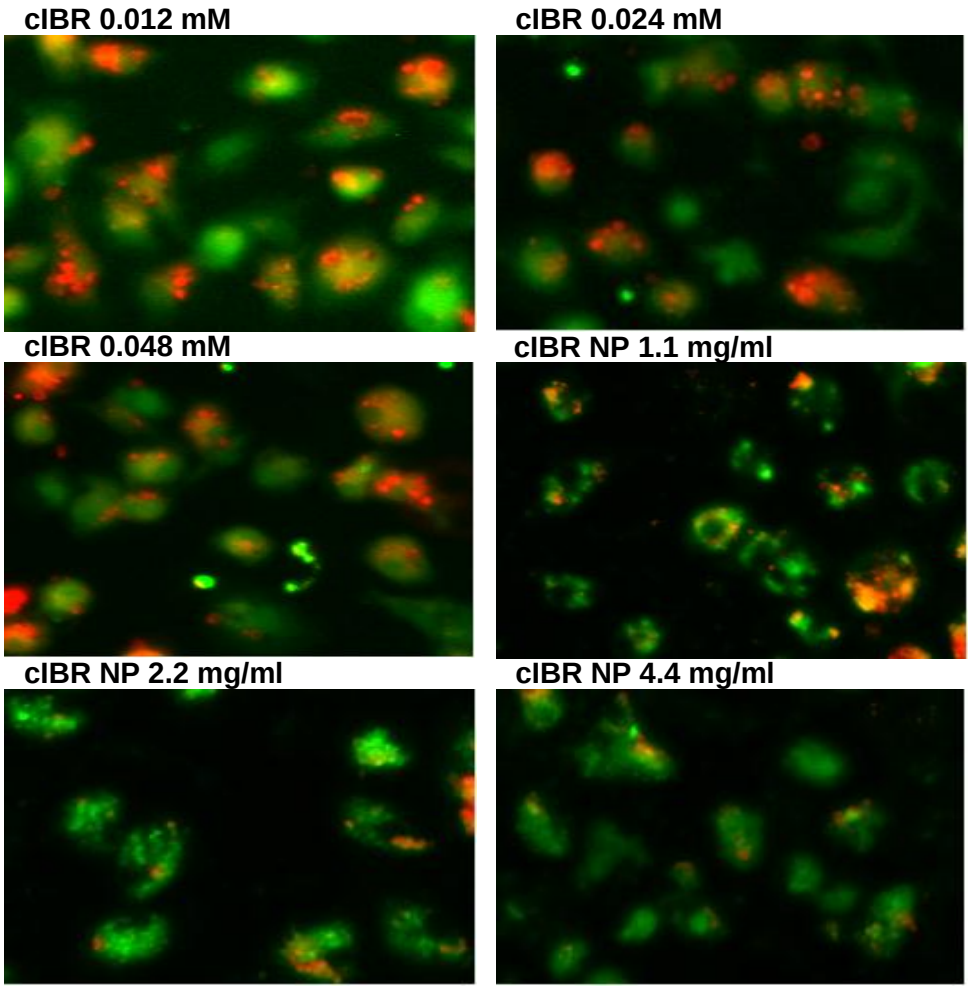
cIBR 0.012 mM
cIBR 0.024 mM
cIBR 0.048 mM
cIBR NP 1.1 mg/ml
cIBR NP 2.2 mg/ml
cIBR NP 4.4 mg/ml

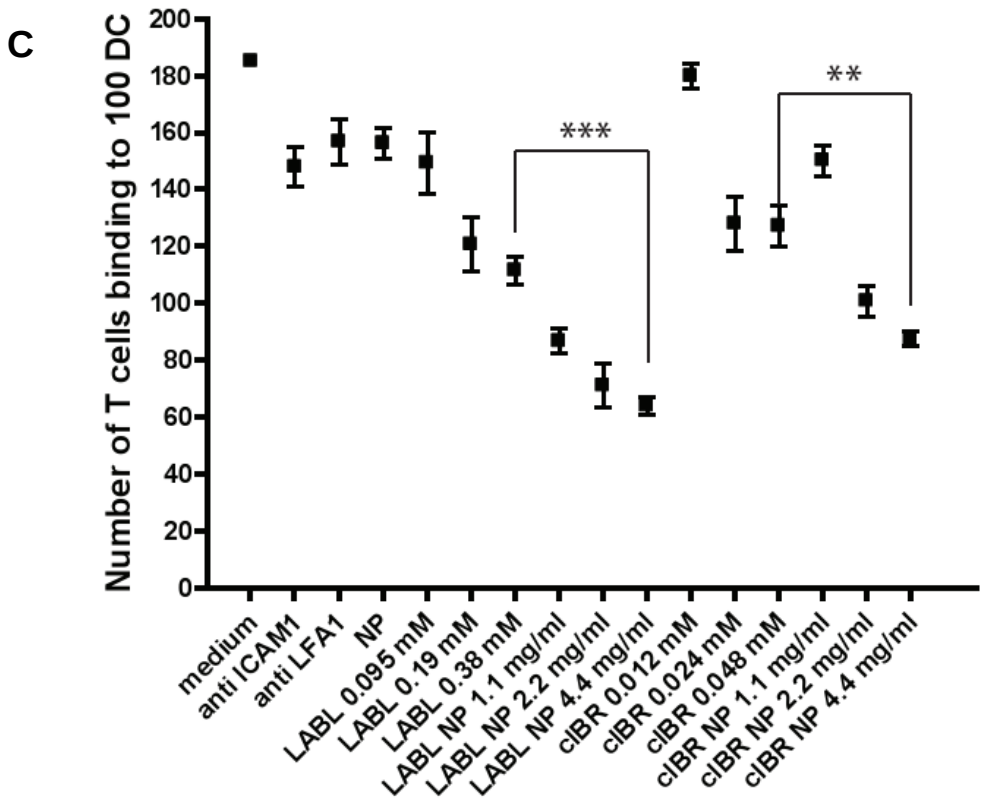

Figure 6 (A) Blocking of DC-T cell conjugate formation. LABL-NPs and cIBR-NPs inhibited the binding of T cells to DCs to a much greater extent than free LABL and cIBR peptides. (B) Micrographs of T cells (red) binding DCs (green). LABL-NPs and cIBR-NPs exhibited greater inhibition of T cell conjugation to Dcs than LABL peptides, anti-ICAM-1, anti-LFA-1, NPs and untreated DCs. DCs were incubated with TNFα and primed with OVA for 24 hrs prior to incubation with samples. DCs were washed and T cells were cocultured for 2 hours and T cells and DCs were imaged and counted. (C) LABL-NPs and cIBR-NPs inhibited the binding of T cells to DCs to a much greater extent than free LABL and cIBR peptides. DCs were incubated with samples for 30 min, washed and cocultured with T cells for 2 hours. T cells and DCs were imaged and counted. *** indicates $p<0.001$.

Effects of LABL-NPs and cIBR-NPs on T cell proliferation

To examine the effect of NPs on T cell proliferation, carboxyfluorescein diacetate succimidyl ester (CFSE) fluorescence dilution in OVA-specific T cells was analyzed after co-incubation with DCs for 24 hrs (1 day) and 168 hrs (7 days). DCs were pretreated with untargeted nanoparticles (NPs), antibodies, free peptides or peptide-conjugated NPs. The three different molar concentrations of free peptides matched the molar concentration of peptide conjugated to NPs. Division of cells was calculated from the percentage of cells having diluted fluorescent intensity using Flowjo software. Untargeted NPs and cIBR-NPs incubated with DCs led to a substantial increase in the number of T cells undergoing division. We observed that 89%, 78% and 41% of T cells divided following co-incubation with DCs which had been pretreated with NPs (2.2 mg/ml) or cIBR-NPs (4.4 and 2.2 mg/ml) for 7 days, respectively. In contrast, T cells incubated with untreated DCs only proliferated ~6%.

The proliferation of T cells incubated with DCs pretreated with anti-ICAM-1, anti-LFA-1, LABL peptide, LABL-NPs (4.4, 2.2 and 1.1 mg/ml) or cIBR peptide were not substantially altered by the treatments (Figure 7). There were no significant differences in the levels of T cell proliferation between the groups of DCs treated with these samples when compared to untreated DCs. T cells alone without DCs were used as a negative control and yielded a T cell proliferation of only ~1.8%.

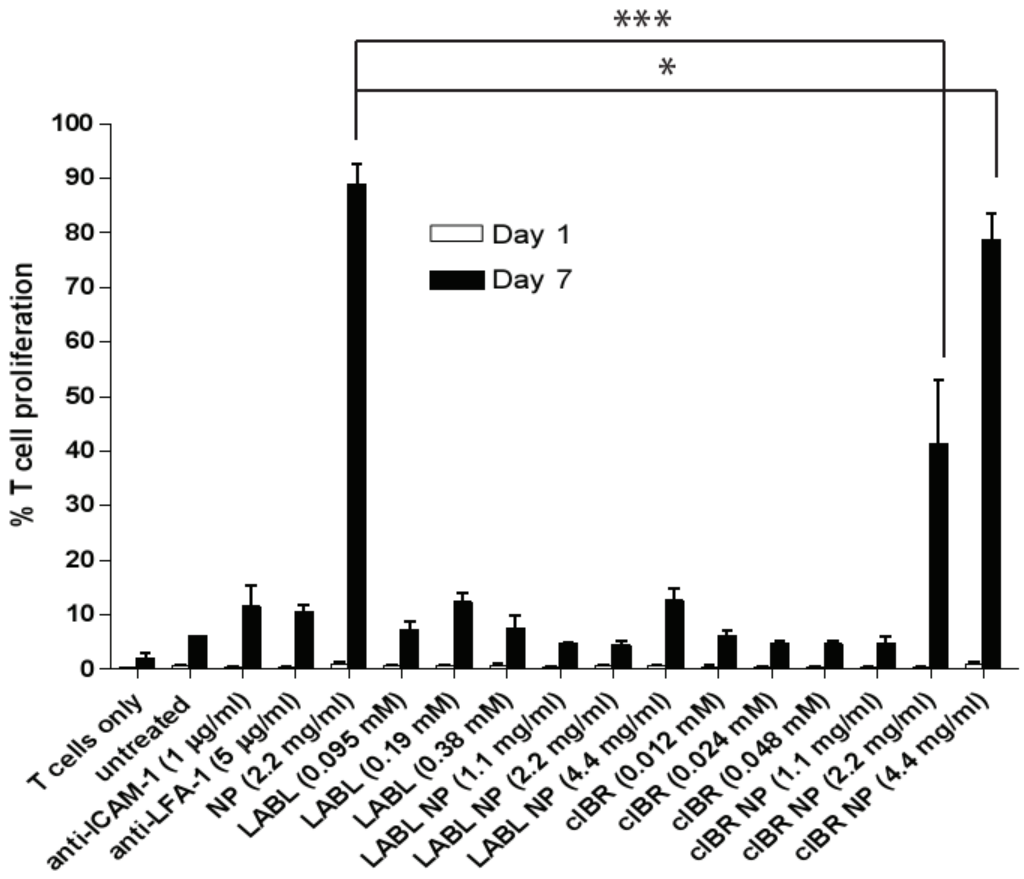

Figure 7 The proliferation of T cells after coculture with DCs treated with samples. The percent of T cells dividing after incubation for 24 hrs (1 day) and 168 hrs (7 days) was determined by flow cytometry. DCs incubated with TNFα and primed with OVA were incubated with samples for 30 min at 37 °C. After removing samples, OVA specific T cells were added and incubated with DCs for 7 days. cIBR-NPs and untargeted NPs stimulated the proliferation of OTII T cells but other samples did not significantly alter T cell proliferation. *** indicates $p<0.001$ and * indicates $p<0.05$.

Cytokine production of DCs and OT-II T cells

One marker for DC maturation and T cell stimulation is the production of cytokines. Cytokines are produced by both antigen presenting cells such as DCs and by T cells. DCs predominantly produce TNF-α, IL-1 and IL-6.[28] IL-2 is produced by CD4+ T cells.[28] To observe cytokine production of DCs after treatment with peptides or nanoparticles, DCs matured with TNF-α and primed with OVA were incubated with LABL peptide, cIBR peptide, LABL-NPs, cIBR-NPs, or NPs for 30 min. DC cultures were washed and then OT-II T cells were cocultured with DCs for 7 days and cytokine production was determined by enzyme-linked immunoassay (ELISA). DCs incubated with LABL-NPs, cIBR-NPs or NPs secreted significantly higher amounts of TNF-α (4-5 fold), relative to untreated DCs. In contrast, the amounts of TNF-α produced by DCs treated with LABL and cIBR peptide solutions were very low similar to untreated DCs (Figure 8A).

Furthermore, the amount of IL-6 produced by coculture of T cells with DCs pretreated with untargeted NPs was not significantly different from the coculture of untreated DCs and T cells. Conversely, the amount of IL-6 produced by coculture of T cells with DCs pretreated with LABL peptide, cIBR peptide, LABL-NPs or cIBR-NPs were lower than coculture of untreated DCs and T cells (Figure 8B). These results suggested that LABL peptide, cIBR peptide, LABL NPs and cIBR-NPs, did not stimulate IL-6 production, which is predominantly produced by DCs.[28] Untargeted NPs did not alter IL-6 production relative to untreated DCs suggesting that these particles neither bound specifically to cell adhesion molecules nor blocked the activation of the OTII T cells.

Proliferation of naïve CD4+ T cells into effector T cells is also regulated by mature DCs. Coculture of OT-II T cells with DCs that had been pre-incubated with untargeted NPs enhanced T cell proliferation and production of IL-17, when compared to other treatments or controls (Figure 8C). From these results we concluded the presence of untargeted NPs promotes activation of T cells and may increase production of TGFβ, which is normally considered immunosuppressive. Yet, in the presence of IL-6, TGF-β promotes the expression of IL-17 and the differentiation of Th17 CD4 cells. [30]These findings are further supported by the low levels of IL-6 produced by LABL, cIBR, LABL-NPs and cIBR-NPs treatments which correlate with the production of IL-17 since IL-6 in combination with TGF-β induces Th17 differentiation from naïve CD4+ T cells.[30] Finally, the amount of IL-2 was undetectable in all media of DCs cocultured with OT-II T cells.

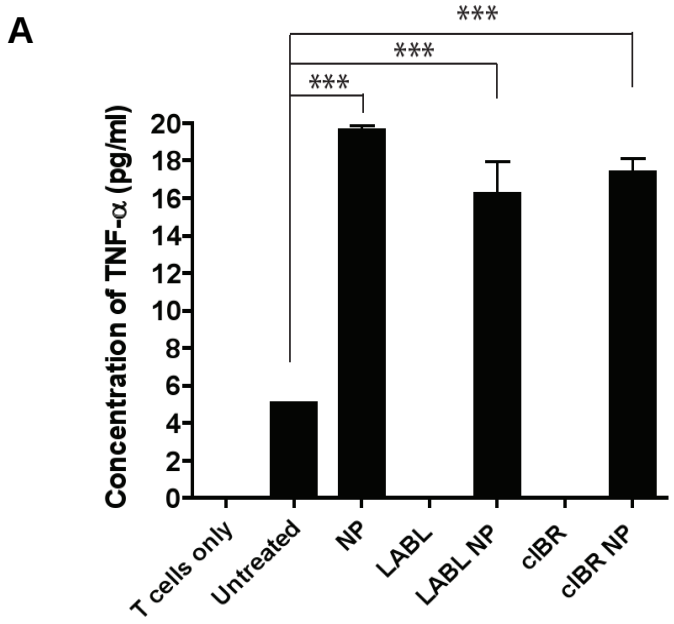

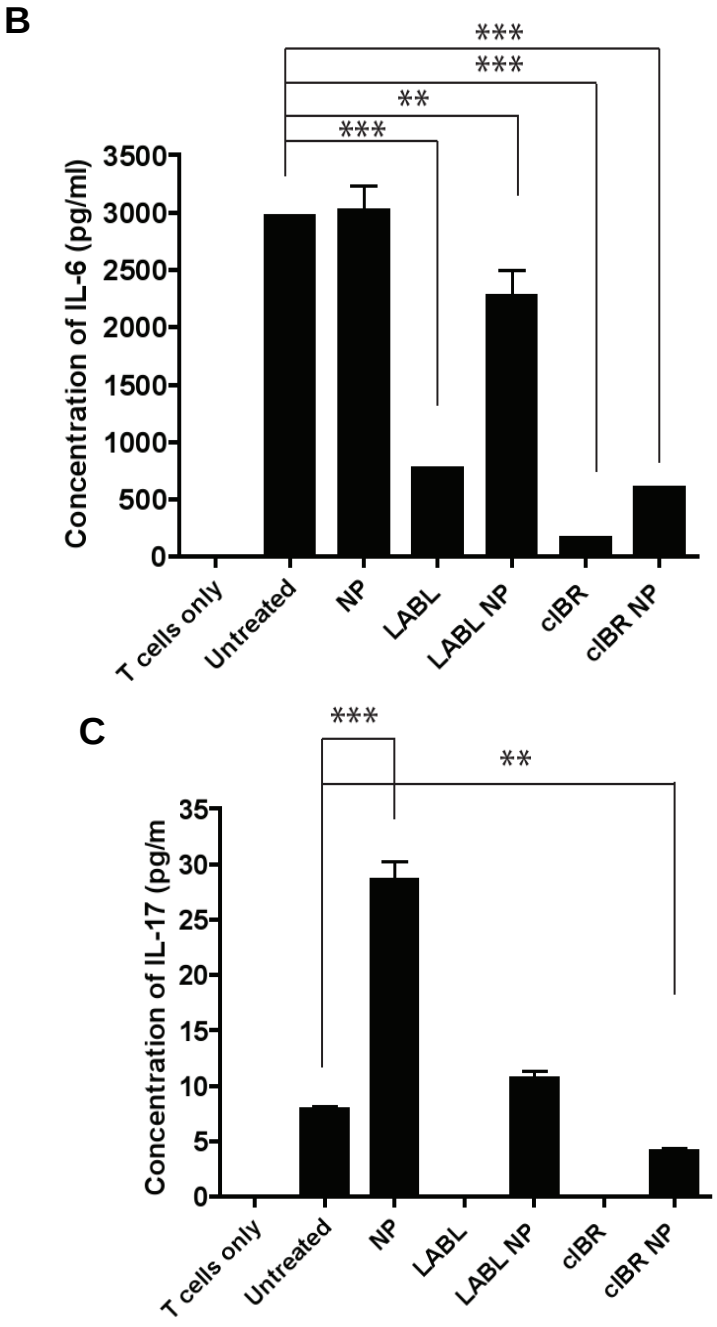

Figure 8 The production of cytokines in cocultures where DCs were pretreated with LABL-NPs, cIBR-NPs, untargeted NPs, LABL peptide or cIBR peptide. (A) All nanoparticles increased the secretion of TNF-α compared to untreated DCs. (B) LABL-NPs, cIBR-NPs, LABL and cIBR peptides decreased the amount of IL-6 detected in the coculture of DCs and T cells relative to untreated DCs. Untargeted

NPs increased the level of IL-6 production in the coculture of DCs and T cells (C) Untargeted NPs induced the production of IL-17 from activated OT-II T cells. LABL-NPs, cIBR-NPs, LABL and cIBR peptides did not stimulate the production of IL-17. *** indicates $p<0.001$ and ** indicates $p<0.01$.

4.4 Discussion

A critical step in the development of an immune response is the activation of T cells. This process transitions naïve CD4+ T cells into effector cells. T cell activation begins with antigen recognition through a highly specific interaction between T cell receptor (TCR) and antigenic peptide presented by major histocompatibility complex (MHC) molecules on the surface of antigen presenting cells.[1] The activation of a T cell by an APC requires the reorganization of receptors and ligands to form an immunological synapse. This dynamic and highly organized structure maintains the cell-cell interaction.[31]The immunological synapse is formed by a re-arrangement of receptors that form supramolecular activation clusters. The central cluster is comprised of TCR-peptide-MHC interaction which is surrounded by LFA-1 and ICAM-1 adhesion molecules, among others, in the mature immunological synapse.[32] The binding of TCRs to peptide-MHC complexes further activates LFA-1 on T cells that recognize and bind ICAM-1 on APC.[2] This interaction strengthens the conjugation of APC and T cells and completes the immunological synapse which can lead to efficient T cell activation.[29-30]

ICAM-1 belongs to the immunoglobulin superfamily and is expressed constitutively at low levels on APC, endothelial cells, and other cell types.[16] The upregulation of ICAM-1 can be induced by inflammatory mediators such as IL-1.[31]

Generally, the binding of cell adhesion molecules is enhanced by oligomerization and clustering of the adhesion molecules.[16] ICAM-1 rearranges into non-covalent homodimers on the cell surface *via* interactions between domain 4 (D4).[16] Moreover, D4-D4 dimers can then be non-covalently linked by interaction of domain 1, resulting in a "W" shaped tetramer that forms linear arrays that are likely bent into circular arrays. This organization of ICAM-1 influences formation of the immunological synapse (Figure 1).[16]

The binding of LFA-1 to ICAM-1 is also tightly regulated. The interaction of LFA-1 to ICAM-1 is driven by cluster formation and a change in LFA-1 conformation leading to higher avidity and affinity, respectively.[17] Binding of TCRs to peptide-MHC complexes generates intracellular signals leading to an increase in avidity of LFA-1 binding by forming a cluster.[17, 34] The adhesion of DCs and T cells involves LFA-1 and ICAM-1 clusters, made up of thousands of molecules.[16] The high densities of ICAM-1 on APCs and LFA-1 on T cells are necessary for firm, long-lasting conjugation. Thus, the nature of T cell conjugation to DCs suggests that multivalent inhibitors may pose an interesting intervention.

LABL and cIBR peptides have been shown to bind specifically to ICAM-1 and LFA-1, respectively.[19-20] These peptides also specifically bind their respective ICAM-1 and LFA-1 receptors when conjugated to nanoparticles.[23, 25] Presenting these as multivalent arrays on the nanoparticle surface was hypothesized to provide more potent intervention strategies due to enhanced binding avidity, triggered endocytosis of receptors, and changes in cell response (Figure 1).[35-36]

In this study, pretreatment of DCs with LABL-NPs yielded up to a ~76% decrease in T cell conjugate formation with DCs suggesting that LABL-NPs bound to ICAM-1 on DCs and blocked the availability of ICAM-1 to interact with LFA-1 on T cells. Similar results were obtained when DCs were pre-treated with cIBR-NPs. The quantity of T cells binding to DCs treated with cIBR-NPs was reduced by 78% when compared to untreated control. LABL-NPs and cIBR-NPs blocked T cell conjugation to DCs to a greater extent than LABL peptide, cIBR peptide, anti-ICAM-1 antibody, anti-LFA-1 antibody and unconjugated NPs.

Inhibition of T cell conjugation to DCs was most likely due to an increase in the binding avidity of multivalent peptides and perhaps internalization of cell adhesion molecules facilitated by the nanoparticles.[35-36] Multiple copies of LABL or cIBR peptide conjugated to the surface of nanoparticles were hypothesized to induce the clustering of LFA-1 and ICAM-1, hence enhancing the binding avidity of peptides to activated, high-density receptors. Welder et al has shown that monovalent soluble ICAM-1 is unable to bind efficiently to LFA-1 expressing cells unless it is rendered multivalent by coupling to polystyrene microspheres.[36] Furthermore, the peptide-NPs were suspected to sustain inhibition by inducing receptor internalization. Internalization of clustered ICAM-1 on endothelial cells is known to be triggered by multimeric anti-ICAM-1 conjugated on microspheres, whereas monomeric anti-ICAM-1 was not efficiently internalized.[35] LABL-NPs and cIBR-NPs have also been shown to be internalized into lung epithelial cells and HUVEC cells expressing ICAM-1 and T cells expressing LFA-1, respectively.[23-25] Here, the punctate staining

patterns observed in DCs treated with NPs indicated uptake, and presumably receptor internalization.

LABL-NPs, cIBR-NPs, and NPs induced TNF-α production which may result from endocytosis or processing of particles in DCs.[37] Indeed, PLGA nanoparticles have been shown to induce proinflammatory cytokine production and increase T cell proliferation.[38-40] Co-incubation of T cells with DC that had been pretreated with untargeted NPs led to high levels of TNF-α, IL-6 and IL-17 and augmented T cell proliferation relative to untreated DCs. A similar observation was previously reported in DCs treated with PLGA microspheres.[41] LABL-NPs decreased the production of IL-6 from DCs and/or OT-II T cells and also resulted in a decrease the amount of IL-17, presumably by inhibiting T cell differentiation into Th17 cells.

DCs pretreated with cIBR-NPs also induced TNF-α production and proliferation of OT-II T cells in a dose dependent manner. Significantly lower levels of IL-6 and IL-17 were produced when comparing cIBR-NPs to other NPs or to untreated coculture. In addition, it was unclear whether the T cells that proliferate following stimulation of T cells with cIBR-NP treated DC were Th1, Th2 or Th17 cells. Based on previous reports, LFA-1 does not seem to deliver a costimulatory signal but improves engagement of TCR by promoting adhesion of T cells to APC.[3] Blockade of LFA-1 on DCs would, therefore, not be expected to inhibit T cell activation by DCs. However it could change the T cell differentiation by changing the microenvironment of T cell during activation. Although cIBR-NPs blocked T cell conjugation to DCs initially, this effect was most likely transient, since substantial T

cell proliferation was observed at day 7. Data also showed that increasing cIBR-NP dose ultimately increased T cell proliferation.

4.5 Conclusion

Chemical conjugation of LABL and cIBR peptides to PLGA NPs generated efficient targeting to ICAM-1 and LFA-1 receptors on DCs, respectively. LABL-NPs and cIBR-NPs were found to be effective inhibitors of T cell conjugation to DCs. LABL-NPs and cIBR-NPs blocked T cell conjugation to DCs more efficiently than untargeted NPs, free peptides and antibodies. Compared to controls, T cell proliferation was arrested when T cells were incubated in the presence of DCs treated with LABL-NPs, whereas DCs treated with cIBR-NPs or untargeted NPs dramatically stimulated the division of T cells. These findings suggested the potential of LABL-NPs to change the character of mature DCs, yet block immunological synapse formation without stimulating T cell proliferation and point to cIBR-NPs as inducers of T cell expansion. All NPs increased the production of TNF-α compared to free ligands or untreated controls, but the amount of IL-6 or IL-7 depended on NP type. Collectively, results suggested that LABL-NPs and cIBR-NPs function as distinct immune modulators that dramatically differ from soluble peptide inhibitors of ICAM-1 or LFA-1.

References

1 Dustin ML, Shaw AS (1999) Costimulation: Building An Immunological Synapse. *Science***,** 283, 649-650.

2. Dustin ML (2008) T-cell Activation Through Immunological Synapses and Kinapses. *Immunol Rev*, 221,77-89.

3. Bachmann MF, McKall-Faienza K, Schmits R, Bouchard D, Beach J, Speiser DE, Mak TW & Ohashi PS (1997) Distinct Roles for LFA-1 and CD28 During Activation of Naive T cells: Adhesion Versus Costimulation. *Immunity*, 7,549-557.

4. Van Seventer GA, Shimizu Y, Horgan KJ, Shaw S (1990) The LFA-1 Ligand ICAM-1 Provides An Important Costimulatory Signal for T cell Receptor-Mediated Activation of Resting T cells. *J Immunol* , 144, 4579-4586.

5. Springer TA, Dustin ML, Kishimoto TK, Marlin SD (1987) The Lymphocyte Function-Associated LFA-1, CD2, and LFA-3 Molecules: Cell Adhesion Receptors of The Immune System. *Annu Rev Immunol*, 5, 223-252.

6. Lunsford KE, Koester MA, Eiring AM, Horne PH, Gao D, Bumgardner GL (2005) Targeting LFA-1 and CD154 Suppresses The In Vivo Activation And Development of Cytolytic (CD4-Independent) CD8+ T cells. *J Immunol.*, 175, 7855-66.

7. Simnick AJ, Valencia A, Liu R, Chilkoti (2010) A. Morphing Low-Affinity Ligands into High-Avidity Nanoparticles by Thermally Triggered Self-Assembly of a Genetically Enclosed Polymer. *ACS Nano*, 4, 2217-2227.

8. Stukel JM, Li RC, Maynard HD, Caplan MR (2010) Two-Step Synthesis of Multivalent Cancer-Targeting Constructs. *Biomacromolecules*, 11, 160-167.

9. Hong A, Leroueil PR, Majoros IJ, Orr BG, Baker JR, Banaszak Holl MM (2007) The Binding Avidity of a Nanoparticle-Based Multivalent Targeted Drug Delivery Platform. *Chemistry and Biology*, 14, 107-115.

10. Johnson RN, Kopeckova P, Kopecek J (2009) Synthesis and Evaluation of Multivalent Branched HPMA Copolymer-Fab' Conjugates Targeted to the B-Cell Antigen CD20. *Bioconjugate Chem.*, 20, 129-137.

11. Ding H, Prodinger WM, Kopecek J (2006) Identification of CD21-Binding Peptides with Phage Display and Investigation of Binding Properties of HPMA Copolymer-Peptide Conjugates. *Bioconjugate chem.*, 17, 514-523.

12. Carlson CB, Mowery P, Owen RM, Dykhuizen EC, Kiessling LL (2007) Selective Tumor Cell Targeting Using Low-Affinity, Multivalent Interactions. *ACS Chem Biol.*, 2, 119-27.

13. Puffer EB, Pontrello JK, Hollenbeck JJ, Kink JA, Kiessling LL (2007) Activating B Cell Signaling with Defined Multivalent Ligands. *ACS Chem Biol.*, 2, 252-62.

14. Gordon EJ, Sanders WJ, Keissling LL (1998) Synthetic Ligands Point to Cell Surface Strategies. *Nature*, 392, 30-31.

15. Mowery P, Yang ZQ, Gordon EJ, Dwir O, Spencer AG, Alon R,Kiessling LL (2004) Synthetic Glycoprotein Mimics Inhibit L-Selectin-Mediated Rolling and Promote L-Selectin Shedding.*Chem Biol.*, 11, 725-32.

16. Lebedeva T, Dustin ML, Sykulev Y (2005) ICAM-1 Co-stimulates Target Cells to Facilitate Antigen Presentation. *Curr Opin Immunol*, 17, 251-258.

17. Hogg N, Laschinger M, Giles K, McDowall A (2003) T-cell Integrins: More Than Just Sticking Points. *J Cell Sci*, 116, 4695-4705.

18. Anderson ME, Siahaan TJ (2003) Targeting ICAM-1/LFA-1 Interaction for Controlling Autoimmune Diseases: Designing Peptide and Small Molecule Inhibitors. *Peptides*, 24, 487–501.

19. Anderson ME, Siahaan TJ (2003) Mechanism of Binding and Internalization of ICAM-1-Derived Cyclic Peptides by LFA-1 on The Surface of T cells: A Potential Method for Targeted Drug Delivery. *Pharm Res*, 20, 1523-1532.

20. Jois SDS, Siahaan TJ (2003) A Peptide Derived from LFA-1 That Modulates T-cell Adhesion Binds to Soluble ICAM-1 Protein. *J. Biomol. Struc. Dyn*, 20, 635-644.

21. Tibbetts SA, Seetharama JD, Siahaan TJ, Benedict SH, Chan MA (2000) Linear and Cyclic LFA-1 and ICAM-1 Peptides Inhibit T cell Adhesion and Function. *Peptides*, 21,1161-1167.

22. Tibbetts SA, Chirathaworn C, Nakashima M, Jois DS, Siahaan TJ, Chan MA & Benedict SH (1999) Peptides Derived from ICAM-1 and LFA-1 Modulate T cell Adhesion and Immune Function in A Mixed Lymphocyte Culture. *Transplantation*, 68, 685-692.

23. Chittasupho C, Manikwar P, Krise JP, Siahaan TJ, Berkland C (2010) cIBR Effectively Targets Nanoparticles to LFA-1 on Acute Lymphoblastic T cells. *Mol Pharm*, 7,146-155.

24. Zhang N, Chittasupho C, Duangrat C, Siahaan TJ, Berkland C (2008) PLGA Nanoparticle-Peptide Conjugate Effectively Targets Intercellular Cell-Adhesion Molecule-1. *Bioconjug Chem*, 19 , 145-152.

25. Chittasupho C, Xie S, Baoum A, Yakovleva T, Siahaan TJ, Berkland C (2009) ICAM-1 Targeting of Doxorubicin-Loaded PLGA Nanoparticles to Lung Epithelial Cells**.** *European Journal of Pharmaceutical Sciences*, 37, 141-150.

26. Lutz MB, Kukutsch N, Ogilvie AL, Rössner S, Koch F, Romani N & Schuler G (1999) An Advanced Culture Method for Generating Large Quantities of Highly Pure Dendritic Cells from Mouse Bone Marrow. *J Immunol Methods*, 223,77-92.

27. Guerrouache M, Karakasyan C, Gaillet C, Canva M, Millot MC (2006) Immobilization of A Functionalized Poly(ethylene glycol) onto β-Cyclodextrin-Coated Surfaces by Formation of Inclusion Complexes:

Application toThe Coupling of Proteins. *J Applied Polym Sci*., *100, 2362-2370*.

28. Commins SP, Borish L, Steinke JW (2010) Immunologic Messenger Molecules: Cytokines, Interferons, and Chemokines. *J Allergy Clin Immunol***,** 125, S53-72.

29. Zhu J, Yamane H, Paul WE (2010) Differentiation of Effector CD4 T cell Populations. *Annu Rev Immunol*, 28, 445-489.

30. Miossec P, Korn T, Kunchroo VK (2009) Mechanisms of Disease

Interleukin-17 and Type 17 Helper T Cells. *Th e new england journal of medicine*, 361, 888-898.

31. Dustin ML (2005) A Dynamic View of The Immunological Synapse. *Semin Immunol*, 17, 400-410.

32. Dustin ML (2009) Modular Design of Immunological Synapses and Kinapses. *Cold Spring Harbor Perspect Biol*, 1, a002873.

33. Rothlein R, Dustin ML, Marlin SD, Springer TA (1986) A Human Intercellular Adhesion Molecule (ICAM-1) Distinct from LFA-1. *J Immunol*, 137, 1270-1274.

34. Dustin ML, Springer TA (1989) T-cell Receptor Cross-Linking Transiently Stimulates Adhesiveness Through LFA-1. *Nature*, 341, 619-624.

35. Muro S, Wiewrodt R, Thomas A, Koniaris L, Albelda SM, Muzykantov VR, Koval M (2003) A Novel Endocytic Pathway Induced by Clustering Endothelial ICAM-1 or PECAM-1. *J Cell Sci.*, 116, 1599-609.

36. Welder CA, Lee DHS, Takei F (1993) Inhibition of Cell Adhesion by Microspheres Coated with Recombinant Soluble ICAM-1. *Journal of Immunology, 150, 2203-2210.*

37. Yoshida M, Babensee JE (2006) Molecular Aspects of Microparticle Phagocytosis by Dendritic Cells. *J. Biomater. Sci. Polymer*, 17, 893-907.

38. Semete B, Booysen LIJ, Kalombo L, Venter JD, Katata B, Ramalapa JA, Verschoor JA, Swai H (2010) In Vivo Uptake and Acute Immune Response to Orally Administered Chitosan and PEG Coated PLGA Nanoparticles. *Toxicology and Applied Pharmacology*. (e-published)

39. Molavi O, Mahmud A, Hamdy S, Hung RW, Lai R, Samuel J, Lavasanifar A (2009) Development of a Poly(D,L-lactic-*co*-glycolic acid)Nanoparticle Formulation of STAT3 Inhibitor JSI-124:Implication for Cancer Immunotherapy. *Molecular Pharmaceutics,* 7, 364-374.

40. Steenblock E, Fahmy TM (2008) A Comprehensive Platform for *Ex Vivo* T-cellExpansion Based on Biodegradable PolymericArtificial Antigen-presenting Cells. *Molecular Therapy*, 16, 765-772.

41. Yoshida M, Babensee JE (2006) Molecular Aspects of Microparticle Phagocytosis by Dendritic Cells. *J. Biomater. Sci. Polymer*, 17, 893-907.

Chapter 5

Targeting ICAM-1 and LFA-1 by hyaluronic acid conjugates for potential treatment of autoimmune diseases

5.1 Introduction

An ideal therapeutic intervention for autoimmune diseases would target the cells that are actively involved in the pathogenesis of the autoimmune disease while keeping protective immune responses intact. Since APCs express many different antigens, it may be possible to selectively block an MHC molecule that is associated with each autoantigen. In this approach, targeting only the subpopulation of offending T cells could minimize global immunosuppression. To this end, antigen-specific inhibition of the immunological synapse (IS) by simultaneously blocking antigen recognition (Signal 1) and costimulation (Signal 2) has been explored.[1, 2]

A number of antigen peptide analogs have been shown to bind to MHC molecules resulting in inhibition of antigen presentation to antigen specific T cells and also a reduction in T cell proliferation.[3] In addition, receptors participating in adhesion or costimulation have become attractive targets for immune suppression. Cell-cell communication at the IS includes both of these signals, orchestrated in thousands of receptor-ligand interactions. Valency, geometry, and duration of the IS are well known affect T cell activation.[4-8]

The choice of material for multivalent ligand presentation is also important. Some polymeric materials used for drug delivery have been shown to modulate immune responses. For example, the synthetic polymers poly(lactic acid) (PLA) and poly(lactic-co-glycolic acid) (PLGA) are biodegradable and biocompatible, but their hydrophobicity has been shown to cause immune responses.[9, 10] Studies have also shown that PLGA nanoparticles coated with polyethylene glycol were efficiently

taken up by phagocytes such as macrophages resulting in an increase in T cell proliferation and proinflammatory cytokine production.[11, 12] In the previous chapter, untargeted PLGA NPs also induced T cell activation by stimulating T cell proliferation and the production of proinflammatroy cytokines including TNF-α, IL-6 and IL-17.

Furthermore, dendritic cells treated with chitosan or PLGA films increased DC maturation by inducing expression of costimulatory molecules (CD86 and CD40) similar to LPS-matured dendritic cells. In contrast, DCs treated with alginate or hyaluronic acid (HA) films decreased the expression levels of these same molecules.[13]

In this study, an ovalbumin (OVA) antigen and a peptide targeting ICAM-1 (LABL) were conjugated to hyaluronic acid (HA). HA conjugates with OVA antigen, LABL, or a 1:1 ratio of these peptides were studied to determine DC binding, T cell proliferation and cytokine production.

5.2 Materials and Methods

Materials

LABL peptide (ITDGEATDSG, Mw 964.95) and OVA peptide (ISQAVHAAHAEINEAGR, Mw 1773.93) were synthesized on a Pioneer peptide synthesizer (PerSeptive Biosystems, CA). Hyaluronic acid (HA, Mw ~31 kDa) was purchased from Lifecore (MN, USA). RPMI 1640 medium was obtained from Cellgro (Manassas, VA, USA). Tumor Necrosis Factor-α (TNF-α) was purchased from Promega (Madison, WI, USA). Granulocyte Macrophage-Colony Stimulating

Factor (GM-CSF) was purchased from Peprotech Inc. (Rocky Hill, NJ, USA). Carboxyfluorescein diacetate succimidyl ester (CFSE) and 5-(and-6)-(((4cloromethyl) enzoyl)amino)tetramethylrhodamine (Orange CMTMR)were purchased from Invitrogen Corporation, (Carlsbad, CA). Ovalbumin was purchased from Sigma (St. Louis, MO). Penicillin, streptomycin and L-glutamine were purchased from Cellgro (Manassas, VA, USA). IL-2 was generously provided by Dr. Christophe Nicot at the University of Kansas Medical Center. C57BL/6-TgN(OT-II.2a)-Rag1 mice were purchased from Taconic Farms (Hudson, NY). C57BL/6 wildtype mice were purchased from Jax labs (Bar Harbor, ME).

Methods

Cell culture and isolation

Bone marrow derived dendritic cells were generated from C57BL/6 wildtype mice as described[36]. Briefly, 2 x 10^6 cells were isolated from bone marrow, plated on bacterial Petri dishes and cultured in 10 ml DC media (RPMI 1640, 10% heat inactivated fetal bovine serum, 100 µg/ml penicillin-streptomycin, 50 µM β-mercaptoethanol, 20 ng/ml murine granulocyte macrophage colony stimulating factor (GM-CSF) (R&D), and 2 nM L-glutamine. At 72 hours (Day 3), 10 ml of fresh DC media was added to each dish. On days 6 and 8, 10 ml of supernatant and cells were removed, cells recovered by centrifugation (90 x *g*) and added back to the dish with fresh DC medium. On day 9 non-adherent cells were collected.

On day 10, T cells were isolated from C57BL/6-TgN(OT-II.2a)-Rag1 spleens by passing spleens through a wire mesh. T cells were purified using a negative

selection, mouse T cell enrichment kit according to manufacturers' directions (EasySep).

Conjugation of LABL and OVA peptide to HA polymer

The aminooxy group of peptide was linked to amide group of hyaluronic acid. Peptides were mixed in a 1:2 molar ratio to the polymer reactive sites. Peptide-HAs were prepared by dissolving HA polymer (10 mg) in acetate buffer solution (20 mM, 5 ml) of pH 5.5 ± 0.1. Then, LABL peptide (13.9 mg) or OVA peptide (24.7 mg) was added and mixed gently. Reaction solutions were then stirred at 500 RPM using magnetic stir bars for 24 hrs at room temperature. LABL-OVA-HA was prepared by adding LABL (6.9 mg) and OVA (12.4 mg) peptides simultaneously. The solution of peptide conjugated with HA (peptide-HA) was then transferred to dialysis bags (MWCO 3500 Da) and was dialyzed for 24 hrs with changing of water at least once to remove free peptides. The peptide-HAs were lyophilized.

Characterization of LABL and/or OVA conjugated HA

The amount of LABL and OVA peptides conjugated on HA were quantified by determination of free peptides in reaction medium by gradient reversed phase HPLC (SHIMADZU) using a C_{18} column. The HPLC consisted of SCL-10A SHIMADZU system controller, LC-10AT VP SHIMADZU liquid chromatograph, SIL-10A XL SHIMADZU autoinjecter set at 30 μl injection volume, DGU-14A SHIMADZU degasser, sample cooler, and SPD-10A SHIMADZU UV-Vis detector (220 nm). The HPLC-UV system was controlled by a personal computer equipped with SHIMADZU class VP Software. All separations were carried out using a Vydac®

HPLC Protein and Peptide C_{18} column. Gradient elution was carried out to determine the amount of LABL and OVA peptide at constant flow of 1 ml/min. Gradient elution was carried out to determine the amount of LABL peptide at constant flow of 1 ml/min, Mobile phase compositions were (A) acetronitrile-water (5:95) with 0.1% TFA and (B) 100% acetonitrile with 0.1% trifluoroacetic acid (TFA).

Binding and uptake of HA, LABL-HA, OVA-HA and LABL-OVA-HA into DCs

The binding and uptake of HA, LABL-HA, OVA-HA and LABL-OVA-HAconjugated with FITC was monitored using fluorescence microscopy. DCs (1 x 10^5 cells/ml) were added in an 8 well-plate (200 μl/well) and matured with TNF-α (1,000 U/ml) and primed with OVA (50 μg/ml) for 24 hrs. DCs were washed with PBS and incubated with HA, OVA-HA, LABL-HA and LABL-OVA-HAconjugated with FITC (2 mg/ml, 300 μl) at 37 °C for 15 min. Cells were washed three times with PBS and fixed with 4% paraformaldehyde. Fluorescence micrographs were acquired using the FITC filter set of a Nikon Eclipse 80i microscope equipped for epifluorescence. Micrographs were captured using an Orca ER camera (Hamamatsu, Inc., Bridgewater, NJ) and analyzed by Metamorph, version 6.2 (Universal Imaging Corp., West Chester, PA). All images were corrected for variations in excitation light intensity. Mean fluorescent intensity of cells incubated with HA conjugates was determined by using ImageJ software.

The binding/uptake of HA conjugates into DCs was also determined and analyzed by using fluorescence plate reader. DCs were matured with TNF-α (1,000 U/ml) and primed with OVA (50 μg/ml) for 24 hr. Cells were washed three times

with serum free RPMI1640 and incubated with HA, OVA-HA, LABL-HA and LABL-OVA-HA in serum free medium (2 mg/ml) for 15 min. After incubation, cells were washed three times with ice-cold PBS. HA conjugates associated with the DCs were detected and compared using a fluorescence plate reader (Spectramax M5; ex: 450 nm, em: 500 nm).

T cell proliferation assay

Primary T cells isolated from C57BL/6-TgN(OT-II.2a)-Rag1 mice were labeled with CFSE (5 μM) for 10 min at 37 °C, 5% CO_2 to observe cell division by CFSE dilution. The dye reaction was quenched by the addition of 5 volumes of culture medium into T cells and incubated 10 min at 4°C. DCs (4 x 10^5 cells/ml) were matured with TNF-α (1,000 U/ml) and primed with OVA (50 μg/ml) for 24 hrs in 24-well plate. DCs were treated with HA, LABL-HA, OVA-HA and LABL-OVA-HAconjugated with FITC (2 mg/ml) for 30 min, at 37 °C, 5% CO_2 and washed three times with PBS. T cells (2 x 10^6 cells/ml) in serum free RPMI1640, IL-2 and 1% penicillin-streptomycin were incubated with DCs 7 days at 37°C, 5% CO_2.T cells collected after 24 hrs (1 day) and 168 hrs (7 days) were centrifuged at 16,089 gfor 2 minutes and fixed with 4% paraformaldehyde. The CFSE dilution was measured by using FACScan flow cytometer. The percent of T cell proliferation was analyzed by calculating the percent of cells with diluted CFSE using FlowJo software.

Quantification of cytokines in cell culture supernatants by ELISA

DCs were matured with TNF-α (1,000 U/ml) and primed with OVA (50 μg/ml) for 24 hrs in 24-well plate. DCs were treated with HA, LABL-HA and LABL-OVA-HA

(2 mg/ml) for 30 min, at 37 °C, 5% CO_2 and washed three times with PBS. T cells (2 x 10^6 cells/ml) in serum free RPMI1640, IL-2 and 1% penicillin-streptomycin were incubated with DCs 7 days at 37°C, 5% CO_2.Supernatants of cell cultures were collected for cytokine detection. Secreted IFN-γ, TNF-α, IL-4, IL-10 and IL-17 were measured by ELISA assay (Cytokine Core Lab, Baltimore, Maryland). ELISA was performed in Nunc Maxisorb ELISA strips freshly coated with capture antibody for 16 hours before the assay was performed. Detecting antibody and the streptavidin-peroxidase conjugate were added into standard, all samples and controls. Premixed substrate solution (Neogen) was then added. The plate was read on a Molecular Divices ELISA plate reader. Curve fitting was selected among linear, quadratic and 4-point based on the best regression coefficient using the SoftPro software package.

Statistical analysis

Statistical evaluation of data was performed using an analysis of variance (one-way ANOVA). Newman–Keuls was used as a post-hoc test to assess the significance of differences. To compare the significance of the difference between the means of two groups, a *t*-test was performed; in all cases, a value of $p < 0.05$ was accepted as significant.

5.3 Results and Discussion

Characterization of peptide-HAs

The conjugation of peptides to HA was based on a novel *N*-oxime reaction scheme. Peptides capped with an aminooxy group at the N-terminus were reacted to the

carbonyl group of *N*-acetyl amides on HA. Both LABL and OVA peptides were successfully grafted to HA using this conjugation reaction. The amounts of unreacted LABL and OVA peptides were quantified after the conjugation reaction. The conjugation efficiency of LABL and OVA peptides were greater than 80% in all cases according to HPLC data (Table 1). For these studies, the total peptide concentration was held constant for all reactions; therefore, LABL-OVA-HA had a ~1:1 ratio of grafted peptide, but the same total peptide content.

Table 1 Percent of peptide conjugated to HA polymer.

	OVA-HA	**LABL-HA**	**LABL-OVA-HA**
% conjugation of LABL	-	80.9 ± 2.7	88.2 ± 0.5
% conjugation of OVA	93.0 ± 0.2	-	89.8 ± 4.8

Binding of peptide-HAs to DCs

The binding of HA, LABL-HA, OVA-HA and LABL-OVA-HA to DCs was investigated *in vitro* by fluorescence microscopy and fluorescence spectroscopy. DCs were matured with TNF-α and primed with OVA for 24 hrs prior to addition of HA conjugates labeled with the fluorophore FITC. Fluorescence microscopy revealed that DCs incubated for 15 min with LABL-HA and LABL-OVA-HA exhibited ~2 and 2.5 fold higher fluorescent intensities than DCs incubated with HA, respectively. DCs

incubated with LABL-OVA-HA were significantly more fluorescent than those treated with LABL-HA (Figure 1A and B). The result was confirmed by fluorescence spectroscopy. Incubating DCs with LABL-HA and LABL-OVA-HA resulted in a significant increase in fluorescence intensity of DCs when compared to HA (Figure 1C).

Unanue et al. reported that free synthetic peptides can also bind directly to class II MHC molecules and be recognized by T cells specific for this antigen.[15-17] The higher fluorescence induced by LABL-OVA-HA suggested that a binding event involving the OVA peptide may augment the fluorescence achieved by LABL-OVA, whereas the OVA alone did not bind DC efficiently. These result suggested that OVA conjugated on HA and OVA conjugated on LABL-OVA-HA may bind MHC molecules with different conformations. The internalization of these peptide-HAs will need to be further studied.

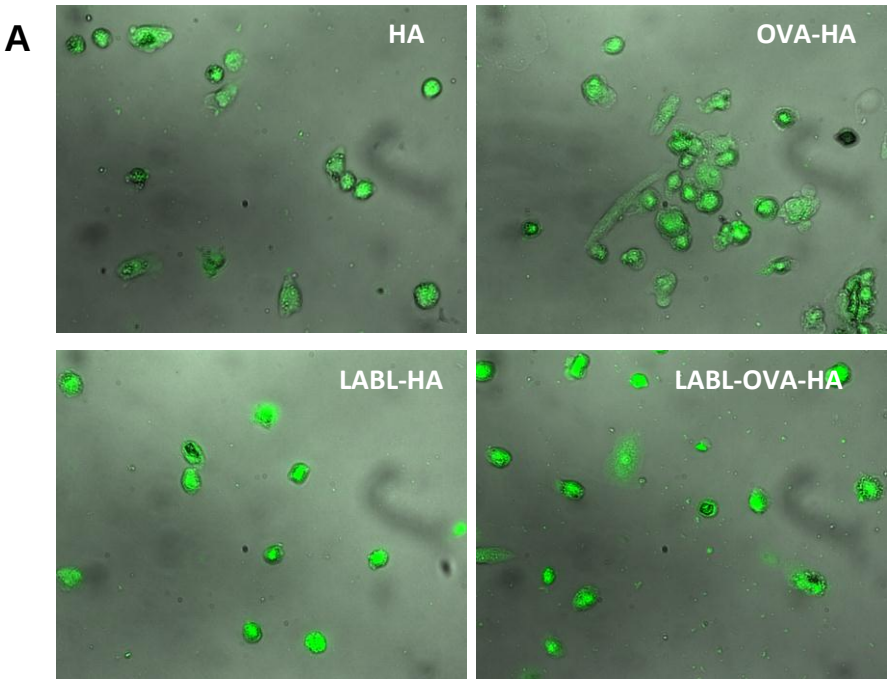

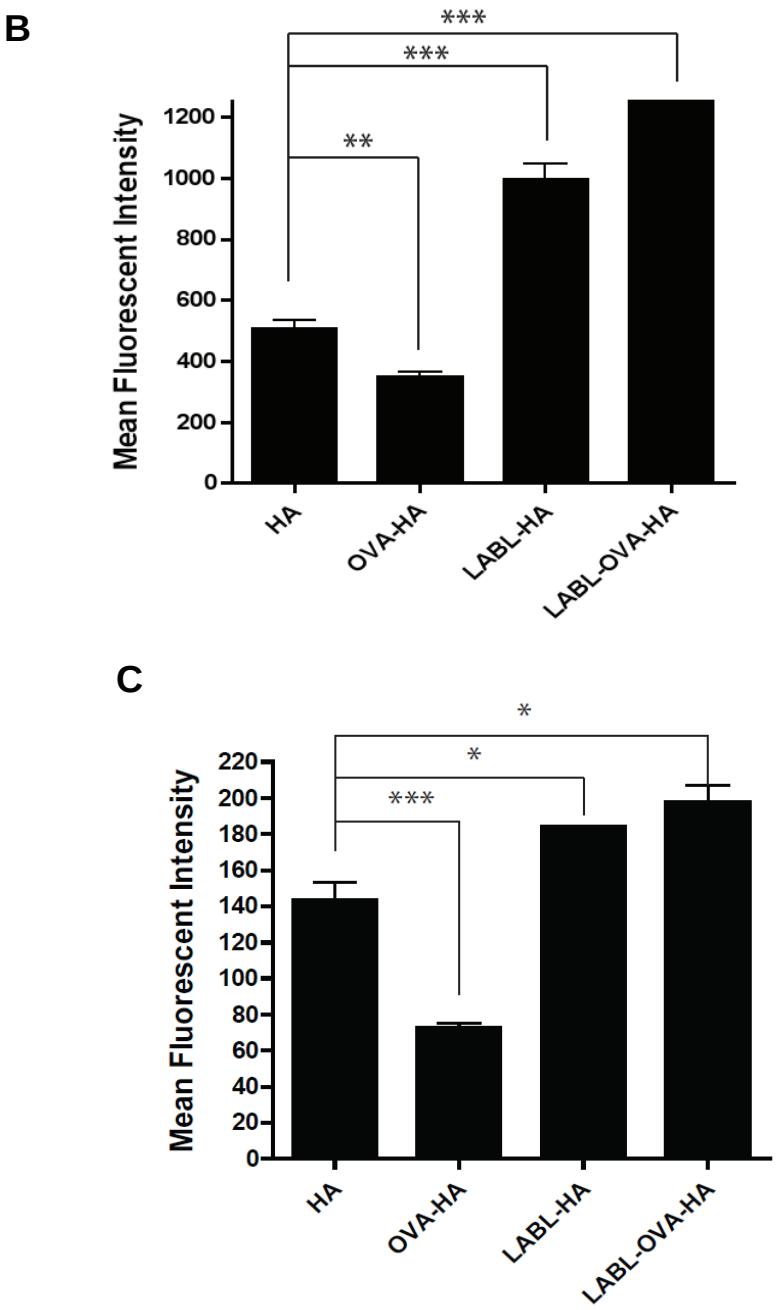

Figure 1 Binding of HA conjugates to dendritic cells matured with TNF-α and primed with OVA. (A) Micrographs of DCs incubated with HA conjugates for 15 min. (B) Fluorescent intensities of DCs as quantified from fluorescence micrographs. (C) Fluorescent intensities of DCs were confirmed using fluorescence specotroscopy.

Data presented as mean ± S.D. (n=3). *** indicates $p<0.001$ and ** indicates $p<0.05$ and * indicates $p<0.01$.

T cell proliferation was reduced by the peptide-HA conjugates

The degree of T cell proliferation was determined after coculture of DCs matured with TNF-α and primed with OVA and OVA-specific T cells. DCs were pretreated with HA, LABL-HA or LABL-OVA-HA for 30 min and then cocultured with OVA specific T cells. After 24 hrs (day 1) and 168 hrs (day 7), OVA-specific T cell proliferation was measured by dilution of fluorescent dye (CFSE) using FACScan flow cytometer. The percent of T cell proliferation was analyzed by calculating the percent of cells with diluted CFSE using FlowJo software. LABL-OVA-HA and LABL-HA incubated with DCs led to a statistically significant decrease in the number of T cells undergoing division compared to the untreated group (Figure 2). There were no significant differences in the level of T cell proliferation between DCs treated with HA compared to untreated DCs. T cells alone without DCs were used as a negative control and yielded a T cell proliferation of only ~0.6%.

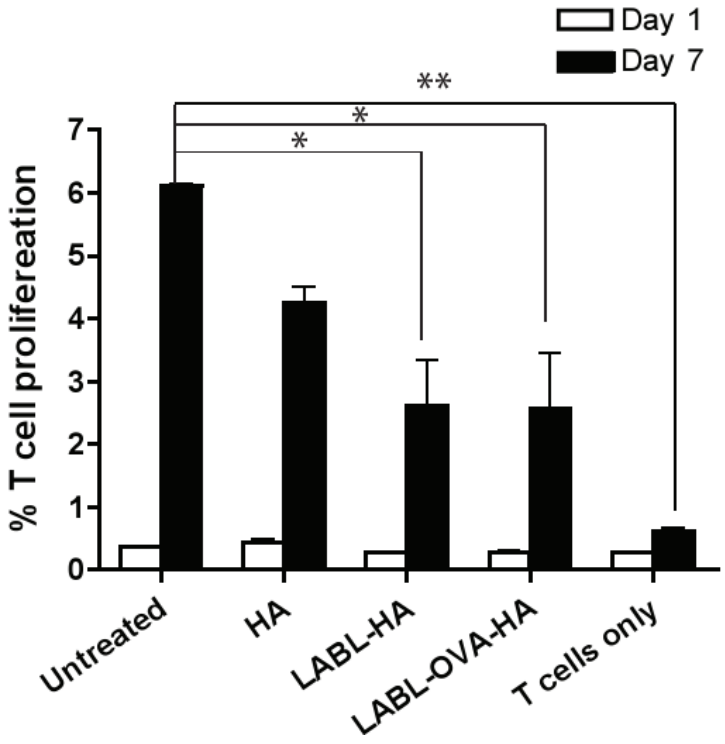

Figure 2 Proliferation of T cells cocultured with DCs for 1 day and 7 days. T cell proliferation was determined by using flow cytometry. Data presented as mean ± S.D. (n=3). ** indicates $p<0.01$ and * indicates $p<0.05$.

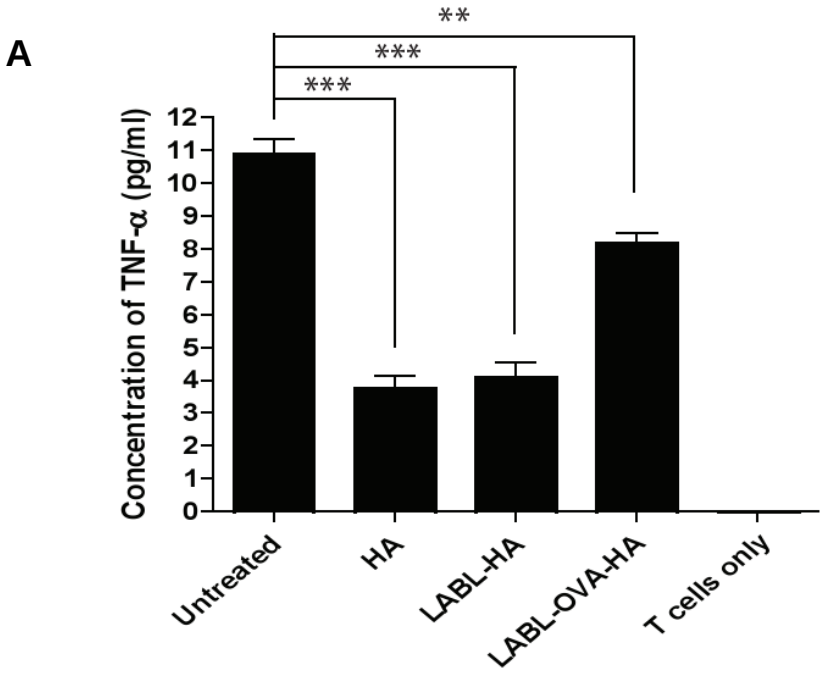

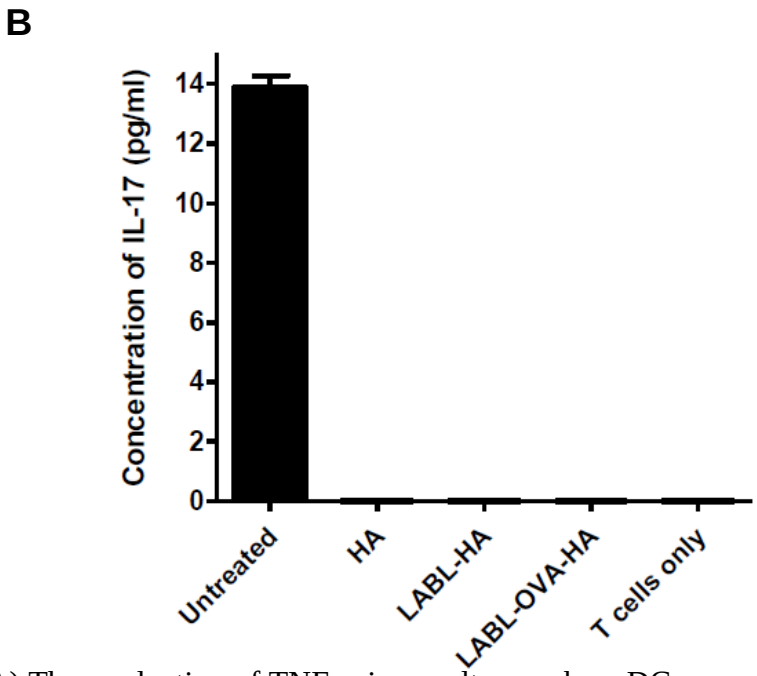

Figure 3 (A) The production of TNF-α in cocultures where DCs were pretreated with HA, LABL-HA or LABL-OVA-HA. HA and peptide-HAs decreased the secretion of TNF-α compared to untreated DCs. *** indicates $p<0.001$ and ** indicates $p<0.01$. (B) The production of IL-17 in coculture of DC and T cells. The amount of IL-17 in coculture of T cells and DCs pretreated with HA, LABL-HA and LABL-OVA-HA were undetectable. Data presented as mean ± S.D. (n=3).

HA and peptide-HAs reduced cytokine production of DCs and OT-II T cells.

Blocking of T cell proliferation by HA and peptide-HAs suggested that HA and peptide-HAs may also regulate cytokine production. To determine the effect of HA and peptide-HAs on cytokine production, DCs matured with TNF-α and primed with OVA were pretreated with HA, LABL-HA and LABL-OVA-HA for 30 min, washed with PBS, and cocultured with primary OT II T cells for 7 days. TNF-α , IFN-γ, IL-4,

IL-10 and IL-17 were then quantified by ELISA (Table 2). After 7 days, all cocultures of DCs and T cells showed undetectable levels of IFN-γ, IL-4, and IL-10. HA and peptide-HAs did not induce the production of IFN-γ, IL-4 and IL-6 suggesting that HA and peptide-HAs had no effect on DC and T cell activation.Compared with untreated DCs, the levels of TNF-α and IL-17 were significantly reduced in the presence of HA, LABL-HA and LABL-OVA-HA. The amount of TNF-α in the medium of cells exposed to HA, LABL-HA and LABL-OVA-HA was reduced from 10.9 (untreated) to 3.7, 4.1 and 8.2 ng/ml, respectively. This result suggested that the production of TNF-α by DCs, which can induce inflammation, was inhibited in the presence of HA and peptide-HAs.[18] Since TNF-α promotes inflammatory responses, dysregulation of TNF-αcan lead to the pathogenesis of various inflammatory and autoimmune diseases.[19] Blockade of TNF-α has shown therapeutic efficacy in a number of T cell-dependent autoimmune diseases such as rheumatoid arthritis, juvenile idiopathic arthritis, Crohn's disease, inflammatory bowel disease and psoriasis.[19, 20]

IL-17 has been associated with the pathogenesis of a wide range of inflammatory and autoimmune diseases including asthma, psoriasis, rheumatoid arthritis (RA), inflammatory bowel disease, systemic sclerosis and systemic lupus erythematosus (SLE).[21, 22] IL-17 produced from untreated cells was 13.9 ± 0.7 ng/ml, whereas the amount of this cytokine secreted from cells in the presence of HA and peptide-HAs was undetectable. The decrease in cytokine production suggested that HA and peptide-HAs inhibited the differentiation of Th17 CD4 cells. The binding of

HA and peptide-HAs to DC inhibited T cell and DC conjugate formation, hence inhibiting T cell proliferation and any ensuing cytokine production.

The binding of peptide-HAs to DCs, the reduction of T cell proliferation, the suppression of TNF-α and IL-17 production, and the lack of IFN-γ, IL-4 and IL-6 suggested that these HA conjugates may be useful for targeting dendritic cells involved in inflammatory and autoimmune diseases. The fact that HA and peptide-HA were not able to induce proinflammatory cytokines (IFN-γ, IL-4 and IL-6) suggested that LABL-HA and LABL-OVA-HA have potential as a multivalent, antigen-specific immune modulator.

Table 2 Summary of assayed cytokines and their functions.

Cytokines	Cell expression	Functions
TNF-α	Mononuclear phagocytes (major) and T cells (minor) [18, 23]	-Induces leukocyte extravasation -Upregulates adhesion molecules on endothelial cells -Regulates maturation and migration of APCs.[18]
IFN-γ	Effector T cells (Th1 cells) (major) and DCs and Natural Killer (NK) cells (minor)[31]	-Increases MHC class I and II expression and stimulates antigen presentation and cytokine production by APCs. -Stimulates the adherence and phagocytosis of mononuclear phagocytes[31]
IL-4	Th2 cells (major) and basophils, NK T cells, eosinophils and mast cells (minor)[31]	-Stimulates T cellproliferation and differentiation[31]
IL-10	Regulatory T cells, monocytes and B cells[24]	-Inhibits cytokine production from T cell and mononuclear phagocytes. -Inhibits the expression of the costimulatory molecules CD80 and CD86 by DCs and other APCs.[24]
IL-17	Activated T cells, particularly Th17 cells[21, 22]	-Induces expression of a variety of cytokines and chemokines such as IL-6, IL-11, granulocyte colony-stimulating factor, GM-CSF and TGF-β from non-hematopoietic cells.[24]

5.5 Conclusion

A novel *N*-oxime chemistry was successfully used to conjugate LABL, OVA and both ligands (LABL and OVA) to HA. HA and peptide conjugated HA rapidly bound to DCs. DCs treated with HA, LABL-HA, and LABL-OVA-HA significantly suppressed T cell proliferation and reduced the production of proinflammatory cytokines TNF-α and IL-17 compared to untreated cells. These results suggested that HA serves as an effective backbone for multivalent ligand presentation. In addition, multivalent display of both antigen and a Signal 2 inhibitor (LABL) may ultimately provide antigen-specific disruption of cellular signaling leading to autoimmunity.

References

1. Wraith DC (2009) Therapeutic peptide vaccines for treatment of autoimmune diseases. *Immunol Lett* 122,134-136.
2. Larche M & Wraith DC (2005) Peptide-based therapeutic vaccines for allergic and autoimmune diseases. *Nat Med* 11, S69-76.
3. De Magistris MT, Alexander J, Coggeshall M, Altman A, Gaeta FC, Grey HM & Sette A (1992) Antigen analog-major histocompatibility complexes act as antagonists of the T cell receptor. *Cell* 68, 625-634.
4. Bachmann MF, McKall-Faienza K, Schmits R, Bouchard D, Beach J, Speiser DE, Mak TW & Ohashi PS (1997) Distinct roles for LFA-1 and CD28 during activation of naive T cells: adhesion versus costimulation. *Immunity* 7, 549-557.

5. Van Seventer GA, Shimizu Y, Horgan KJ, & Shaw S (1990) The LFA-1 ligand ICAM-1 provides an important costimulatory signal for T cell receptor-mediated activation of resting T cells. *J Immunol* 144, 4579-4586.

6. Springer TA, Dustin ML, Kishimoto TK, & Marlin SD (1987) The lymphocyte function-associated LFA-1, CD2, and LFA-3 molecules: cell adhesion receptors of the immune system. *Annu Rev Immunol* 5, 223-252.

7. Kobayashi N, Kobayashi H, Gu L, Malefyt T, & Siahaan TJ (2007) Antigen-specific suppression of experimental autoimmune encephalomyelitis by a novel bifunctional peptide inhibitor. *J Pharmacol Exp Ther* 322, 879-886.

8. Ridwan R, Kiptoo P, Kobayashi N, Weir S, Hughes M, Williams T, Soegianto R & Siahaan TJ (2010) Antigen-specific suppression of experimental autoimmune encephalomyelitis by a novel bifunctional peptide inhibitor: structure optimization and pharmacokinetics. *J Pharmacol Exp Ther* 332, 1136-1145.

9. Raghuvanshi RS, Katare YK, Lalwani K, Ali MM, Singh O & Panda AK (2002) Improved immune response from biodegradable polymer particles entrapping tetanus toxoid by use of different immunization protocol and adjuvants. *Int J Pharm* 245, 109-121.

10. Thomas C, Gupta V, & Ahsan F (2009) Influence of surface charge of PLGA particles of recombinant hepatitis B surface antigen in enhancing systemic and mucosal immune responses. *Int J Pharm* 379, 41-50.

11. Semete B, Booysen LI, Kalombo L, Venter JD, Katata L, Ramalapa B, Verschoor JA & Swai H (2010) In vivo uptake and acute immune response

to orally administered chitosan and PEG coated PLGA nanoparticles. *Toxicol Appl Pharmacol* 249, 158-165.

12. Molavi O, Mahmud A, Hamdy S, Hung RW, Lai R, Samuel J & Lavasanifar A (2010) Development of a poly(d,l-lactic-co-glycolic acid) nanoparticle formulation of STAT3 inhibitor JSI-124: implication for cancer immunotherapy. *Mol Pharm* 7, 364-374.
13. Babensee JE & Paranjpe A (2005) Differential levels of dendritic cell maturation on different biomaterials used in combination products. *J Biomed Mater Res A* 74, 503-510.
14. Oh EJ, Park K, Kim KS, Kim J, Yang JA, Kong JH, Lee MY, Hoffman AS & Hahn SK (2010) Target specific and long-acting delivery of protein, peptide, and nucleotide therapeutics using hyaluronic acid derivatives. *J Control Release* 141, 2-12.
15. Viner NJ, Nelson CA, Deck B, & Unanue ER (1996) Complexes generated by the binding of free peptides to class II MHC molecules are antigenically diverse compared with those generated by intracellular processing. *J Immunol* 156, 2365-2368.
16. Babbitt BP, Allen PM, Matsueda G, Haber E, & Unanue ER (2005) Binding of immunogenic peptides to Ia histocompatibility molecules. 1985. *J Immunol* 175, 4163-4165.
17. Babbitt BP, Matsueda G, Haber E, Unanue ER, & Allen PM (1986) Antigenic competition at the level of peptide-Ia binding. *Proc Natl Acad Sci U S A* 83, 4509-4513.

18. Commins SP, Borish L, & Steinke JW (2010) Immunologic messenger molecules: cytokines, interferons, and chemokines. *J Allergy Clin Immunol* 125, S53-72.

19. Nagar M, Jacob-Hirsch J, Vernitsky H, Berkun Y, Ben-Horin S, Amariglio N, Bank I, Kloog Y, Rechavi G & Goldstein I (2010) TNF activates a NF-kappaB-regulated cellular program in human CD45RA- regulatory T cells that modulates their suppressive function. *J Immunol* 184, 3570-3581.

20. Blanco P, Palucka AK, Pascual V, & Banchereau J (2008) Dendritic cells and cytokines in human inflammatory and autoimmune diseases. *Cytokine Growth Factor Rev* 19, 41-52.

21. Mills KH (2008) Induction, function and regulation of IL-17-producing T cells. *Eur J Immunol* 38, 2636-2649.

22. Song C, Luo L, Lei Z, Li B, Liang Z, Liu G, Li D, Zhang G, Huang B & Feng ZH (2008) IL-17-producing alveolar macrophages mediate allergic lung inflammation related to asthma. *J Immunol* 181, 6117-6124.

23. Pober JS & Cotran RS (1990) Cytokines and endothelial cell biology. *Physiol Rev* 70, 427-451.

24. Steinke JW & Borish L (2006) 3. Cytokines and chemokines. *J Allergy Clin Immunol*117, S441-445.

Chapter 6

Conclusion and Future directions

Multivalent receptor-ligand interactions regulate many important biological responses. In cell-cell recognition events, pairs of receptors and ligands often occur in arrays and elicit a cellular response dictated by valency.[1] For example, the immunological synapse (IS) requires sustained conjugate formation between T cells and APCs mediated by a large member of binding events, due in part to the low affinity and high dissociation rate of the T cell receptor. Therefore, ligands and receptors are clustered and arranged in an orderly manner to prolong the duration of T cell signaling. Multivalent ligand strategies have been shown to increase avidity of ligands conjugated to nanoparticles.[2] In addition, multivalent conjugates can potentially improve the ligand binding specificity, induce ligand-receptor endocytosis, and induce unique cell responses.[3-6] Attaching multiple copies of ligand to polymeric nanoparticles is one of the ways to achieve such multivalency.

The goal of this thesis has been to develop nanoparticles that could be used to target specific cell surface receptors. PLGA nanoparticles (NPs) coated with PEG were synthesized and multiple copies of targeting ligands were attached to a reactive terminus of the PEG. Multiple copies of ICAM-1 or LFA-1 ligands conjugated to NPs were shown to enhance binding and uptake of NPs compared to untargeted NPs, and blocking studies established the specificity of these targeted NPs to ICAM-1 or LFA-1, respectively. *In vitro* studies of cocultures of DCs with T cells also showed the ability of both LABL-NPs and cIBR-NPs to shift cell responses due to NP binding and internalization. NPs did, however, consistently show the production of the proinflammatory cytokine TNF-α, which led to some final studies on water soluble multivalent polymers.

HA and peptide conjugated HA also have potential to target receptor/ligand interactions in the IS and could inhibit T cell proliferation and cytokine production (IL-4, IL-6, IFN-γ, TNF-α and IL-17). These findings have significant implications for the development of new therapeutic strategies in autoimmune diseases or inflammatory diseases in which T cell activation may play an important role. The actions of HA on the immune response are dependent on HA size and the mechanisms remain unknown. HA fragments in the 200-500 KDa range were reported to induce inflammatory cytokines by interacting with CD44 and TLR.[7-9] HA fragments that are smaller than 100 KDa showed various effects. Low molecular weight HA fragments have shown to induce cytokine, chemokine and enzyme production by alveolar and bone marrow derived macrophages.[7, 10] In contrast, Kanawa et al. reported that low Mw HA (3, 22 KDa) did not significantly affect the proinflammatory cytokine production by bone marrow macrophages.[11] In addition, in LPS-treated macrophages, IL-6 and TNF-α production levels were significantly reduced by the addition of low Mw HA (3 and 22 KDa), indicating the inhibitory effect on of low Mw HA on Toll-like receptor (TLR) signaling.[11] Yamasaki et al. also found that large Mw HA induced L-1β release by macrophages, whereas extracellular small HA oligosaccharides did not.[12] In chapter 5, low Mw (31 KDa) HA was used to conjugate targeting peptides. The results have shown that this molecular weight of HA did not stimulate T cell proliferation or proinflammatory cytokine production indicating that HA might be useful as a polymeric multivalent peptide carrier.

Future work with this multivalent ligand targeted drug delivery systems should further investigate the use of HA to inhibit the immunological synapse

formation. This would include the blockade of DC and T cells conjugate formation by using LABL-OVA-HA. Furthermore, the binding mechanism of this peptide-HA could be determined by using anti-MHC antibody and/or anti-ICAM-1 antibody to block the binding of OVA and LABL, respectively to examine the binding sites of this conjugate. In addition, the internalization of peptide-HAs should be determined since it could not be excluded from the mechanism of blocking the IS. Future work should examine the use of peptide-HAs to deplete the clinical scores and symptoms of autoimmune disease animal models to evaluate the clinical efficacy of this conjugate. Furthermore, HA could also be conjugated to other costimulatory molecule ligands expressed on DC including B7, OX40L and LFA-1 to examine the other possibilities to block the IS.

References

1. Kiessling LL, Gestwicki JE, & Strong LE (2006) Synthetic multivalent ligands as probes of signal transduction. *Angew Chem Int Ed Engl* 45, 2348-2368.

2. Caplan MR & Rosca EV (2005) Targeting drugs to combinations of receptors: a modeling analysis of potential specificity. *Ann Biomed Eng* 33, 1113-1124.

3. Johnson RN, Kopeckova P, & Kopecek J (2009) Synthesis and evaluation of multivalent branched HPMA copolymer-Fab' conjugates targeted to the B-cell antigen CD20. *Bioconjug Chem* 20, 129-137.

4. Puffer EB, Pontrello JK, Hollenbeck JJ, Kink JA, & Kiessling LL (2007) Activating B cell signaling with defined multivalent ligands. *ACS Chem Biol* 2, 252-262.

5. Muro S, Dziubla T, Qiu W, Leferovich J, Cui X, Berk E & Muzykantov VR (2006) Endothelial targeting of high-affinity multivalent polymer nanocarriers directed to intercellular adhesion molecule 1. *J Pharmacol Exp Ther* 317, 1161-1169.

6. Muro S, Wiewrodt R, Thomas A, Koniaris L, Albelda SM, Muzykantov VR & Koval M (2003) A novel endocytic pathway induced by clustering endothelial ICAM-1 or PECAM-1. *J Cell Sci* 116, 1599-1609.

7. Horton MR, Shapiro S, Bao C, Lowenstein CJ, & Noble PW (1999) Induction and regulation of macrophage metalloelastase by hyaluronan fragments in mouse macrophages. *J Immunol* 162, 4171-4176.

8. Jiang D, Liang J, & Noble PW (2007) Hyaluronan in tissue injury and repair. *Annu Rev Cell Dev Biol* 23, 435-461.

9. Hodge-Dufour J, Noble PW, Horton MR, Bao C, Wysoka M, Burdick MD, Strieter RM, Trinchieri G & Puré E (1997) Induction of IL-12 and chemokines by hyaluronan requires adhesion-dependent priming of resident but not elicited macrophages. *J Immunol* 159, 2492-2500.

10. McKee CM, Penno MB, Cowman M, Burdick MD, Strieter RM, Bao C & Noble PW (1996) Hyaluronan (HA) fragments induce chemokine gene expression in alveolar macrophages. The role of HA size and CD44. *J Clin Invest* 98, 2403-2413.

11. Kawana H, Karaki H, Higashi M, Miyazaki M, Hilberg F, Kitagawa M & Harigaya K (2008) CD44 suppresses TLR-mediated inflammation. *J Immunol* 180, 4235-4245.

12. Yamasaki K, Muto J, Taylor KR, Cogen AL, Audish D, Bertin J, Grant EP, Coyle AJ, Misaghi A, Hoffman HM & Gallo RL (2009) NLRP3/cryopyrin is necessary for interleukin-1beta (IL-1beta) release in response to hyaluronan, an endogenous trigger of inflammation in response to injury. *J Biol Chem* 284, 12762-12771.